2

NASA CR-112302

SCRAMJET FUEL INJECTOR DESIGN PARAMETERS AND CONSIDERATIONS

DEVELOPMENT OF A TWO-DIMENSIONAL TANGENTIAL FUEL INJECTOR WITH CONSTANT PRESSURE AT THE FLAME

by

Anthony M. Agnone
New York University
Bronx, New York

NASA-CR-112302) SCRAMJET FUEL INJECTOR DESIGN PARAMETERS AND CONSIDERATIONS: DEVELOPMENT OF A TWO-DIMENSIONAL TANGENTIAL FUEL INJECTOR WITH (New York Univ.) ~~104~~ 106 p HC ~~$7.25~~ CSCL 21A G3/28 N73-20829 Unclas 67735

NYU 72-25

The work reported herein was supported by the National Aeronautics and Space Administration under Grant NGR-33-016-131

September 1972

106

ACKNOWLEDGEMENT

The author gratefully acknowledges the suggestions and guidance, as well as the review and presentation of this paper by Dr. Antonio Ferri.

The procurement of the computer program by the Advanced Technology Laboratories, Inc. and collaboration of its personnel especially Dr. S. Dash is appreciated.

This project was sponsored under the auspices of the National Aeronautics and Space Administration under the NASA Grant NGR-33-016-131.

ABSTRACT

The factors affecting a tangential fuel injector design for scramjet operation are reviewed and their effect on the efficiency of the supersonic combustion process is evaluated using both experimental data and theoretical predictions.

A description of the physical problem of supersonic combustion and method of analysis is followed by a presentation and evaluation of some standard and exotic types of fuel injectors. Engineering fuel injector design criteria and hydrogen ignition schemes are presented along with a cursory review of available experimental data.

A two-dimensional tangential fuel injector design is developed using analyses as a guide in evaluating the effects on the combustion process of various initial and boundary conditions including splitter plate thickness, injector wall temperature, pressure gradients, etc.

The fuel injector wall geometry is shaped so as to maintain approximately constant pressure at the flame as required by a cycle analysis. A "viscous characteristics" program which accounts for lateral as well as axial pressure variations due to the mixing and combustion process is used in determining the wall geometry.

A fuel injector performance evaluation scheme is then presented along with the fuel injector cooling considerations. An experiment to evaluate the various analytical tools and theoretical predictions made here is recommended.

TABLE OF CONTENTS

SECTION		PAGE
	ACKNOWLEDGEMENT	
	LIST OF FIGURES	
	ABSTRACT	
I.	INTRODUCTION	1
II.	DESCRIPTION OF THE PROBLEM	6
III.	PHYSICS OF SUPERSONIC COMBUSTION	8
IV.	FUEL INJECTOR DESIGN FOR PRACTICAL APPLICATION	13
	A. REVIEW OF INJECTORS TESTED	13
	B. WALL INJECTORS	16
	C. SOME EXOTIC TYPES OF FUEL INJECTORS	17
	D. FUEL INJECTORS DESIGN CRITERIA	18
V.	HYDROGEN IGNITION SCHEMES AND IGNITION DELAY IN HIGH SPEED FLOWS	20
VI.	DEVELOPMENT OF FUEL INJECTOR DESIGN	22
	A. DESIGN CONDITIONS	22
	B. INITIAL PROFILES USED	23
	C. INJECTOR WALL SHAPE GEOMETRY DEVELOPMENT	26
VII.	FUEL INJECTOR PERFORMANCE EVALUATION - FUEL INJECTOR DRAG	29
VIII.	FUEL INJECTOR COOLING	31
IX.	RESULTS, CONCLUSIONS AND RECOMMENDATIONS	34
	APPENDIX I - INFLUENCE OF VARIOUS INITIAL AND BOUNDARY CONDITIONS ON SUPERSONIC COMBUSTION	37
	REFERENCES	46
	TABLES	53
	FIGURES	57

LIST OF FIGURES

FIGURE		Page No.
1.	Typical two-dimensional fuel injectors	55
2.	Plug injector	56
3.	Three-dimensional fuel injectors a) GASL b) NASA	57
4.	Number of fuel injectors required for a given combustor length to height ratio	58
5.	Exotic injectors	59 - 60
6.	Ignition delay of premixed hydrogen and other hydrocarbons as a function of temperature, pressure and stoichiometric ratio	61 - 62
7.	Influence of hydrogen stagnation temperature on ignition delay	63
8.	Initial profiles used in parabolic mixing analysis	64
9.	Edge of mixing and flame shape from parabolic mixing analysis	65
10.	Flow profiles at various axial stations	66 - 74
11.	Centerline properties	75 - 76
12.	Similar velocity profile with mixing and combustion	77
13.	Pressure variation along the flame and wall of a straight wall injector from viscous characteristics analysis	78
14.	Geometry of a curved wall injector	79
15.	Pressure distributions for injector of Fig. 14	80
16.	Injector wall geometry that gives relatively constant pressure at the flame	81
17.	Pressure distibutions for injector shown in fig. 16	82
18.	Flow profiles in the flow field produced by the injector of Fig. 16	83 - 91
19.	Flow profiles with ideal and real combustion	92
20.	Standard fuel injectors cooling schemes	93

FIGURE		Page No.
21.	Leading edge cooling scheme of Ref. 46	94
22.	Final fuel injector design - flow field and geometry	95
23.	Injector wall cooling calculation with low speed cold hydrogen	96
24.	Influence of pressure gradients on mixing and combustion	97 - 9
25.	Influence of adjacent fuel injectors	99
26.	Qualitative influence of lateral pressure and thermal gradients	100
27.	Effect of splitter plate temperature on ignition delay length	101

I. INTRODUCTION

In a cycle analysis of a scramjet engine, the thermodynamic conditions (pressure and temperature) and fluid dynamic conditions (velocity, etc.) at which the heat release occurs are prescribed along with the combustion efficiency (percent of injected fuel that is burned). Furthermore, the cycle efficiency is fixed by the assumed process (i.e. constant pressure, constant area, constant Mach number, or some other pressure area relation such as the area fields of Crocco, etc.). When this assumption is introduced, the engine efficiency and thrust depend only on the initial and end states. The manner and conditions of the fuel injection is eliminated. In subsonic combustion the velocity is low. Then the possible local variation of pressure are negligible and one-dimensional flow analysis can be used to relate the geometry and the cycle. The case is different when supersonic combustion is considered.

In a supersonic combustion chamber large variations in pressure and temperature in both lateral and axial directions exist. Furthermore, the combustion process can produce shocks. The combustion taking place in a given region can produce an entropy rise in regions outside of the combustion region because of the propagation of shock waves. While interactions with adjacent fuel injectors can be used advantageously to increase the combustion performance. As a consequence the heat release does not occur at either the air or fuel static (burner entrance) conditions. Therefore a means of determining and controlling the conditions at which the heat is released is essential for an efficient scramjet engine combustor design. Since the supersonic combustion process is a highly coupled fluid dynamic and chemical phenomenon, an accurate analytical tool which accounts for the main features of the flow (e.g. wave formation due to

chemical reactions) must be used in designing the fuel injectors, fuel injector arrangement and combustor wall geometry.

This tool has been used in the present investigation to design and to evaluate quantitatively the fuel injector performance and to describe the flow field. However, since the combustion efficiency depends on the mixing efficiency (i.e. the availability of the correct fuel to air ratio at the flame surface) which in turn depends on a not too well known turbulent transport phenomenon (i.e. eddy viscosity), the theoretical predictions must be verified by experiment.

The primary purpose of this investigation is to test the validity of the analytical tool and to determine the flow conditions at which combustion takes place. A secondary purpose of the present investigation is to determine the influence of the various flow and geometric parameters on the supersonic combustion phenomena (i.e. ignition, efficiency of combustion and combustion length). First a qualitative evaluation of several fuel injection schemes is made. The ultimate purpose of this is to design a fuel injector suitable for a scramjet combustor design at a flight Mach number of 6.0 and to select fuel injection conditions more conducive to faster mixing and more efficient combustion. The supersonic combustion phenomenon, i.e. mixing rate, ignition and combustion length as well as the combustion efficiency, depends on many geometrical and flow parameters such as:

1. Fuel type, (i.e. hydrogen, hydrocarbon) and phase (liquid or gas)
2. External stream and jet conditions (temperature, velocity, pressure, Mach number, Etc.)
3. Fuel injector size and type (axisymmetric, two-dimensional, three-dimensional)

4. Injection angle relative to the air stream
5. Initial boundary layer thickness and state
6. Local and/or global three-dimensional jet (such as swirl) and stream nonuniformities
7. Splitter plate thickness and/or bluff base diameter
8. Injector wall geometry
9. Splitter plate wall temperature and material (e.g. platinum)
10. Injector wall temperature
11. Boundary layer growth on injector wall
12. Under and overexpansion of the jet
13. Flow impurities "artificial" or natural (H_2O vapor, OH radical, O_2 or any other combustion products or even metal (platinum) particles injected upstream)
14. End effects, fuel injector nose bluntness, etc.
15. Turbulence levels in the freestream, pressure gradients, etc.
16. Heat release due to change of phase,
17. Three-dimensional protuberance on the injector wall

The individual effects cannot be separated simply because of their mutual interaction role. A parametric study would reveal a desirable fuel injector design by evaluating several injector configurations.

Since the type of configurations are as numerous as the imagination will conceive, the approach here is to first evaluate some typical injectors and injection schemes and the influence that the various parameters have on the combustion. Thus organizing (classify) the imaginable types of fuel injectors and consequently set some design criteria.

The considerations presented here are for a tangential fuel injection scheme. An evaluation of the normal injection scheme versus tangential is given in Ref. 1. The combustion process is assumed to be diffusion controlled, that is the reaction rates are much faster than the mixing rates. The combustion is assumed to occur at supersonic speeds and the flow conditions are such that a turbulent transport phenomenon prevails. The fuel is gaseous hydrogen and the steady state chemical kinetics are the same as used in Refs. 2 and 3, (Table A1 of Ref. 2). An evaluation of different reaction rates constant on the combustion process is described in Ref. 1.

The description of the fluid dynamics and thermo-chemical interaction has been described in Ref. 4 and therefore will not be repeated here. An evaluation of the various turbulent mixing rates (see Table 2 of Ref. 5 and 10.1 of Ref. 6) by investigators, Ref. 5, 6, and 7 generally reveals the unsuitability of the various models to general flow conditions. Theoretical evaluations of various mixing models are subject to scrutiny as theoretical comparisons use numerical programs that inadvertently introduce an artificial numerical viscosity. This error arises when a numerical program has to decrease the number of mesh points in a profile to maintain the calculation time relatively short. In so doing, profiles with large gradients (as a temperature profile with a flame) are smoothed by the elimination of alternate mesh points. This acts like an inviscid viscosity. Numerical calculations of flows with chemical reactions should use finite difference equation using the total enthalpy rather than static temperature.

Experimental correlations of mixing decay rates etc. made with simple configuration are subject to speculation; first, the turbulent mixing phenomenon depends not only on the jet and stream conditions but also on geometry; second, the eddy viscosity, diffusion coefficient, turbulent Lewis

and Prandtl numbers etc. are inferred from flow profiles, (more specifically on their curvature at the centerline e.g. Ref. 8) which although the configuration is axisymmetric, the axis of the jet is seldom co-linear with the experimental apparatus and therefore produce three-dimensional effects; third, initial nonuniformities such as boundary layer growth splitter plate thickness etc. are usually disregarded in the correlations. Hence, disagreement in experimental data with theory is reported by various authors. The viscosity model adopted in the present investigation is described below. In general it has been assumed that the mixing laws are not altered by the combustion phenomenon. The validity of this assumption is explored here.

II. DESCRIPTION OF THE PROBLEM

The design of a supersonic combustion chamber requires the use of multiple mid-stream fuel injectors to keep the combustor length reasonably short. Furthermore, since the flow is supersonic, effects produced at one point are felt elsewhere along Mach waves. Hence the combustion process must be controlled locally where the heat is released rather than to simply shape the combustor walls. Also, the combustor and/or fuel injector designs must be suitable for different flight speeds. The combustor design must necessarily begin with the design of its constituent parts. Therefore we consider first the design of a mid-stream fuel injector. The design of a wall injector follows analogous considerations. However, the additional influences of thicker initial boundary layers and heat loss due to heat transfer to the combustor wall must also be included in the latter design. The complete combustor design requires treatment of interaction due to shock waves, adjacent combustion regions, etc. This is a complex task that is left for future considerations.

The function of a fuel injector is not only to introduce fuel into an air-stream at some selected conditions but rather the fuel injector should be designed as to control the condition at which the heat is released, so as to improve the combustion efficiency. Several experiments with mixing and combustion have been conducted in the past with the aim of establishing the chemical kinetics, mixing rates, influence of various flow and geometric parameters, etc. These experiments have given the designer useful information on the supersonic combustion processes. A partial compendium of the effects produced by influences of various initial and boundary conditions is included in Appendix I of this report for reference and to serve as a guide to the designer in selecting fuel injection conditions and some boundary conditions.

The effects of initial and boundary conditions on mixing and combustion are also presented in Appendix I.

In the absence of an accurate theory to describe the combustion process at supersonic speeds we would only be able to catalogue the above information. Furthermore, we would be at a loss when confronted with a new situation. The analytical tool developed in Ref. 9 will enable the designer to:

1. determine the flow field in different situations
2. evaluate a given fuel injector design
3. select injection conditions and injectors geometries more conducive to efficient combustion, and
4. give a better understanding of the combustion process.

In this theory normal pressure gradients as well as axial pressure gradients and shock waves are included. The governing ewuations are treated as quasi-hyperbolic. Therefore it is a more accurate theory and describes the combustion process better than a parabolic type analysis where the normal pressure gradients are neglected and the possibility of shock waves is not permitted. Unfortunately, the shortcoming of both theories is an accurate knowledge of constants and mixing rate laws and to a minor degree of reaction rate constants under different flow comditions. Because of these reasons a coupled analytical and experimental investigation conducted under carefully controlled conditions should give more details about the supersonic combustion process. Furthermore it will supply the designer with a reliable tool with which to perform his task.

In order to check experimentally these fuel injector design development concepts the first step has been taken here to design a fuel injector which gives constant pressure in the vicinity of the flame using the above theory. Such a design is of practical interest and is deduced from cycle analysis

considerations.

Since the supersonic combustion process is an interplay between the fluid dynamics, heat release and mixing mechanisms, an accurate determination of the last will result by application of the theory to the experimental data since the first two are described fairly accurately by the theory.

III. PHYSICS OF SUPERSONIC COMBUSTION FLAME

A physical description of the supersonic diffusion controlled process is presented here as it will assist in understanding the experiments that have been conducted and in explaining ignition characteristics. The supersonic combustion flame is an extremely complex aerodynamic process where the chemical and fluid dynamic effects strongly interact. Several different types of flames can be generated, depending on the controlling mechanism for the heat release. Only the diffusion controlled turbulent flame is described here as the conditions at the burner entrance are such that this is most likely to occur. A description of a heat conduction flame is given in Ref. 1. A diffusion controlled flame is more stable than a heat conduction flame where the chemical kinetics are slower than the diffusion and hence admit the possibility of a detonation.

Diffusion Controlled Flame

Consider two streams both supersonic: (1) an air stream surrounding (2) a jet of hydrogen. Assume that the two flows have parallel motion. The hydrogen mixes with the air and the diffusion process tends to produce a homogeneous mixture of hydrogen and air. Two limiting cases can be desired. If the static temperature of the mixture everywhere is sufficiently low, then the time required for chemical reaction between the oxygen and the hydrogen to take place is very long; thus mixing takes place first as the time for the fluid dynamic process to be completed is smaller than the time required for chemical reaction. The other limiting case is when the chemical reactions are extremely fast because of the high static temperature of the mixing. Then, as soon as hydrogen is mixed with air, H_2O is formed, and heat is released. When the chemical time (defined as the time to reach chemical equilibrium) is extremely

short, two regions can be defined in the flow divided by a line where the fuel air ratio is stoichiometric ($\varphi = 1$). The flow outside the line contains oxygen, nitrogen, and combustion products. The line corresponding to a $\varphi = 1$ mixture, is the line where heat is released. In this case the change in density is much larger than for the case of no reaction. Because of the heat release, the streamlines obtained in a calculation that assumes constant pressure and uses a mixing type of calculation to simplify the analysis are more curved than in the first case. Therefore, the assumptions of constant pressure or pressures depending mainly on x are not sufficiently accurate and the variation of pressure normal and along streamlines should be taken into account in the analysis. This effect tends to increase initially the static pressure and accelerates chemical reaction. In actual cases, at high temperature, the chemical time is very small; however, it is finite. Thus the heat release occurs in a small region distributed around the line $\varphi = 1$. Because of the high initial temperature and pressure, the isotherms for the two cases are very similar. The rate of chemical reaction decreases and the chemical time increases when either the local static pressure or local static temperature decreases. Then, for some flow conditions, the reaction time becomes of the same order as the mixing time. In this case substantial mixing takes place before heat is released, and thus the zone of reaction is widely extended. When the local static pressure is very low, the reaction rates are small, substantial mixing takes place before reaction occurs and the concentration of hydrogen at the point where reaction starts is below stoichiometric. Thus the local temperature is also low.

The heat release due to chemical reaction tends to decrease the density locally; therefore, it generates local pressure changes. The mixing type of

analysis used by several researchers neglects pressure gradients normal to streamlines, therefore it does not give a correct representation of these effects. In supersonic flames the pressure variations travel along Mach waves which propagate outside the flame region and tend to form shocks. The mixing near the injection region initially is very rapid because of the large gradients of concentration and of velocity and temperature normal to the streamline. There, if the reaction is fast, a large rate of heat release takes place locally, and therefore, strong compressions are generated that tend to form a shock. Downstream, the gradients gradually decrease; therefore, the rate of heat release gradually decreases and thus as the mixing continues the pressure gradually decreases. In a burner design, where combustion starts in a small region of the flow near the injectors, the flow properties outside the flame region change and the Mach number decreases. Therefore these waves diffuse the adjacent flow as in the inlet and can be used to increase the engine efficiency.

The effect of the presence of a pilot flame is of extreme importance even for the case of diffusion controlled flames when applied to supersonic combustion. This effect indicates that if the reaction process produces a heat release sufficient to generate a high temperature region, then combustion will continue even if the static temperature is initially low, and the flame once initiated continues and propagates. In practical applications a boundary layer is always present near the walls of the injector. At hypersonic flight velocity, the static temperature in the boundary layer is higher than free stream, especially if the wall temperatures is higher than free stream. When the two boundary layers from the fuel side and air side mix, they react very rapidly because of the local high temperature of the mixture in this region. Then combustion, once initiated, can continue. As a consequence, in practical

applications the possibility of having reaction depends more on the value of the stagnation temperature of the air and fuel and on the wall temperature, than on the static temperature of the two streams.

IV. FUEL INJECTOR DESIGNS FOR PRACTICAL APPLICATIONS

A. Review of Injectors Tested

Most of the experimental investigations on supersonic combustion Refs. 10 to 16 have been carried out using coaxial free jets because they lend themselves easily to analytical description and are easy to perform. Unfortunately this configuration cannot be used in practical scramjet engines. A summary of the injection conditions used in coaxial mixing and combustion of hydrogen in the above references is presented in Table 1. The geometric configuration of the fuel injectors tested is also depicted in the table. Other experiments on ducted mixing and combustion with simple coaxial configurations have been conducted. However, these are not reviewed here as the combustor wall has significant influence on the mixing and combustion process. Therefore, these data are not pertinent to fuel injector designs but more relevant to a combustor design. Moreover, many more experiments with mixing only of various gases in different environment have been performed to determine the mixing laws. These experiments are not reviewed here as they are too numerous. However, pertinent results are cited here when necessary.

Most of the experimental investigations have been conducted with either subsonic or nearly sonic velocities. At sonic conditions, the product $\rho_j u_j$ is a maximum for a given jet stagnation condition. Some simple typical two-dimensional tangential midstream fuel injectors without afterbody are shown in Fig. 1. These depict various external and internal geometries possible. The external geometry can range from a simple wedge (A) to a wedge-slab (B,C,D) to a wedge-slab-boat-tail (E) combination. If the external flow is supersonic, it is evident that for the same injection flow conditions, the last configuration (E) presents the greatest blockage and drag. Also, the trailing lip shock would

be strongest for this configuration. Furhtermore the external stream static conditions would be reduced to conditions less conducive to auto ignition. Since both a static pressure and temperature drop is experienced by the expansion of the external flow around the boatail of the fuel injector. The possibility of flow separation is greatest in this case. The rotational external flow produced by the curvature of the trailing shock would induce a strong streamwise pressure gradient on the jet stream which are not conducive to efficient combustion. The propensity of the production of these effects decreases drastically on going from configuration E to B,C,D to A. An ogival type fuel injector would produce similar effects as configuration E; while a cusped injector would be like configuration A.

The internal geometry depends on the injection speed as to whether it is subsonic, sonic, or supersonic. The three injection modes are depicted in configuration D,B,C respectively. For the supersonic mode, the nozzle shape may be contoured or conical (wedge like). In the wedge-like configuration, the fuel is transported into the mixing zone not only by a diffusional velocity but also by a v-component of the jet velocity proportional to $u_j \sin \delta$, where δ is the nozzle wedge angle. Unfortunately, compression waves generated at the mixing and combustion zone (plume) negate this effect. These considerations show there is no "control" on the combustion beyond the region of influence of the initial data line with these simple types of fuel injectors. That is, everything is defined by the initial conditions and the line of symmetry.

The fuel injector shown in Fig. 2 overcomes this shortcoming. As shown in Fig. 2 this type of fuel injector has a central body whose geometry can play a significant role on the combustion process as will be evident below. Although

this type of fuel injector has a greater blockage (for the same fuel injection conditions) in proportion to the size of the central body, its drag is less than that without the central body due to the induced pressure of the combustion on the central body. However, the central body affords a more direct control on the combustion process than the combustor walls as the waves would have to travel through several combustion regions before reachingthe intended point of influence.

A three-dimensional fuel injector design was used in Ref. 17. The fuel injector is shown in Fig. 3a. Several of these injectors were mounted on the combustor walls. As shown in Fig. 3a, this injector consists of an axisymmetric injector mounted on a swept-strut. The injection speed could be subsonic or sonic with this injector. The injected mass flow could be increased only by increasing the fuel injection pressure resulting in underexpanded jet conditions. The effects of the interaction of the strut wake on the jet are not clear with this type of injector. The interaction of the strut shock pattern with the boundary layer on the various surfaces which can lead to inlet unstart and the formation of corners lead to complex local three-dimensional flow patterns with multiple interacting and reflecting shocks. This coupled with the need to have a great number of then ~ 0 (100) makes them unattractive for use in a practical scramjet even though the fuel may be distributed more uniformly than some other type of fuel injection scheme, and the combustor length shortened significantly.

The number of axisymmetric fuel injectors vs the number of two-dimensional fuel injectors required to achieve complete mixing of hydrogen and air in a combustor of specified length, shown as a function of the combustor length to height ratio in Fig. 9 of Ref. 18, is shown here in Fig. 4 for reference. This figure shows that for short combustors $H/L \sim 0$ (2 or 3) approximately 10 two-dimensional fuel injectors are required while 100 axisymmetric injectors would

be needed. While for long combustors $H/L \sim O(10)$ only a few injectors either axisymmetric or two-dimensional would ne needed.

In Ref. 19 (Fig. 3b) a swept two-dimensional midstream strut with injection holes normal to the flow was used. This injection scheme avoids some of the shortcomings of normal injection described by Ferri (Ref. 1). Namely, the flow separation produced by the normal injection is not as extensive as wall mounted normal injection holes as the boundary layer is very thin in this case. The inviscid shock patterns, however, still exist. Also a wake and trailing shock is formed by the strut if no injection is used in this region. In Ref. 20, the jet is assumed to have an initial swirl in order to enhance the mixing. It is found that the maximum tangential (swirl) velocity decays slowly and depends inversely as the square root of the initial value of the swirl velocity. The experimental data of Ref.21 indicates that swirl does not enhance mixing. Whereas the results of both theory and experiment of Ref.22 show that the introduction of swirl into an open jet diffusion flame leads to a faster decay of the velocity, and to an increase of flame width and mass entrainment in the downstream direction than non swirling flame. The induction period (ignition delay) is shortened significantly with increasing amounts of swirl. The reduction of the velocity gradients due to swirl lead to a shortening of the potential

B. Wall Injectors

"Conservative" scramjet combustor designers of two-dimensional and axi-symmetric engines (Ref.23-25) have used wall injection in the form of normal injection through orifices or wall slots just downstream of the inlet throat. Since in a two-dimensional or axi-symmetric engine the throat height is small and therefore the fuel need not penetrate too far into the stream. The con-

sequences of the normal injection scheme on the combustion are discussed in Ref. 1. The wall slot injection scheme is analogous to the midstream injector with afterbody except for the presence of a thicker boundary layer on the splitter plate which can reduce the ignition delay length (Ref. 1).

Some mixing experiments of hydrogen injected from a wall slot into a supersonic stream are presented in Refs. 26 to 30. A sharp drop in hydrogen mass fraction at the wall is reported in Reference 30, at the end of the potential core region. The edge of mixing grows approximately linearly downstream of the initial region and its growth rate and decay rates of species mass fraction, and velocity maxima increase with decreasing mass flux ratio $\rho_j u_j / \rho_e u_e$. The data is not sufficient to determine the laws although the species profiles are similar downstream of the initial region.

C. Some Exotic Types of Fuel Injectors

Experimental data shows that the mixing from axisymmetric injectors is more rapid than that produced by a two-dimensional injector as the wetted area of fuel exposed to the air flow is greater in the former than the latter. Furthermore the wetted area growth is also larger; however, the number of axisymmetric fuel injectors required to pass a certain amount of mass flow is considerably larger than a two-dimensional injector. Also the fuel closer to the perimeter diffuses at a faster rate than that closer to the center. Therefore, it would appear that an intermediate shape which enhances the mixing and passes the same amount of fuel flow should exist. The injector cross-section normal to the fuel flow which gives the same maximum mixing rate to all fuel particles passing through the injector can be developed using three-dimensional mixing equations and variational calculus. Intuitively this injector cross section shape would be lobed somewhat similar to the cross-section of the red

blood cells as shown in Fig. 5. Downstream, the initial three-dimensional pattern would decay becoming axisymmetric as the lateral gradients diminish (Ref. 31).

The initial external flow pattern (shocks, expansions, slip-stream, etc.) produced by this type of fuel injector would be quite complex and the installation of this injector in a standard combustor would be problematical. However, the concept can be used in two-dimensional fuel injectors by "corrugating" the cross-section at a radial support strut point for instance as shown in Fig. 5a.

Additional exotic types of axisymmetric and planar swept fuel injectors are depicted in Figs. 5a through 5 . Their relative merits can be conjectured at this point as no theoretical or experimental means of evaluating the .

D. Fuel Injector Design Criteria

In view of the great number of possibilities of injecting the fuel, several engineering design and fluid dynamic criteria are enumerated here to assist in evaluating and designing a fuel injector. Some of these criteria are:

1. Obtain short combustor lengths by using multiple mid-stream injectors.

2. Obtain the required local pressure at the combustion region.

3. Minimize under and over expansion losses over the range of combustor pressure.

4. Operate over a range of flight Mach numbers and internal flow field conditions.

5. Enhance mixing and insure high combustion efficiency.

6. Establish a diffusion flame very near to the injector lip.

7. Achieve a favorable fuel air distribution without shock losses or flow instability that can cause inlet unstart in the outside flow.

8. Establish ignition and stabilize the flames.

These qualitative injector design criteria are supplemented below by quantitative fuel injector performance evaluation criteria.

V. HYDROGEN IGNITION SCHEMES AND IGNITION DELAY IN HIGH SPEED FLOWS - EXPERIMENTAL AND THEORETICAL CONSIDERATIONS

The combustion properties (flame temperature, burning velocity, quenching distance, flammability limits, detonation properties, spontaneous ignition, etc.) of hydrogen in air at low speed has been documented very well in Ref. 32. However, in high speed air flows the auto-ignition limits, flame initiation and stabilization are not documented as well although a substantial amount of theoretical and experimental data is presently available.

The experimental evidence of hydrogen ignition in high speed air flows is presented in Refs. 33 to 41. The various methods used for igniting hydrogen in a high speed air flow even at low air temperature are:

1. Preheating of the injected hydrogen to 1900°R (Ref. 33) estanlishes auto-ignition independent of air temperature.

2. Piloting-using hot combustion products to heat up the fuel and air as they mix (Ref. 15).

3. Platinum acts as catalyst in the induction period to form OH radicals. (Ref. 33)

4. Oxygen injection - (Ref. 34)

5. Ultra violet irradiation has been used to sensitize the injected hydrogen and form OH radicals (Ref. 35)

6. Bluff bases and thick splitter plates present stagnation flow regions with high stagnation temperature and long residence times (Ref. 36, 37)

7. Shock induced ignition is obtained through the increased static temperature and pressure of the mixture and/or air streams (Ref. 38, 39)

8. Upstream Injection - (Ref.40)-

9. Resonance Ignitor - (Ref.41) - resonance of a jet into a dead-end tube produces unsteady shock oscillations which lead to temperature rises well above the stagnation temperature of the jet.

More recently Ferri has suggested that the injection of small amounts of hydrogen into the boundary layer on the injector wall to act both as a coolant and to form OH radicals. In this case, the static temperature in the boundary layer is higher than that in the free stream and the residence time is increased by the low velocities in the boundary layer, and therefore are conducive to combustion initiation. Also the splitter plate can be made of platinum to further assist in the ignition. This last scheme has been adopted in the fuel injector design presented below. See also Ref. 11.

The criteria for selecting a hydrogen ignition scheme are its reliability, efficiency and simplicity. The ignition delay time (induction period) for premixed hydrogen fuel and oxydizer (O_2 or Air) using the various technique enumerated above has been well documented as a function of temperature, pressure, stoichiometric ratio, etc. Some of the correlations taken from various references are shown in Fig. 6. A comparison with other hydrocarbons is also shown. The influence of other factors such as those mentioned in the introduction however are not known as clearly. The induction period for jet initial temperature, much different from the air temperature, must be determined using the various mixing theories.

VI. DEVELOPMENT OF FUEL INJECTOR DESIGN

A. Design Conditions

The present fuel injector design was developed for a scramjet operation at a free stream Mach number of 6.0. The Mach number after combustion is supersonic at this condition. This condition simplifies the analysis of the combustion region. The nominal burner entrance conditions corresponding to a flight Mach number of 6.0 and an altitude of 80 k ft P_∞ = 60 psf. were taken to be as follows:

Mach number (after fuel injector shock) = 2.5	u = 5137 ft/sec
Air static temperature = 1000° K	T_{o_e} = 3036°R
Air static pressure = 1 atm	P_{o_e} = 20 atm

These conditions assume that the pressure recovery of the inlet (stagnation pressure) is 0.434. Therefore the static pressure rise is 40.

The fuel injector design developed here is for use in a three-dimensional integrated fixed geometry scramjet engine. This is the high speed $6.0 \leq M \leq 10$ propulsion system of a large vehicle with take-off weight on the order of one million pounds. As a consequence the frontal area of the air induction system of the scramjet engine is approximately 1200 ft^2 and its length is 200 ft. The captured streamtube is compressed to a swept annular gap, at the throat of the inlet, approximately 2 ft high on a central body of $\sim$ 30 ft average radius. A more detailed description of the inlet design is given in Ref. 42.

To maintain the combustor length reasonably short relative to the inlet size, multiple midstream fuel injectors are required. Assuming the fuel is injected at the local burner entrance pressure, the ratio of fuel injector area to burner entrance area is given by (mass flow requirements)

$$\frac{n A_j}{A_b} = \frac{0.11 \quad \phi \quad M_b}{\sqrt{T_{o_b}/T_{o_j}} \quad M_j} \sqrt{(2 + (\ - 1) M_b^2) \Big/ (2 + (\ - 1) M_j^2)}$$

where n is the number of fuel injectrrs while subsript j denotes jet conditions and subscript b denotes burner entrance conditions. Subscript o denotes stagnation conditions and ϕ is the stoichiometric fuel air ratio.

Therefore to maintain the number of injectors at a minimum, it would be advantageous to have high jet Mach number M_j and low jet stagnation temperatures, T_{o_j}, and low air stream Mach number and stagnation temperatures. The air stream and fuel injection conditions stated above were selected by a compromise of these ideas, a cycle analysis, and ignition condition requirements.

The fuel injector slot height (two-dimensional) was taken as 0.45 inches as this would require n = 6 injectors for the above condition. These conditions were selected as a good compromise of several different requirements. The fuel injection conditions were taken as follows:

Mach number 2.0	Velocity $\sim$ 9870 ft/sec
Static temperature - 440°K	Stagnation Temperature $\sim$ 1500°R
Static pressure = 1 atm	Stagnation pressure $\sim$ 8 atm

B. Justification of Initial Conditions Selected

Since the ignition delay length, flame length, etc. are strongly affected by the fuel injection conditions, an initial investigation was undertaken to determine the dependence of these on the hydrogen injection conditions and air external conditions. Several calculations were made using the parabolic mixing program (Refs. 43 and 44).

In these calculations, the Lewis number was assumed equal to unity and the pressure field was assumed uniform throughout. The eddy viscosity was assumed

to be initially given by $\mu_t = 0.5\times10^{-3}\,\rho_e\,|u_e - u_\ell| + 1.0\times10^{-4}$ up to when $U_{\mathbb{C}} = .99\,U_{jet}$ followed by a model suggested in Ref. 8 : $\mu_t = K\,r_{\frac{1}{2}}|\rho_o u_o|$ where $r_{\frac{1}{2}}$ is the height to where $\rho u = \frac{1}{2}(\rho_e u_e + \rho_o u_o)$. and K= 0.045.

If the presence of the boundary layer is neglected, then the flow initially has a step profile; however, this simplification gives an incorrect representation of the actual phenomenon. Using step profiles, the hydrogen stagnation temperature was varied to determine the ignition delay length. The results shown in Fig. 7 demonstrate that a significant ($\sim$ 0(1 ft)) ignition delay exists in spite of the high stagnation temperature of the hydrogen. This is due to the fact that the mixing cools the flow before ignition takes place. The actual situation is different when the presence of the boundary layer is considered. The boundary layer produced by the splitter plate was introduced in the analysis. The boundary layer reduces the mixture speed and increases the mixture static temperature in the initial region if the temperature of the wall is sufficiently high. In the calculations a 1/7th power law velocity profile was assumed on the air side, and the temperature profile was assumed given by a Crocco integral relation. The splitter plate temperature was assumed equal to the hydrogen stagnation temperature. A heat transfer analysis shows this to be nearly the case due to the very high thermal conductivity of the hydrogen. Similar conditions were assumed for the hydrogen boundary layer. The temperature profile exhibited a maximum greater than the freestream static temperature. The boundary layer on the hydrogen side was assumed thin due to the short hydrogen nozzle length. These assumed initial profiles are shown in Fig. 8 . The analysis showed that the boundary later acts as a pilot and decreases the ignition delay length to 0.43 ft., the bulge in the temperature profile and the velocity defect decreased very rapidly in the initial region.

In order to acellerate ignition and further decrease the ignition delay length, some hydrogen was injected into the boundary layer on the splitter plate sufficiently far upstream (approximately $\sim$ .5 ft) in order to produce a slight temperature rise in the boundary layer (T_{max} = 1400°K) and increase locally the radicals O, H, OH, concentrations. This change reduced the ignition delay to approximately 0.194 ft. Actually the splitter plate finishes with finite thickness that produces a wake. This effect was introduced artificially in the analysis by introducing in the velocity profile a small region where the velocity is equal to 100 ft/sec. This resulted in an ignition delay length of 0.0055 ft.

Similar results have been obtained by introducing small amounts of hydrogen on the leading edge and along the splitter plate surface at very low velocity for cooling purposes. The scheme is shown in Fig. 22. The flow field, edge of mixing and flame, obtained with this final configuration of initial conditions are shown in Fig. 9. The flame length is observed to be approximately 10 ft. long. This gives a combustor with a height to length ratio of 5. The flow profiles are shown in Fig. 10 for the various axial stations while the centerline velocity decay and temperature rise and hydrogen concentration and Mach number are shown in Fig. 11. The centerline hydrogen mass fraction, the parameter $(u_{C_L}-u_e)/(u_j-u_e)$, the mixing width b, the entrainment ψ_e/ψ_j, and turbulent viscosity approached a power law behavior, i.e., $\sim x^n$, $n \approx 1$. Flow similarity was observed for $(u-u_{\mathfrak{L}})/(u_e-u_{\mathfrak{L}})$ as a function of ψ/ψ_e, where ψ_e is the stream function at the edge of mixing. The similar profile is shown in Fig. 12. The temperature profiles are similar downstream of where the flame reaches the axis. Lean combustion occ rs in the region $5. < x < 9.$ ft. This is evident by the increase in the oxygen mass fraction inside the flame. For $x < .5$ ft., the small amount of O_2 inside the flame present in the initial profile is consumed

If the expression for the eddy viscosity is changed, the above results can be reinterpreted by a suitable shift in the axial location according to x' where

$x' = \int \mu(x)/\mu'(x)\, dx$. This is only possible in view of the assumptions of two-dimensionality, constant pressure, and Lewis and Prandtl numbers of unity. These simplified analyses have shown the importance of including the initial boundary layer to determine ignition delay in actual flow conditions. On this basis the following configuration has been designed.

C. Fuel Injector Wall Shape Design

Compression waves are generated by the mixing and combustion process of hydrogen in a supersonic air stream (Ref. 4). The strength ($\Delta P/P_\infty$) of the pressure waves depends on the rapidity of the combustion process which in turn depends mainly on the hydrogen and/or air static temperature and mixing rate. To assess the strength of these waves and their effect on the combustion process, a "viscous" characteristic program (Ref. 45) was used to calculate the flow field. The initial flow profiles at the exit of the injector were taken to be the same as those used in the parabolic mixing program. However, the centerline of the mixing calculation was replaced by a solid wall whose shape was altered to produce various pressure distributions on the flame.

At first the wall was assumed straight. The pressure distribution shown in Fig. 13 , shows a pressure rise along the wall of approximately 40% while at the center of the flame, defined as the region where ($T = T_{max}$), the initial pressure rise is approximately half or 24%. This shows that pressure waves of strength $\Delta p/p_\infty \cong .24$ propagate both in the air stream and jet stream away from the mixing and combustion zone which initiates near the splitter plate. The waves which propagate into the jet stream are reflected at the wall and tend to form shocks at some distance from the plate. In addition, the waves on passing through the mixing and combustion zone, are of sufficient strength to generate subsonic flow locally in the region of the velocity defect produced by the

splitter plate.

In order to avoid region having too low velocity, and at the same time eliminate formation of shocks in the outside flow the pressure waves must be cancelled. Therefore, a wall geometry has been developed from the parabolic mixing program by shifting the centerline in such a way as to produce no deflection in the streamlines in the external air stream that approaches the flame. This wall injector shape is shown in Fig. 14 . The pressure distribution along the wall and the flame are shown in Fig. 15 for this configuration. Again, with this configuration a pressure peak is evident at the flame. However, the waves are partly cancelled at the wall producing a smaller pressure rise there and on passing through the combustion zone a secondary pressure peak is found. Further downstream a pressure decay is experienced both at the flame and at the wall as the heat released is not sufficient to overcome the expansion waves that emanate from the wall.

The combustion efficiency is impaired if the pressure is allowed to decrease. In addition the temperature also varies in a like manner degrading the combustion process. Therefore, an injector wall geometry which maintains the pressure essentially constant in the region of heat release (i.e. flame) was developed by a step by step numerical calculation.

First, to decrease the strength of the initial waves produced by the combustion, expansion waves were introduced in the initial profile. The expansion waves start on the lower wall of the fuel injector inside of the jet nozzle, at a point sufficiently far upstream of the lip of the splitter plate so as to affect the initial region of the combustion (see Fig. 16). A 4° expansion was too strong as it caused a pressure peak followed by a pressure decay at the flame front. A 2° expansion decreased the initial pressure rise at the flame to

approximately 10% and was implied as satisfactory. Subsequently downstream the combustion process sustained this selected pressure level, the waves generated by the flame were cancelled at the wall by turning it 4.8°. This required the pressure generated by the flame tends to decrease, therefore it is required that the necessary turning be of the order of 1.8°. Further downstream however, the wall generates compressions to sustain the pressure at the flame. The wall then remains straight with an inclination of -3°. The resulting wall geometry and pressure distributions are shown in Figs. 16 and 17 respectively. In this analysis, the flow upstream of the injector is assumed uniform. However in a practical case waves are present in the flow. Some flow profiles with this injector are shown in Figs. 18a through 18i.

The initial profiles were taken two splitter plate thicknesses downstream of the injection station to have a completely supersonic profile. The subsonic region due to the wake of the splitter plate was neglected. The static pressure and temperature drop due to the 2° expansion are represented in the figure 18a along with the boundary layer on the external surface. The flow direction is also shown. The temperature maximum is greater when the lateral pressure gradients are considered. This is due to the induced pressure due to the combustion. In the initial region (x .2 ft.) the static pressure profiles show a pressure pelse moving away from the flame. While the lateral extent of the influence of the pressure waves due to combustion is greater than that due to mixing and combustion.

The injector wall geometry must be shaped to account for interactions with waves from the main stream flow and/or combustor wall. The analysis could have included initial nonuniformities or even discontinuities in both the jet and external streams since the computer program is equipped to do so. However the nature of the non-uniformities were not known at this point and hence were not considered.

VIII. FUEL INJECTORS PERFORMANCE DESIGN EVALUATION

A measure of the efficiency of the combustion can be obtained by evaluating the amount of unburned pure hydrogen at any station downstream of where the flame reaches the centerline. Unity less the ratio of the mass of unburned hydrogen to the injected hydrogen flow rate times a ratio which measures the amount of heat released in the stream to the theoretical maximum heat release, can be taken as the combustion efficiency. This ratio is proportional to the ratio of H_2O mass flow rate at end of combustion to the maximum H_2O flow rate possible with the injected hydrogen flow rate. A third ratio would be necessary to measure if the heat released is used in forming radicals or in increasing the thermal energy of the stream. This last is proportional to 1.0 minus the total mass fraction of all radicals present. Therefore, the combustion efficiency may be expressed as

$$\eta_{comb} = \left(\frac{\int_o^\infty Y_{H_2} \rho u \, dy}{\dot{m}_j} \right) \left(\frac{\int_o^\infty Y_{H_2O} \rho u \, dy}{0.24 \int_o^\infty \rho u \, dy} \right) \left(1 - \frac{\int_o^\infty (Y_O + Y_{OH} + Y_N + \ldots) \rho u \, dy}{\int_o^\infty \rho u \, dy} \right)$$

The species profiles for complete combustion (100% efficiency) are shown in Fig. 19 for comparison. In the ideal case (100% efficiency) the fuel and oxidizer reach the flame in stoichiometric proportion. Therefore no fuel is on the outside of the flame while no oxidizer is present on the inside of the flame. In the real case, however, oxidizer which had diffused into the fuel unreacted in the initial region when the flame burned less is dissipated downstream. While the fuel which is not burned at the flame simply diffuses and is lost. The maximum mass fraction of combustion products are reduced by inefficient combustion.

The fuel injector drag is evaluated from a pressure and momentum integral su a control surface surrounding the fuel injector. Drag or thrust of a standard and a plug injector with and without fuel injection respectively are evaluated as follows.

The fuel injector drag of a standard tanjential fuel injector (Fig. 1) is due to its forebody and its base, i.e.

$$D/A_j = (p_w - p'_{\infty}) - (p_{base} - p'_{\infty}) + c_f A_w/A_j$$

Where A_j is the jet area (the splitter plate thickness is neglected) and A_w is the wetted surface of the fuel injector. An average pressure is used in the above formula although these can be replaced by pressure integrals. The prime denotes free stream conditions just upstream of the fuel injector tip.

Depending on the monentum of the jet, the drag can become thrust. In this case the fuel injector axial force is

$$F_{ax}/A_j = (p_w - p'_{\infty}) - {}_j p_j M_j^2 - (p_j - p'_{\infty}) + c_f A_w/A_j$$

In which the second term is due to the momentum of the jet.

The drag of a plug type fuel injector (Fig. 2) is

$$D/A_f = (p_w - p'_{\infty}) - (p_{base} - p'_{\infty})A_j/A_f - (p_{plug} - p'_{\infty})(1 - A_j/A_f) + c_f A_w/A_f$$

Where A_f is the frontal area of the injector and the third term represents the pressure force acting on the plug. With injection the axial force is

$$-F_{ax}/A_f = (p_w - p'_{\infty}) - {}_j p_j M_j^2 A_j/A_f - (p_j - p'_{\infty})A_j/A_f - (p_{plug} - p'_{\infty})(1 - A_j/A_f) + c_f A_w/A_f$$

With typical supersonic injection conditions, the thrust produced by the jet is several times larger than the forebody drag. This gain is lost if normal injection is used. The estimated drag and thrust of the present fuel injector design is presented is presented in section X.

Other performance parameters (such as mixing rate, combustion and induction length, etc.) are readily obtained from the flow field analysis.

IX. FUEL INJECTOR COOLING SCHEMES

Due to the inlet diffusion the fuel injector is exposed to a more harsh environment than the aircraft's surfaces as the pressure and temperature are much higher at the combustor entrance than in the free stream. The fuel injector must retain its structural integrity at high temperatures and under strong aerodynamic pressure loads and intensive heating and cooling rates (thermal fatigue). High temperature and/or refractory materials (Molybdenum, etc.) may be used in certain regions of the fuel injector and cooling techniques in other regions. Further heating is received by the radiation from the combustion zone.

The three types of injector cooling schemes are shown in Fig. 20 taken from Ref. [18]. The transpiration cooling scheme with hydrogen appears to be the best for maintaining the injector wall temperature below 2000°R. Whereas film cooling is least effective. A leading edge cooling scheme was suggested in Ref. 46 by Ferri. This cooling scheme consists of an upstream slot injection as shown in Fig. 21.

The walls of the injector can be thermally protected by a film cooling technique by using cold hydrogen. The cooling length is determined from the correlation given by Zakkay in Ref. 47 (H_2 injection, $T_w/T_{o_e} = .6$, $M_j = 1.0$, $M_e = 6.0$, $u_j/u_e = 1.5$)

$$\frac{\ell_{cooling}}{S} = 1100\,\lambda^{0.8}$$

where $\lambda = \rho_j u_j/\rho_e u_e$, and S is the slot height and ℓ is the cooling length. If we select $M_j = 1.0$ and $T_{o_j} = 530°R$, then a cooling length of 364 slot heights is obtained. Or to cool a 1 ft long surface a slot height of .033 inches would be

needed. This implies a coolant hydrogen flow rate to injected hydrogen flow rate ratio of approximately 7%. To supplement the experimental data of Zakkay on cooling which was taken at $M_e = 6.0$, a calculation was made using a parabolic mixing analysis to simulate a wall slot of cold H_2 injected tangentially into a Mach 2.5 stream and $1000^{\circ}K$ static temperature ($T_o \approx 3100^{\circ}R$). The coefficient of viscosity was assumed to be K = 0.02 and the viscosity law was taken to be that of the potential core model as the actual physical configuration would be a series of smaller slots located sequentially at the end of each of the potential cores. The boundary layer was not considered in this analysis. The air was assumed vitiated in the calculation and the slot height .01 ft was assumed. This coolant hydrogen mass flow rate corresponds to 20% of the injected hydrogen flow rate. The results of this calculation are shown in Fig. 23.

A lean burning flame appears at about 0.5' (50 slot heights) from the slot. However, in spite of the flame the centerline (or wall temperature) reaches a value of 1000°K at about 1 ft (100 slot heights) from the injection point. A very slow speed hydrogen jet (u_j = 10 ft/sec) was also investigated. The centerline temperature reached $1000^{\circ}K$ in .23 ft in this case. The reason being that the coolant mass flow in this case is 0.1% of the injected mass flow. Therefore if the same mass flow as in the first case were to be injected, the surface would reach $1000^{\circ}R$ after 41 ft by using a very low speed jet. Alternatively if 10 coolant slots are used with very low H_2 injection speed, the coolant mass flow would be about 1% of the injected hydrogen and the wall temperature would be kept much below $1000^{\circ}K$. Unfortunately in this case the total injection slot is 1.2". To overcome this, the coolant flow should be passed through 10 quasi-tangential slots (about 1 inch apart) of .1 inches high as shown in Fig. 22 . The base

flow like region typical of low speed slot injection and ensuing expansion and shock system is avoided and an effective cooling system is obtained,

X. RESULTS AND CONCLUSIONS

An experimental and theoretical review of most geometrical and fluid-dynamic factors which influence the supersonic combustion of hydrogen has shown a qualitative and quantitative dependence of supersonic combustion parameters (ignition delay, mixing rate, centerline decay, jet spreading, etc.) on these factors. Although both experiment and theory are wanting an indication of the choice of fuel injector condition and injector geometric parameters more conducive to an efficient diffusion controlled combustion flame is afforded to the fuel injector designer. The philiosophy adopted in the present design is to control, through the selection of the parameters, what takes place naturally in order to obtain what is desired to occurr.

The fuel injector design shown in Fig. 22 incorporates most of the essential qualities of an efficient fuel injector developed in this report. The concept is not restricted to a symmetrical configuration. Symmetry is used here for convenience. This fuel injector uses a central body to increase the low mixing rate normally experienced by a two-dimensional mid-stream injector relative to the higher mixing rate of an axisymmetric injector, to that typical of a wall slot. Secondly, the central body geometry (Fig. 16) was designed so as to maintain relatively constant pressure at the flame so as to improve the combustion efficiency and to prevent diffusive separation due to lateral thermal and pressure gradients. The initial wedge angle of 5° was selected somewhat arbitrarily. The hydrogen injection conditions (stagnation temperature, Mach number, etc.) are selected following a theoretical evaluation of several initial conditions on the ignition delay length. The tip cooling scheme is as shown in Fig. 21 while porous cooling is used on the faces and central body surfaces of the injector. The ignition scheme utilizes normal injection of hot hydrogen

at a point just downstream of an expansion fan to insure high penetration into the air stream and the formation of OH radicals prior to the main injection station. The injection Mach number is selected so as to retain a supersonic flow at the flame. The splitter plate thickness and boundary layer growth on the injector splitter plate provides a velocity defect and temperature excess to ensure the flame is stabilized.

Some of the flow field characteristics of this injector are shown in the upper half of Fig. 22. These were determined from the patching of various analyses presented in the text of this report. Some flow profiles have been presented in the main text of this report (Figs. 18a to 18h).

The injector drag determined by a pressure integral and momentum integral plus an estimate of the skin friction drag show a net thrust coefficient $C_T = 0.447$ based on the fuel injector frontak area and the free stream conditions upstream of the fuel injector tip. Without fuel injection, the drag coefficient of the present fuel injector is 0.15.. This can be minimized by injecting a coolant fluid when the scramjet is not functioning. The injector net thrust coefficient, in terms of free stream flight conditions and engine frontal area ($A_c = 1200$ ft^2), is $C_t = 0.003$. Therefore for stoichiometric fuel flow, a tangential injector increases the engine thrust ($C_T = 0.45$ at $M_{oo} = 6.$) by approximately 1%. The losses with normal injection are considerably more than this (for the same type of engine etc.) as the normal shock losses due to normal injection are not included in the above figure.

The combustion efficiency of the present fuel injector design, as evaluated from the various integrals desgribed in the main text, was approximately 0.94%, for the initial region up to x=0.43 ft. No discernable difference was noted in the fuel injector desribed in fig. 14 due to the numericalt accuracy of the results and the numerical integration.

An experimental investigation of the present furl injectoe design and comparison with a standard fuel injector design is recommended with a slightly reduced scale version of the design shown on fig. 22 to compliment and verify the present analysis.

APPENDIX I

INFLUENCE OF VARIOUS INITIAL AND BOUNDARY CONDITIONS ON SUPERSONIC COMBUSTION

As stated in the introduction, the mixing and combustion phenomenon is affected by many flow and geometric parameters. A qualitative influence of these parameters on the mixing, i.e. jet spreading, potential core lengths, centerline decay, etc. is made here for hydrogen combustion with tangential injection only.

A. External Stream and Jet Conditions

When the jet is fully expanded, i.e. matched pressures ($p_j = p_e$), the stream and jet parameters that influence the mixing are the ratio of jet to stream velocity, u_j/u_e, static temperature T_j/T_e, individual Mach numbers M_j, M_e, mass flux ratio $\lambda = \rho_j u_j/\rho_e u_e$, momentum flux $\rho_j u_j^2/\rho_e u_e^2$, molecular weights ratio W_j/W_e, and specific heat ratios γ_j, γ_e. Depending on the values of each of these parameters the mixing zone may either enlarge or neck down as in a wake. The effects of these parameters on the mixing is discussed in various references (Refs. 8, 12, 18, 48, 49). The basic conclusions of the mixing analyses and experiments are that the centerline properties (species, velocity, and temperature defect) decays inversely with the square root of distance along the axis of the jet for a two-dimensional injector and inversely with the distance for axi-symmetric jets (except for the investigations by Ferri and his co-workers who found that for H_2 the mixing rate in the near field $x/r_j \leq 10$ is much faster and produces a decay rate inversely with the square of the distance.) While for a wall slot the power is 0.8. Furthermore the power is independent of the slot design, the environment (injection and stream conditions) or molecular weight. Whereas the potential core length and factors of proportionality do vary with these and other parameters. Their dependence is not known very well. These studies imply

that the use of gaseous fuel of low molecular weight and high velocity relative to the local air stream is conducive to high mixing rates. Also it is important to expand the fuel to a pressure close to or below the local combustion chamber pressure.

The cases of equal velocity, temperature and/or mass flux are discussed further in Ref. 27 as the mixing laws which depend on differences of these parameters are not suited to these cases. The potential core length for the hydrogen concentration is correlated by Zakkay in Ref. 50 who gives the following formula to evaluate the species potential core length, x_o, in terms of the jet and stream conditions

$$\frac{x_o}{r_j} = 2. + 6.0 \left(\frac{\rho_j}{\rho_e}\right)^{\frac{1}{4}} M_j^{\,2} \left[1 + M_j^{\,2} \exp\left\{-\left(\frac{M_e}{M_j} - 1\right)^2/2\right\}\right]^{-2}$$

The velocity and temperature potential core lengths are not correlated as well as they are assumed to be of the same order as the species potential core length when the Lewis and Prandtl number are unity.

Additional influences of initial jet and free stream conditions on mixing and combustion can be determined from the theory of Libby Ref. 51. For example, the centerline velocity decay can be shown to be inversely proportional to the square of the distance x.

$$\text{i.e.} \quad \frac{u_e - u_j}{u_e - u_j} = \exp\left[-\frac{36.4}{(x/a)^2}\left(\frac{\rho_e}{\rho_o}\right)\frac{1}{(1-u_j/u_e)}\right]$$

while the potential core length is given by

$$\frac{x_{pot}}{a} = 8.5\sqrt{\frac{\rho_j}{\rho_o}\left|\frac{u_j/u_e}{1-u_j/u_e}\right|}$$

Similar results are inferred for the stagnation enthalpy and species as the governing equations are identical in form under the assumption of the theory (i.e. $Le = Pr = 1$, $\frac{\partial p}{\partial x} = 0$).

B. Influence of Impurities on Combustion

The influence of stream impurities such as H_2O vapor and small amounts of CO_2 have been studies theoretically in Refs. 52, 53, and 54. These studies have shown that the induction time is increased by approximately 16%. The reaction time is also increased due to the diluting effects which reduces the mean reaction temperature. The effect of initial free radicals ($y_{OH} \sim 10^{-5}$ and 0) is to reduce the induction periods. The inclusion of bimolecular or shuffle reactions (Ref. 55) show that the ignition delay time is prolonged at high temperatures and shortened at low temperatures. While the presence of hydroperoxyl HO_2 radical lengthens both ignition and reaction times.

C. Influence of Streamwise Pressure Gradients on Mixing and Combustion

Some effects of streamwise pressure gradients on mixing and combustion are discussed by Ferri (Ref. 10) in regard to the possible flow reversal. Schetz (Ref. 5) has suggested the study of the effect of strong pressure gradient on mixing rates. Since the pressure field in a scramjets combustor is most likely to be nonuniform, the influence of streamwise pressure gradients was assessed here theoretically using a parabolic mixing program (Ref. 43) and the jet initial conditions given in Section VI of the main text.

A constant favorable and adverse pressure gradient equal to 1/4 of an atmosphere per foot (for the initial region only, i.e. $x < 1$ ft) was used in this analysis. That is, the pressure variation was assumed equal to

$$p = p_\infty (1 + 0.25\, x/L) \quad \text{for } x \quad 1 \text{ ft} \quad \text{and } p_\infty = 2116.9$$

The adverse pressure gradient was found to increase the viscosity (Fig.24) and therefore to enhance the mixing. The potential core length decreased for an adverse pressure gradient and increased for a favorable pressure gradient (Fig.24). This is due to a faster decay of the velocity on the centerline to

a value of .99 of the initial jet velocity in the case of adverse pressure gradient than in the case of favorable pressure gradient. The edge of mixing and flame shape (Fig.24) are relatively unchanged by the pressure gradients. For stronger gradients than the one assumed above the effects on the edge of mixing and flame shape are expected to be similar to those produced on the potential core.

The effect of injector wall (i.e. centerline) conditions such as temperature, hydrogen concentration (as in a porous wall), boundary layer growth, and heat transfer rate, lateral pressure gradients, etc. could not be assessed with this computer program. However, the effects of adjacent injectors was assessed in a preliminary manner. Since the number of parameters (distance apart, downstream location, etc.) involved in this case is numerous, and the eddy viscosity law in the interaction region is unknown, an investigation of this effect is discussed in Ref. 4. An additional case is presented here to show the effects when the fuel injectors are too close. This configuration is shown in Fig.25. Since the local flow is fuel rich, the flames merge into a single surface.

D. Under and Over Expansion of the Jet

Some effects of under expansion of a jet core are studies analytically in Ref. 56.. It is found that for an under expanded jet strong streamwise favorable pressure gradients are generated along the axis of the jet. The ignition is delayed due to a pressure and temperature drop in the mixing and combustion zone when the expansion fan originating at the lip of the injector reflects on the axis and passes through the combustion zone. These effects are not clearly shown by the example presented in the reference. Unfortunately, the reduction in under expansion, i.e. strength of the expansion fan, could not be assessed.

The case of over expansion has not been presented there. However, this is believed more beneficially to combustion than the under expansion case. In either case, the pressure field becomes uniform in a short distance ~ 0 (10 to 20) jet diameter.

E. Lateral Pressure and Thermal Gradient Effects

In general the mixing process is controlled by gradients, in species, pressure and temperature normal to streamlines and by their cross-effects. That is, the mass flux of a certain species is proportioned to

$$\rho_1 \bar{V}_1 = \frac{\rho_1 D_{12}}{\mu_t} \left[\frac{\mu_t}{Y_1} \bar{\nabla} Y_1 + \frac{W_2}{W_1} \frac{\rho D_{ij}}{T} K_t \nabla T + \frac{W_2}{W_1} Y_1 (1-Y_1) \frac{1}{p} \nabla p \right]^*$$

Where the first term is the flux due to species gradients, the second due to temperature and the third is due to pressure gradients. Usually the assumption is made that the diffusion due to species gradients dominates and the diffusion due to thermal and pressure gradients is neglected as the laws of turbulent diffusion are not known very well so that the equations are simplified. In the energy transport phenomena, besides neglecting heat transfer due to species and pressure gradients, heat transfer by radiation is also neglected.

In a supersonic combustion process these assumptions may not be valid in certain regions of the flame. For example, in the near field of the splitter plate, the species gradient may easily overshadow the thermal and pressure gradients in the absence of combustion. While the presence of shock waves and/or combustion induced waves can generate lateral pressure gradients which are comparable to species gradients. Further downstream where the flame is well developed, the thermal gradients may overshadow the species gradients while the

* The Boussinessq assumption for momentum transport has been extrapolated here for the cross-effects analogous to laminar mixing.

lateral pressure gradients will have decayed substantially. An order or magnitude analysis in these different regions follows with some qualitative implication of these considerations.

Analogous to laminar diffusion, the diffusion velocity may be expressed as in Ref. 57, for a mixture and using turbulent coefficients, as

$$\rho_1 \bar{V}_1 = - \rho_1 D_{12} \left[\frac{\partial}{\partial r} (\ln Y_1) + \frac{W_2^2 - W_1^2}{W_1 W_2} (1 - Y_2) \frac{\partial}{\partial r} (\ln p) + \right.$$

$$\left. + \frac{(W_1 + W_2)^2}{W_1 W_2} \frac{K_t}{Y_1} \frac{\partial}{\partial r} (\ln T) \right]$$

where $\rho_1 = Y_1 \rho \equiv$ partial density of species11

$\bar{V}_1$ = Diffusion velocity

D_{12} = Binary diffusion coefficient (turbulent)

$Y_1 = \rho_1/\rho \equiv$ mass fraction of species 1

W_1 = Molecular weight of species 1

W_2 = Molecular weight of species 2

$p \equiv$ Pressure

T = Temperature

$K_t = \rho D_1^T / D_{12} W_1 W_2 n^2$ = ratio of thermal to diffusion coefficients

Simplifying for $W_2 >> W_1$ (W_2 = 28.9 for air, W_1 = 2.0 for hydrogen)

$$\rho_1 \bar{V}_1 = \rho D_{12} \left[(Y_1)_r + \frac{W_2}{W_1} Y_1 \frac{(1-Y_1)}{P} p_r + \frac{W_2}{W_1} \frac{K_t}{T} T_r \right]$$

Nondimensionalizing so that all terms are of the order unity requires four separate length scales: (1) physical scale $\sim r_j$, (2) thermal scale proportional to the flame thickness, (3) a pressure scale proportional to com-

pression fan scale $\sim x \tan \mu$ and (4) a diffusion scale $\sim$ mixing zone. The shock wave thickness scale is much too small (on the order of a few mean free paths) at pressures encountered in the combustor and is therefore disregarded as the length is not sufficient to cause diffusive separation even with moderately strong shocks ($\frac{\Delta p}{p_\infty} \sim 10.$).

The pressure and temperature are nondimensionalized w.r.t. the free stream pressure and temperature respectively. The order of magnitude of the corresponding gradients are then

<u>Species</u> $$Y^{-1}\frac{\partial Y_1}{\partial r} = Y_{1_\mathcal{E}}^{-1}\frac{Y_{1_\mathcal{E}} - Y_{1_{flame}}}{b}$$ inside the flame b is the flame width

$\longrightarrow 0$ outside the flame

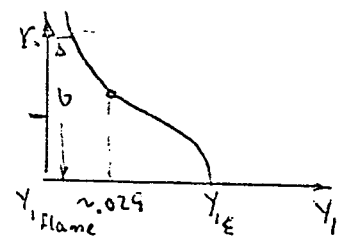

<u>Pressure</u> $$p^{-1}\frac{\partial p}{\partial r} = p_{avg}^{-1}\frac{p - p_e}{x\tan\mu_e}$$

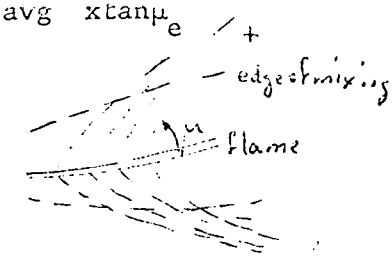

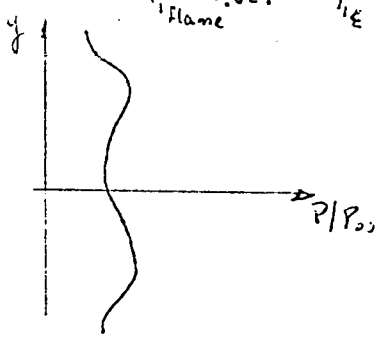

<u>Temperature</u> $$T^{-1}\frac{\partial T}{\partial r} \doteq \frac{2}{T_j + T_e}\frac{T_e - T_j}{b}$$ initial region (x 5 r_j)

$$= \frac{2}{T_j + T_{flame}}\frac{T_{flame} - T_j}{t_{flame}} \cong \frac{2}{t_{flame}} \gg 1$$ inner region

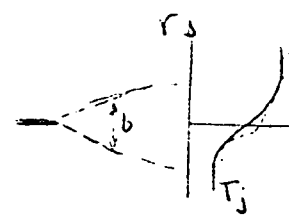

$$= \frac{2}{T_{flame} + T_e}\frac{T_e - T_{flame}}{t_{flame}}$$ outer region

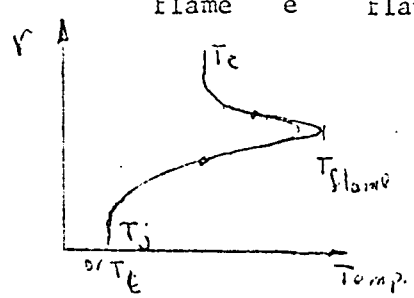

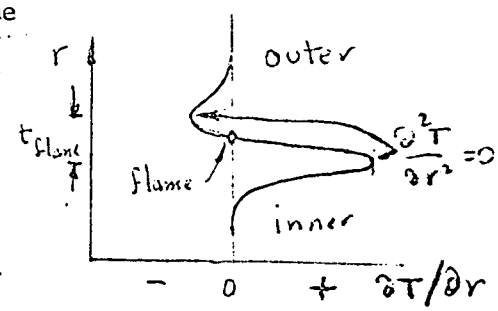

In Ref. 58, it is shown that even for infinite Damkohler Number (ratio of the characteristic relaxation time of the energy containing eddies to that of the molecular chemical reaction), the thickness of the flame zone is of the local scale of turbulence which, in a pure shear-produced turbulence is of the order of the shear layer thickness. Furthermore the heat conduction takes place in the direction of increasing mean temperature in certain regions of the flame. Seemingly defying the 2nd law of thermodynamics. This last is not verified by "standard" theories which assume Le=1, Pr = 1, and neglect diffusion due to thermal and pressure gradients.

An order of magnitude analysis of each of the three terms shows that in the far field of the flame the temperature gradients may induce a larger diffusion velocity than the species gradients while pressure gradients produce effects which are subordinate to both species and temperature gradients simply because the pressure effects travel along Mach waves which except at very high hypersonic speeds spread laterally faster than a mixing zone.

Assuming the conditions are propitious to diffusion by all three mechanisms the consequences of the inclusions of these effects on the combustion can be qualitatively assessed from profiles generated in the absence of diffusion by pressure and thermal gradients. In Fig.26, the flow field, and typical flow and concentration profiles are shown along with the directions of the lateral pressure and thermal gradients. The pressure gradients would tend to establish fluxes of lighter species in the same direction as the decreasing pressure as shown in Fig.26a. The net effect of which would be that the flame initially would burn leaner than stoichiometric. Then as the pressure pulse moves away from the zone, the trend reverses and the flame burns fuel rich. The temperature gradients would also likewise establish fluxes of lighter elements away from high temperature regions and therefore would result in lean burning.

A fuel injector as shown in Fig. 2 can be designed to generate pressure waves to counter the effects produced by a natural induced lateral pressure gradient. The effects of thermal gradient are not as easily countered.

F. Splitter Plate Temperature Effects

The splitter plate temperature affects the growth of the boundary layer of the viscous flow on it. The boundary layer thickness is thicker at higher wall temperatures; therefore, it provides longer residence time which results in shorter ignition delay lengths. A trend in the ignition delay length dependence on the splitter plate temperature is shown in Fig. 27. This shows a considerable decrease in ignition delay at higher wall temperatures. The effects of much higher wall temperatures (1500 T_w 4500 °R) are presented in Ref. 11 in Fig. 14 and are reproduced here in Fig. 27.

REFERENCES

1. Ferri, Antonio, "Mixing Controlled Supersonic Combustion," New York University Aerospace Laboratory, Bronx, New York. Review of Journal of Fluid Mechanics, January 1973, p. 122-135.

2. Moretti, G., "A New Technique for the Numerical Analysis of Nonequilibrium Flows," General Applied Science Labs, Inc., Westbury, New York, AIAA Journal, Vol. 3, No. 2, February 1965, p. 223.

3. Pergament, H.S., "Theoretical Analysis of Non-Equilibrium Hydrogen-Air Reactions in Flow Systems," General Applied Science Labs, Inc., Westbury, New York. Hypersonic Ramjet Conference, Naval Ordnance Laboratory, White Oak, Md., April 23-25, 1963.

4. Ferri, A. and Fox, H., Twelfth Symposium (International) on Combustion, 1969, The Combustion Institute, Pittsburgh, Penna.

5. Schetz, J.A., Unified Analysis of Turbulent Jet Mixing, Johns Hopkins University Silver Springs, Md., NASA C-1382, July 1969.

6. Harsh, Philip, Thomas, "Free Turbulent Mixing: A Critical Evaluation of Theory and Experiment," ARO Inc. AEDC TR-71-36, 1971.

7. Putre, Henry A., "Improved Data Agreement Using New Eddy Viscosity Equations in a Coaxial Free Jet Computer Code," Lewis Research Center, Cleveland, Ohio, NASA TN-D-5835.

8. Zakkay, V., Krause, E., Woo, S.D.L., "Turbulent Transport Properties for Axisymmetric Heterogeneous Mixing," Polytechnic Institute of Brooklyn, AIAA Journal, Vol. 2, No. 11, November, 1964, p. 1939.

9. Ferri, A., Moretti, G., and Slutsky, S., "Mixing Processes in Supersonic Combustion," Journal of Soc. of Industrial and Applied Math, Vol. 13, No. 1, March 1965, p. 229.

10. Ferri, A., Libby, P., and Zakkay, V., "Theoretical and Experimental Investigation of Supersonic Combustion," reprinted from High Temperatures in Aeronautics, Turin, 10-12 September 1962, Tamburini Editore, Milan, Pergamon Press.

11. Da Riva, I. , Urrutia, J. L., "Ignition Delay in Diffusive Supersonic Combustion", Instituto Nacional de Tecnica Aerospcial, Madrid, Spain, AIAA paper No. 67-496, July 1967.

12. Osgerby, I.T., "An Investigation of Supersonic Combustion and Heterogeneous Turbulent Jets Mixing Related to the Design/Operation of Scramjets," Ph.D. Thesis, submitted to the University of Sheffield, Department of Fuel Technology and Chemical Engineering, October 1965.

13. Anderson, G.Y. and Vick, A.R., "An Experimental Study of Flame Propagation in Supersonic Premixed Flows of Hydrogen and Air," Langley Research Center, Langley Station, Hampton, Va., NASA TND-4631, June 1968.

14. Cohen, L.S. and Guile, Ray, N., "Investigation of the Mixing and Combustion of Turbulent Compressible Free Jets," United Aircraft Research Labs, East Hartford, Conn., NASA CR-1473, December 1969.

15. Anderson, G.Y., Agnone, A., and Russin, W.R., "Composition Distribution and Equivalent Body Shape for a Reacting, Coaxial, Supersonic Hydrogen-Air Flow," Langley Research Center, Hampton, Va., NASA TND-6123, January 1971.

16. Beach, H.L., "Supersonic Mixing and Combustion of a Hydrogen Jet in a Coaxial High Temperature Test Gas," NASA Langley Research Center, Hampton, Va. Presented at the AIAA/SAE Eight Propulsion Joint Specialist Conference, New Orleans, Louisiana, November 24 - December 1, 1972.

17. Peschke, W. and Reiss, E., "Diffusion Controlled Supersonic Combustion Analysis and Design of Combustors," General Applied Science Laboratories, Westbury, New York, TR-672, November 1967.

18. Hawkins, R., "The Feasibility of Supersonic Combustion Ramjets for Low Hypersonic Speeds," Bristol Siddley Engines, England, NATO AGARDoraphs 103 Aerodynamics of Power Plant Installation, Part I, October 1965.

19. Becker, J.V., "New Approaches to Hypersonic Aircraft," NASA Langley Research Center, Hampton Va., 7th Congress of the International Council of Aeronautical Sciences, ICAS Rome Italy, September 14-18, 1970.

20. Schetz, J.A., "Approximate Analysis of a Turbulent, Swirling Jet in a Co-Flowing Stream," Deutsch Forschung-und Versuchsanstalt fur Luft-und Raum Fahrt-Institut fur Theoretische Gasdynamick Aachen Germany, Forschungsbericht 71-80, 1971.

21. Povinelli, Louis A. and Ehlers, Robert C., "Swirling Base Injection for Supersonic Combustion Ramjets," NASA Lewis Research Center, Cleveland, Ohio. AIAA Tech. Note Vol. 10, No. 9, p. 1243-1244.

22. Chervinsky, Amnon, "Turbulent Swirling Jets Diffusion Flames," Israel Institute of Technology, Haifa, Israel, AIAA Journal, Vol. 7, No. 10, October 1969, p. 1877.

23. Mac Farlin, David V. and Kepler, Edward C., "Mach 5 Tests Results of Hydrogen-Fueled Variable Geometry Scramjet," United Aircraft Research Laboratories Technical Report, AFAPL-TR-68-116, October 1968, Confidential.

24. Bahr, D.W., et al "Scramjet Exploratory Development Program ," General Electric, NASA Contract No. NAS 1-8544, NASA CR-1502, December 1969, Confidential.

25. Marguet, R. and Huet, Charles, "Research of an Optimum Solution for a Fixed Geometry Ramjet in the Mach 3 to Mach 7 Range, with Successively Subsonic and Supersonic Combustion," ONERA France T.P. N° 656 E (1968).

26. Dunn, J., Agnone, A., Feeley, H., Soll, D., "An Experimental Investigation of Supersonic Turbulent Slot Injection," GASL, Westbury, New York, TR NO. 420, June 1964.

27. Alpinieri, Louis J., "Turbulent Mixing of Coaxial Jets," Polytechnic Institute of Brooklyn, Freeport, No. 7, AIAA Journal, Vol. 12, No. 9, p. 1560, 1964.

28. Krause, E., Maurer, F., and Pfeiffer, H., "Some Results of Investigations of Problems Relating to Supersonic and Hypersonic Combustion," DFVLR Porz-Wahn, Germany, ICAS 8th Congress, ICAS Paper No. 72-21, September 1972.

29. Kordulla, W. and Krause, E., "Heat Addition by Oxidation of Hydrogen in Laminar Boundary Layers," DFVLR Porz-Wahn, Germany, June 1971, DLR-71-13.

30. Yates, C.L., "Two-Dimensional Supersonic Mixing of Hydrogen and Air Near a Wall," The John Hopkins University, Applied Physics Laboratory, Silver Springs, Md., NASA CR-1793, March 1971.

31. Steiger, M.H., Werner, H., and Sforza, P., and Trentacoste, N., "Studies in Three-Dimensional Free-Mixing: I. Finite Difference Solutions- II. Experimental Results," Polytechnic Institute of Brooklyn, Freeport, N.Y., AIAA Paper No. 65-49, January 1965.

32. Drell, I.L. and Belles, F., "Survey of Hydrogen Combustion Properties," Lewis Flight Propulsion Laboratory, Cleveland, Ohio, NACA RME 57024, July 26, 1957.

33. Suttrop, F., "Ignition of Gaseous Hydrogen Fuels in Hypersonic Ramjets,"

Institut fur Luftstrahlantriebe, Deutsch Forschungs - und Versuchsanstalt fur Luftund Raumfahrt. Presented at 1st International Symposium on Air Breathing Engines, Marseille, 19-23 June 1972.

34. DA Riva, I. and Urutia, J.L., "Ignition Delay in Diffusive Supersonic Combustion," Instituto Nacional de Tecnica Aerospacial, Madrid, Spain, AIAA 3rd Propulsion Joint Specialist Conference, Washington, D.C., July 17-21, 1967, AIAA Paper No. 67-496.

35. Levy, M.E. and Cerkanowicz, A.E., "Ignition of Subatmospheric Gaseous Fuel-Oxydant Mixtures by Ultraviolet Irradiation," Vitro Labs, West Orange, New Jersey, AIAA Paper No. 69-88, January 1969.

36. Townsend, L.H. and Reid, J., "Some Effects of Stable Combustion in Wakes Formed in A Supersonic Stream," Royal Aircraft Establishment, Farnborough, England.

37. Winterfield, J.G.,"Flame Stabilization in Supersonic Flows at Low Gas Temperatures," Deutsche Versuchsanstalt fur Luft-und Raumfahrt E.V. Institut fur Lufts trahlantriebe Porz-Wahm, September 1966, Royal Aircraft Establishment Library Translation No. 1230, N-68-12850.

38. Rubins, P.M., Cunningham, T.H.M., "Shock Induced Supersonic Combustion in a Constant Area Duct," ARO, Inc. Arnold Air Force Station, Tenn., Journal of Spacecrafts & Rockets, Vol. 2, March-April, 1965, p. 199-205.

39. Strehlow, R.A., Rubins, P.M., "Experimental and Analytical Study of H_2-Air Reaction Kinetics Using a Standing-Wave Normal Shock," University of Illinois Urbana, Ill. ARO, Inc., Arnold Air Force Station, Tenn., AIAA Journal, Vol. 7, No. 7, July 1969, p. 1335.

40. Douglas, G.W., O'Loughlin, J.R., "Studies of Combustion Efficiency and Flame Shape for Opposed-Jet Flameholders," Tulane University, New Orleans,

AIAA Journal, Vol. 6, No. 4, p. 672, April 1968.

41. Phillips, Bert, Pa lin, Albert J. and Conrad, W., "A Resonance Ignition for Hydrogen-Oxygen Combustors," NASA Lewis Research Center Cleveland, Ohio, Journal of Spacecraft and Rockets, Vo No. 5, May 1970, p. 620.

42. Agnone, A., "Design and Theoretical Performance Estimates of a Three-Dimensional Fixed Geometry Inlet for an Integrated Scramjet Engine to Propell a launch Vehicle," N.Y.U. Aerospace Laboratory, Bronx, New York, NYU-73-01, January 1973.

43. Siegelman, D., Fortune, O., "Computer Programs for the Mixing and Combustion of Hydrogen in Air Streams," General Applied Science Labs, Inc., Westbury, New York, GASL TR 618, July 1966.

44. Rudman, S., "Three-Dimensional Jet Mixing with Hydrocarbon Chemistry," Advanced Technology Laboratory, Inc. Jericho, N.Y. ATL-TM-150, March 1970.

45. Dash, S., "An Analysis of Internal Supersonic Flows with Diffusion, Dissipation and Hydrogen-Air Combustion," Advanced Technology Laboratory, Inc., 400 Jericho Turnpike, New York, NASA CR-111783, May 1970.

46. Piva, R.,"Leading Edge Cooling by Upstream Injection," New York University Aerospace Laboratory, Bronx, New York, NASA CR-111965, 1971.

47. Parthasarathy, K., Zakkay, V., "Turbulent Slot Injection Studies at Mach 6.0", New York University Aerospace Laboratory, Bronx, New York, Wright-Patterson AFB, Ohio, ARL 69-0066, April 1969, (see also AIAA Journal, Vol. 8, No. 7, July 1970, p. 1302-1307.)

48. Ferri, A., "A Critical Review of Heterogeneous Mixing Problems," New York University, Astronautica, Vol. 13, pp. 453-465.

49. Ferri, A., "Review of Problems in Application of Supersonic Combustion," Seventh Lanchester Memorial Lecture, Journal of the Royal Aeronautical Society, Vol. 68, No. 645, September 1964.

50. Zakkay, V., Sinha, R. Nomura, S.; "Prediction and Evaluation of Eddy Viscosity Models for Free Mixing" New York University Aerospace Laboratory, Bronx, New York, NYU 72-06

51. Libby, P. A.;"Theoretical Analysis of Turbelent Mixing of Reactive Gases with application to Supersonic Combustion of Hydrogen", General Applied Science, Labs., Westbury, N.Y. ARS J. vol. 32, No. 3, pp. 388-396 March 62

52. Abbett, M. A.;"The Effects of Water on the Combustion History of a Hydrogen-Air System", General Applied Science Labs, Westbury, N Y. TR427, March 64

53. Edelman, R., Spadaccini, L. "Analytical Investigation of the Effects of Vitiated Air Contamination on Combustion and Hypersonic Airbreathing Engine Ground Tests," AIAA Paper NO. 69-338, April, 1969.

54. Ericks , W. d., Klich, G. F. ;"Analytical Chemical Kinetic Study of the Effect of Carbon Dioxide and Water Vapor on Hydrogen Air Constant- Pressure combustion," Langley Research Center, Hampton, Va., NASA TND 5768, April, 1970.

55. Brevig, O., Shahrokhi, F.;"On the Free Turbulent Mixing and Combustion between Coaxial Hydrogen and Air Streams," Convair Aerospace/General Dynamics Corporation, San Diego, California, AIAA 9th Aerospace Sciences Meeting New York, January 1971, AIAA Paper No. 71-5.

56. Edelman, R., Weilerstein, G.;"A Solution of the Inviscid-Viscid Equations with applications to Bounded and Unbounded Mult component Reacting Flows," General Applied Science Laboratories, Westbury, N.Y., AIAA Paper No. 69-83, January 1969.

57. Dorrance, W. H.;"Viscous Hypersonic Flow", Mc Graw Hill 1962.

58. Chung, P. M.;"Structure of Turbulent diffusion Flames," University of Illinois, Chicago, Ill. AIAA J. Vol. 9, No. 11.

59. Richmond, J. K., Shreeve, R. P., "New Technique for obtaining Kinetic Data with Shock Induced Combustion," Boeing Reasearch Laboratiries, Seattle Washington, AIAA Paper No. 67=105, Jan. 1967.

60. Hawthorn, R. D., Nixon, A. C.,"Shock Tube Ignition Delay Studies of Endothermic Fuels," Shell Development Co., Emeryville California, AIAA J. Vol. 4, No. 3, March, 1966.

61. Leuchter, O.,"Etude des Evolutions Chimique dans une Couche de Melange Hydrogene - Air," Office National D'Etude et de Recherches Aerospatiales, Chatillon France, T. P. No. 981, 1971.

Table 1 Nominal Fuel Injection Conditions used in Previous Experiments

Ref.	Date	Injector Geometry Radius Sketch	Injection Conditions: Mach No. T_t (°K) P_t (psia)	Injection Conditions: Velocity (ft/sec) Temp (°K) Pressure (psia)	Ignition System	Air Stream Conditions: Mach No. T_t (°K) P_t (psia)	Air Stream Conditions: Velocity Temperature °K Pressure (psia)	$\rho_j u_j / \rho_e u_e$ u_j/u_e T_j/T_e	$R_{e_{co}}$ 1/ft
10	1962	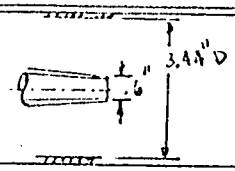	0.3 | .7 | .9	1200 | 2280. | 3420.	auto-ignition	1.55	3000.	.022 | .05 | .09	$.5\times10^6$
			300. | 1000.	200. | 676.		1300.	880.	.4 | .76 | 1.14	
			50.	14.7		60.	14.7	.23 | .77	
11	1963			4000.	auto-ignition	4.2	10000.		
			1000.	1000.		1300.	1300.	.40	
								.77	
12	1965	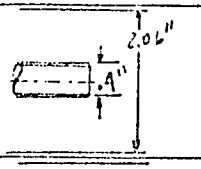	1.0	1050.		3.0	4560.	.02 to 2.	$1.\times10^7$
			300.	250.		1500.	535.	.23	
			28.	14.7		560.	14.7	0.47	
13	1968	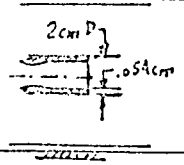	1.0	2800.	pilot pre-mixed	1.5	1550.	.20	1.8×10^7
			1400.	1120.		300. & 450.	207. & 310.	1.80	
			50.	14.7		55.0	14.7	5.4 & 3.6	
14.	1969	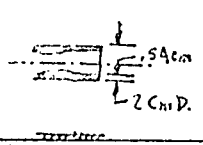	1.46	5300.	auto-ignition	1.86	1670. | 2040.	.425	3×10^6
			300.	210.		1500 & 1750.	890. | 1040.	32. | .26	
			46.	13.2			13.2	24 | .20	
15.	1971	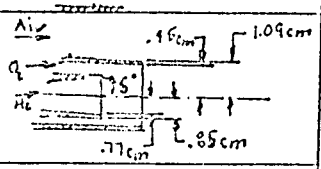	2.0	6450.	pilot & O_2	2.0	1690.	0.262	3.3×10^7
			300.	165.		300.	165.	3.82	
			120.	14.7		120.	14.7	1.00	
16	1972	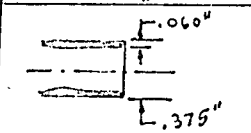	2.0	6953.	auto-ignition	2.0	4060.	582.	3.6×10^6
			347.	192.		1800.	1120. &	1.71	
			120.	14.7		120.	14.7	0.171	

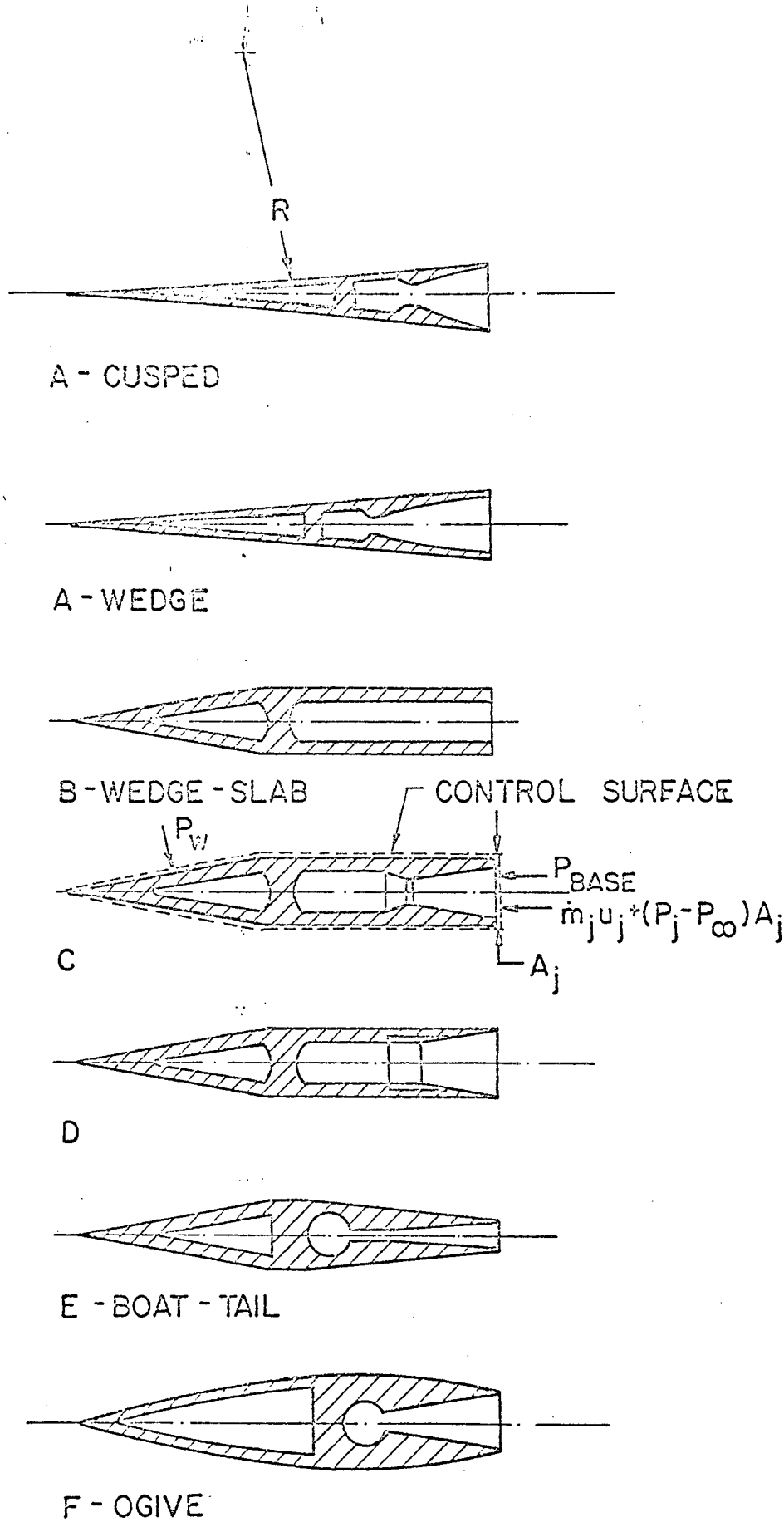

Fig. 1 Typical two-dimensional fuel injectors

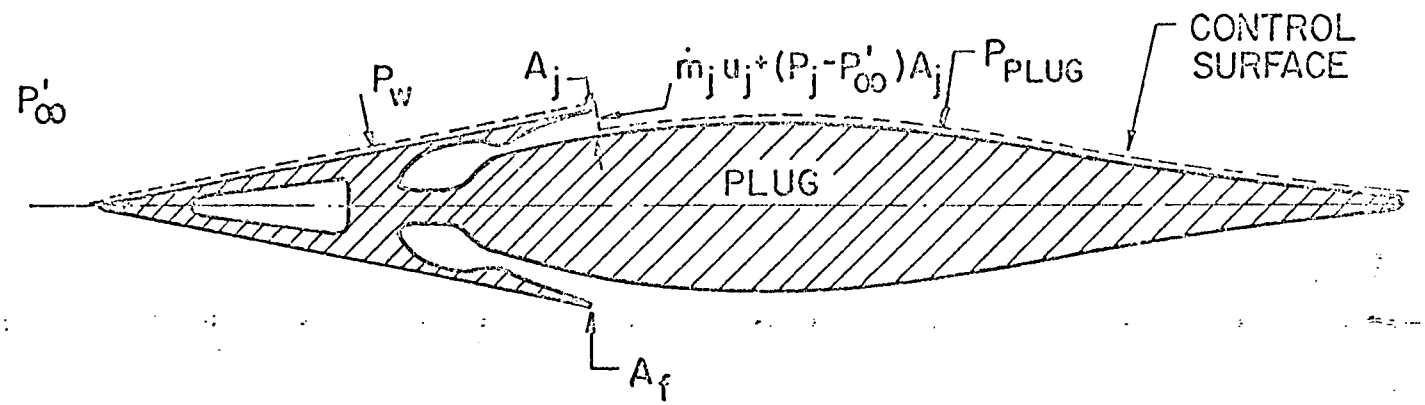

Fig. 2 Plug type injector

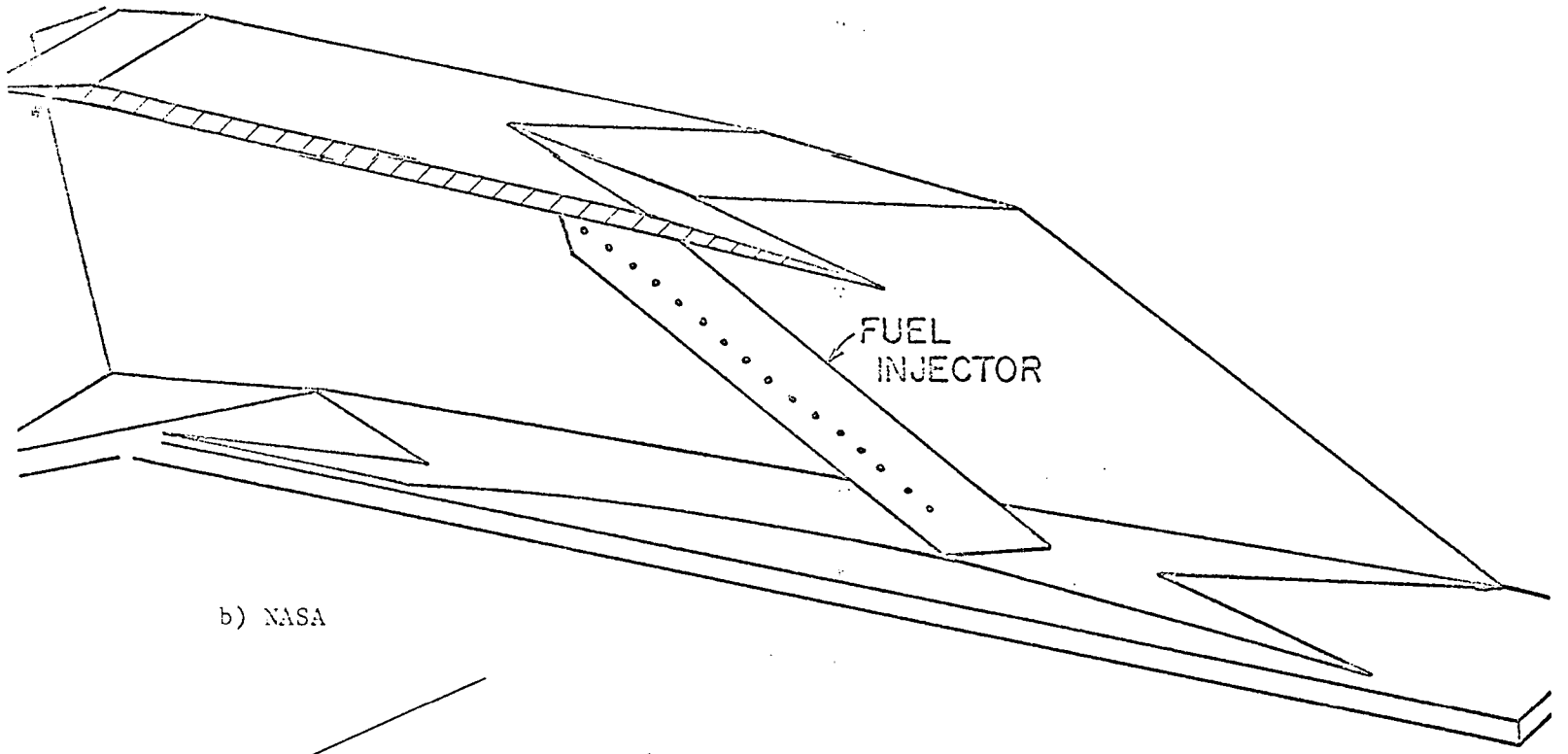

b) NASA

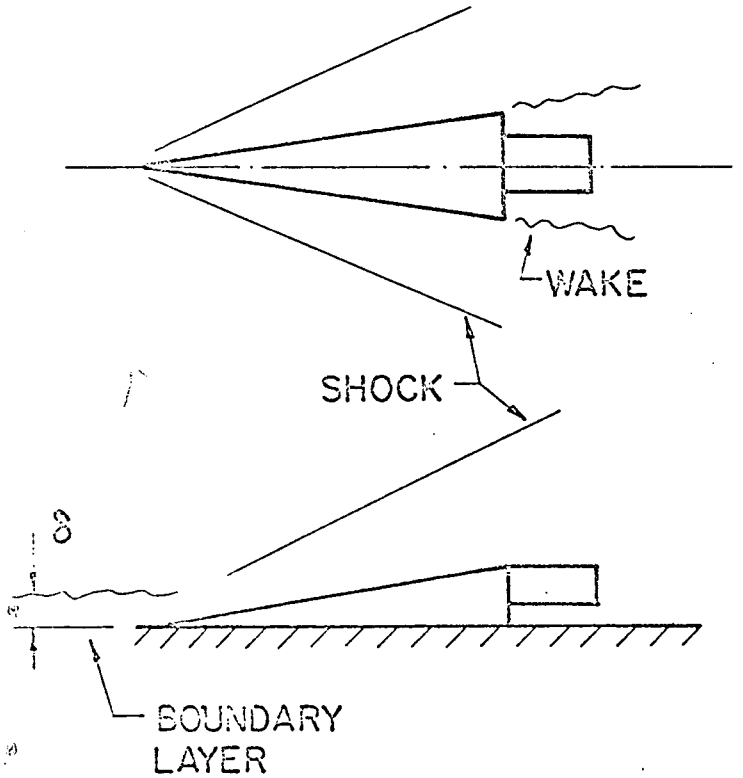

a) GASL

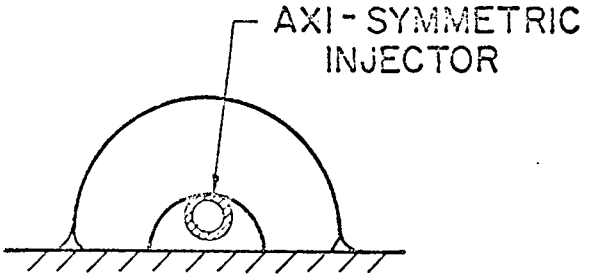

Fig. 3 Three dimensional fuel injectors

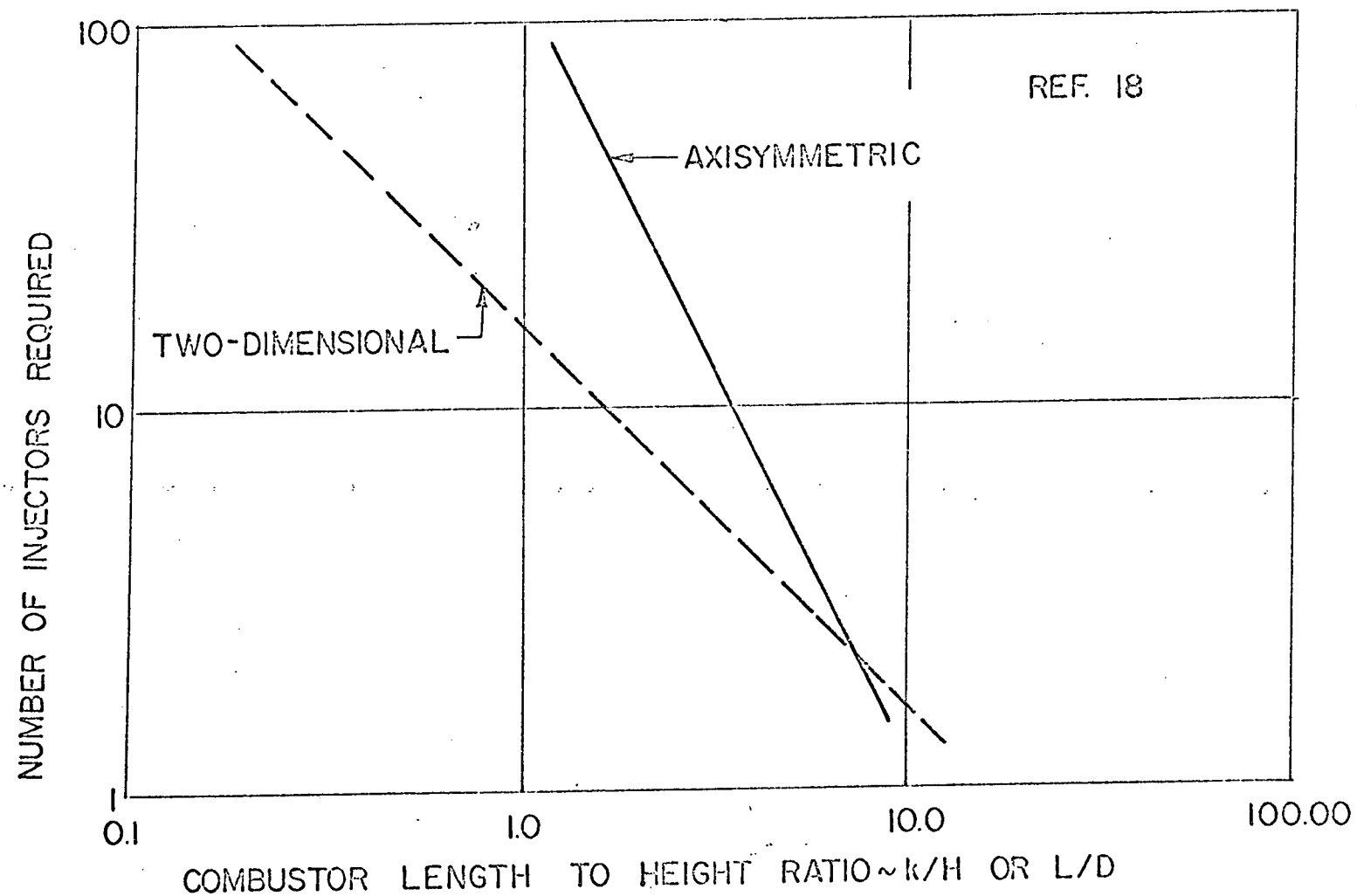

Fig. 4 Number of fuel injectors required for a given combustor length to height ratio

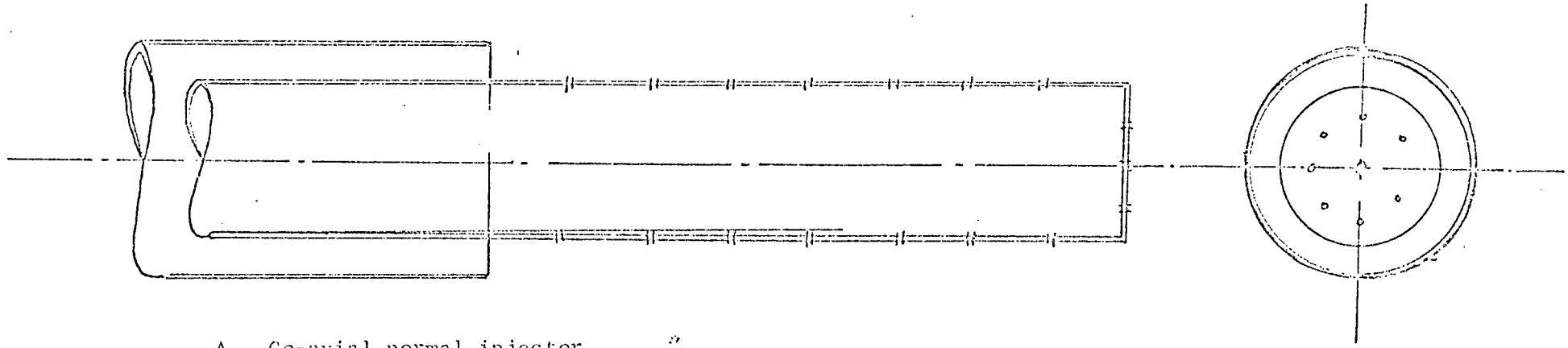

A. Co-axial normal injector

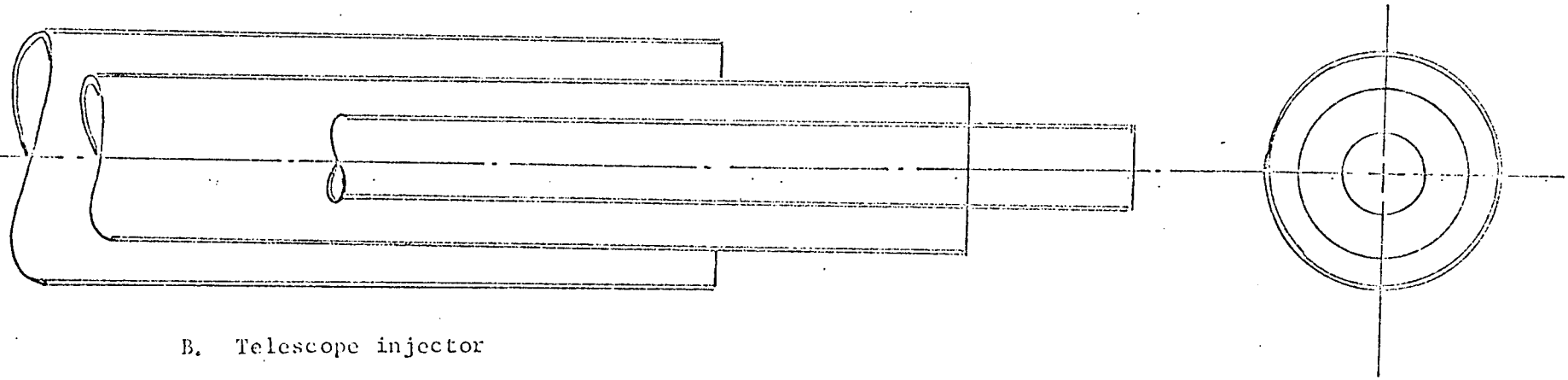

B. Telescope injector

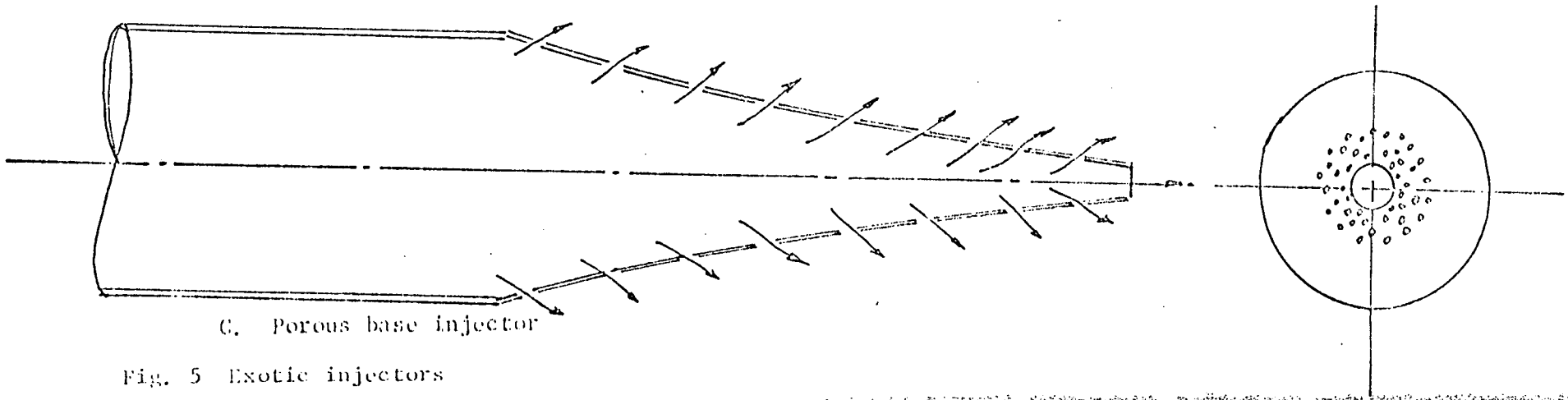

C. Porous base injector

Fig. 5 Exotic injectors

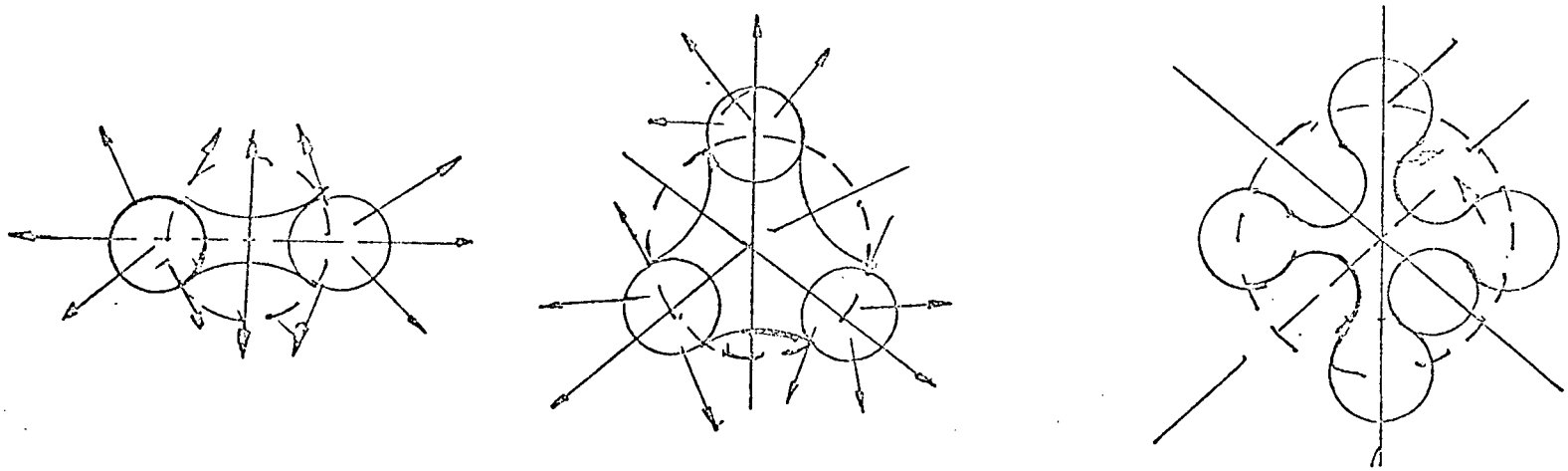

A. Lobed injectors

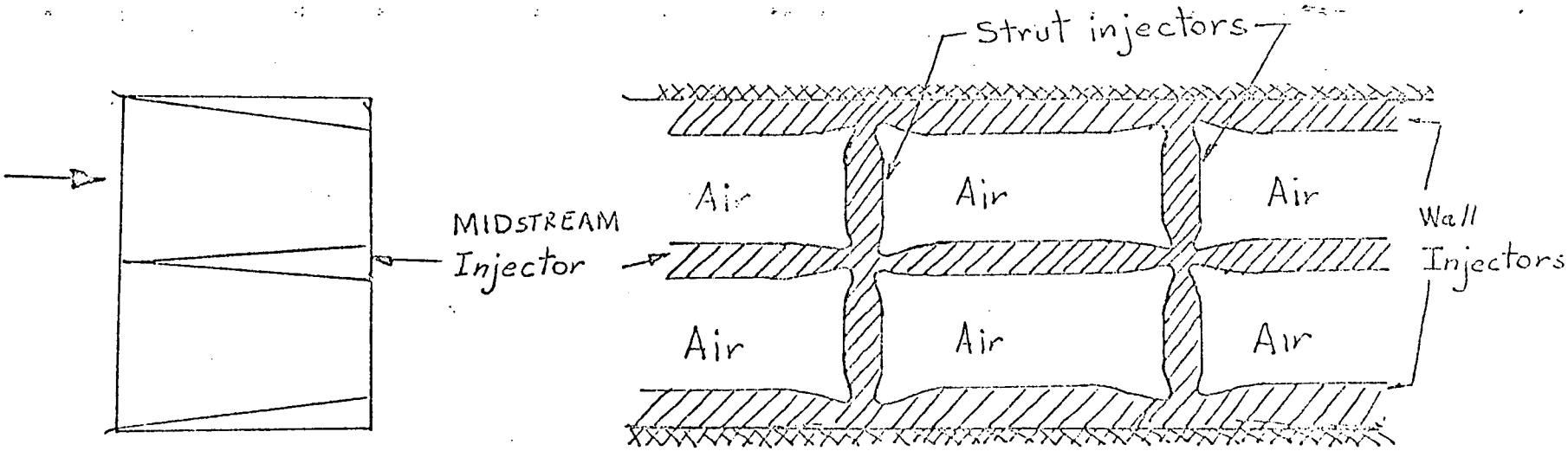

B. Corrugated injectors

Fig. 5a Exotic injectors

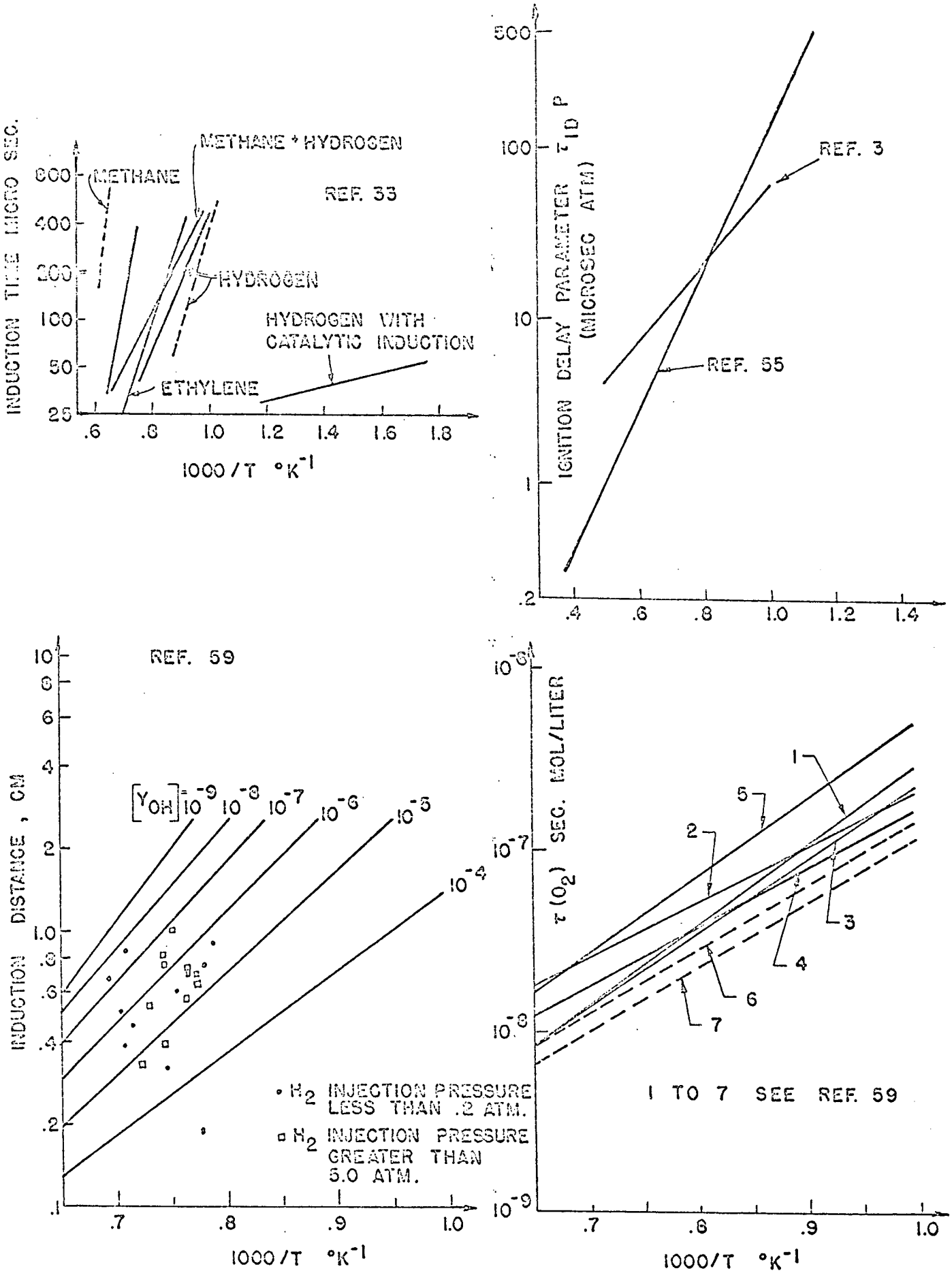

Fig. 6 Ignition delay of premixed hydrogen and other hydrocarbons as a function of temperature, pressure and stoichiometric ratio

61

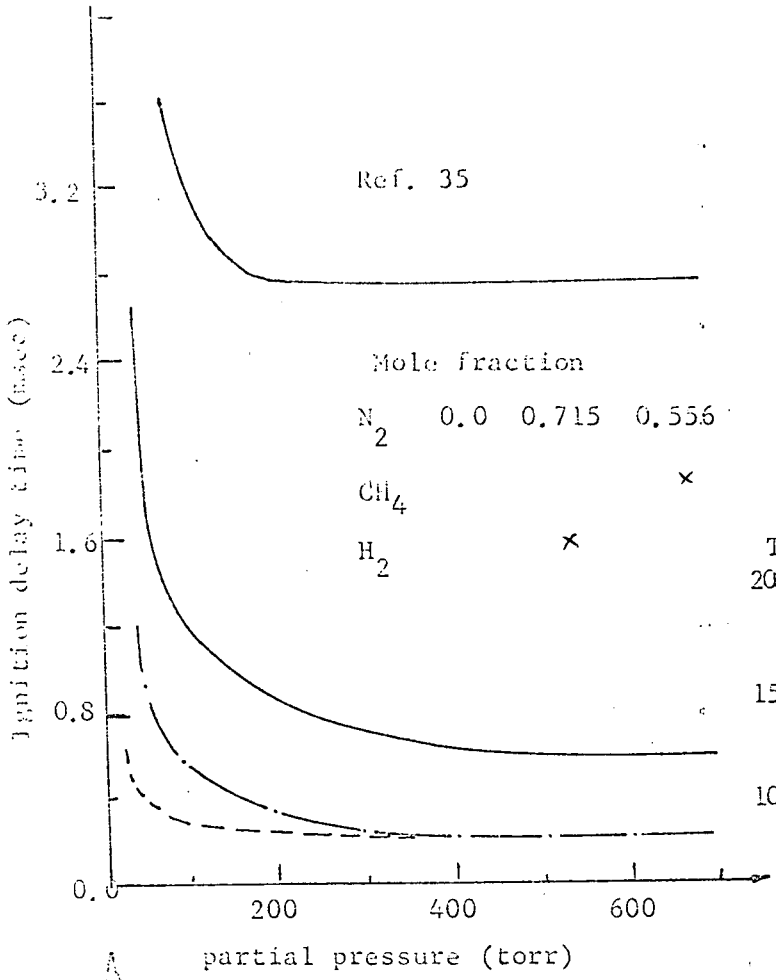

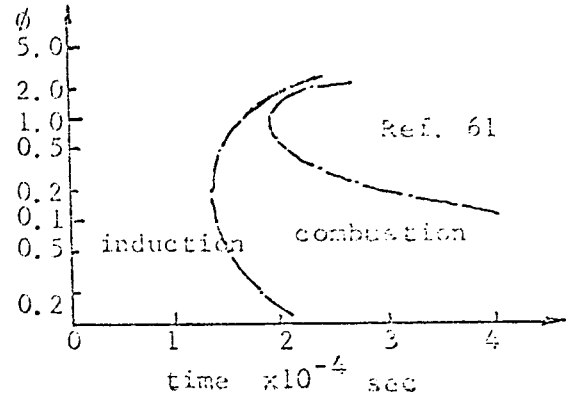

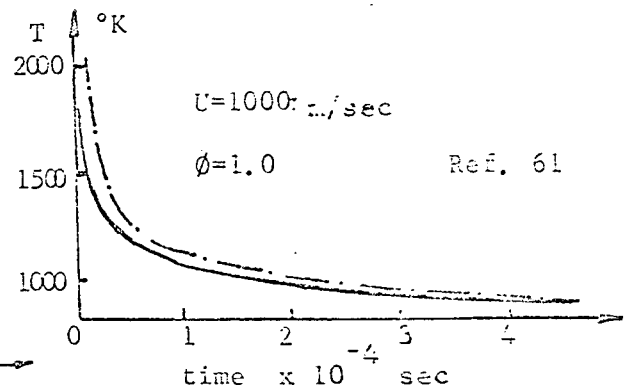

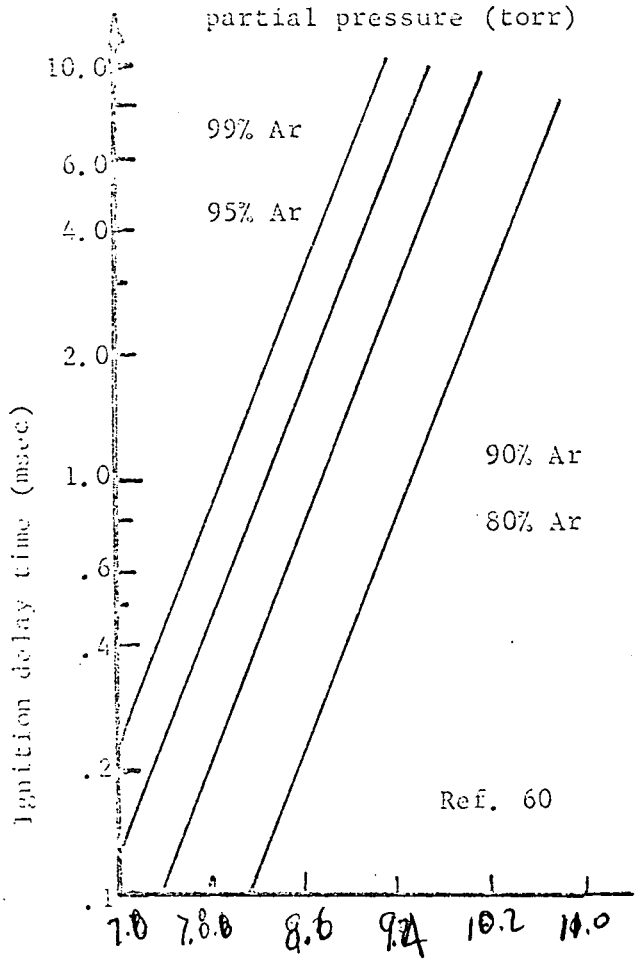

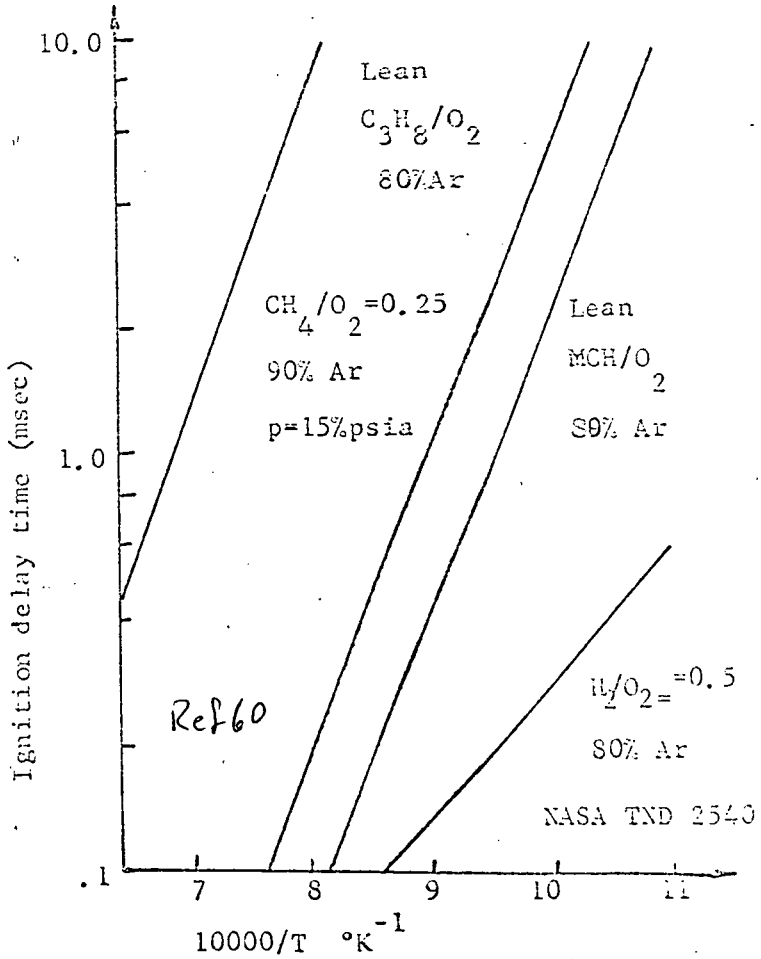

Fig. 6 Concluded.

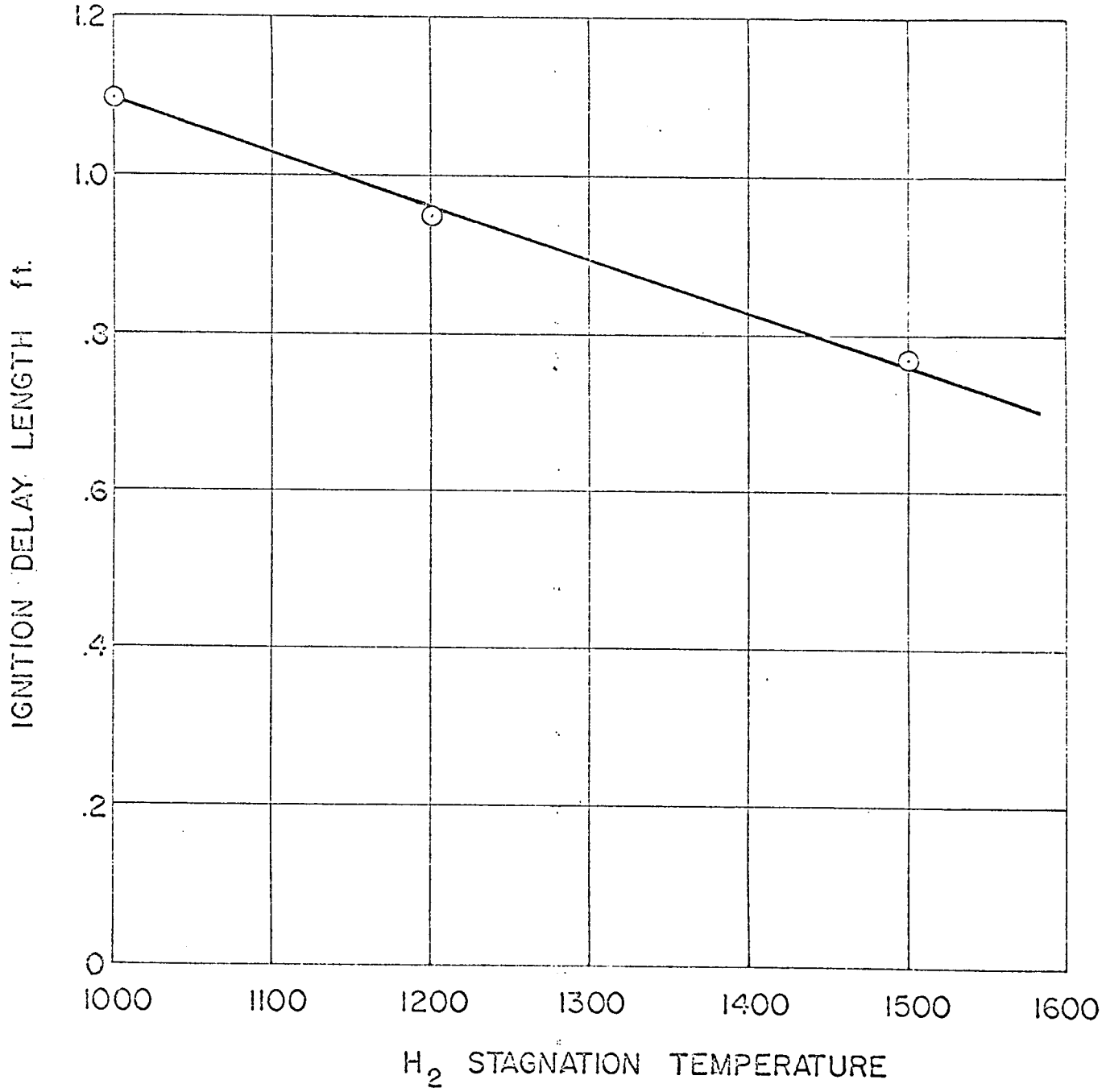

Fig. 7 Influence of hydrogen injection stagnation temperature on ignition delay

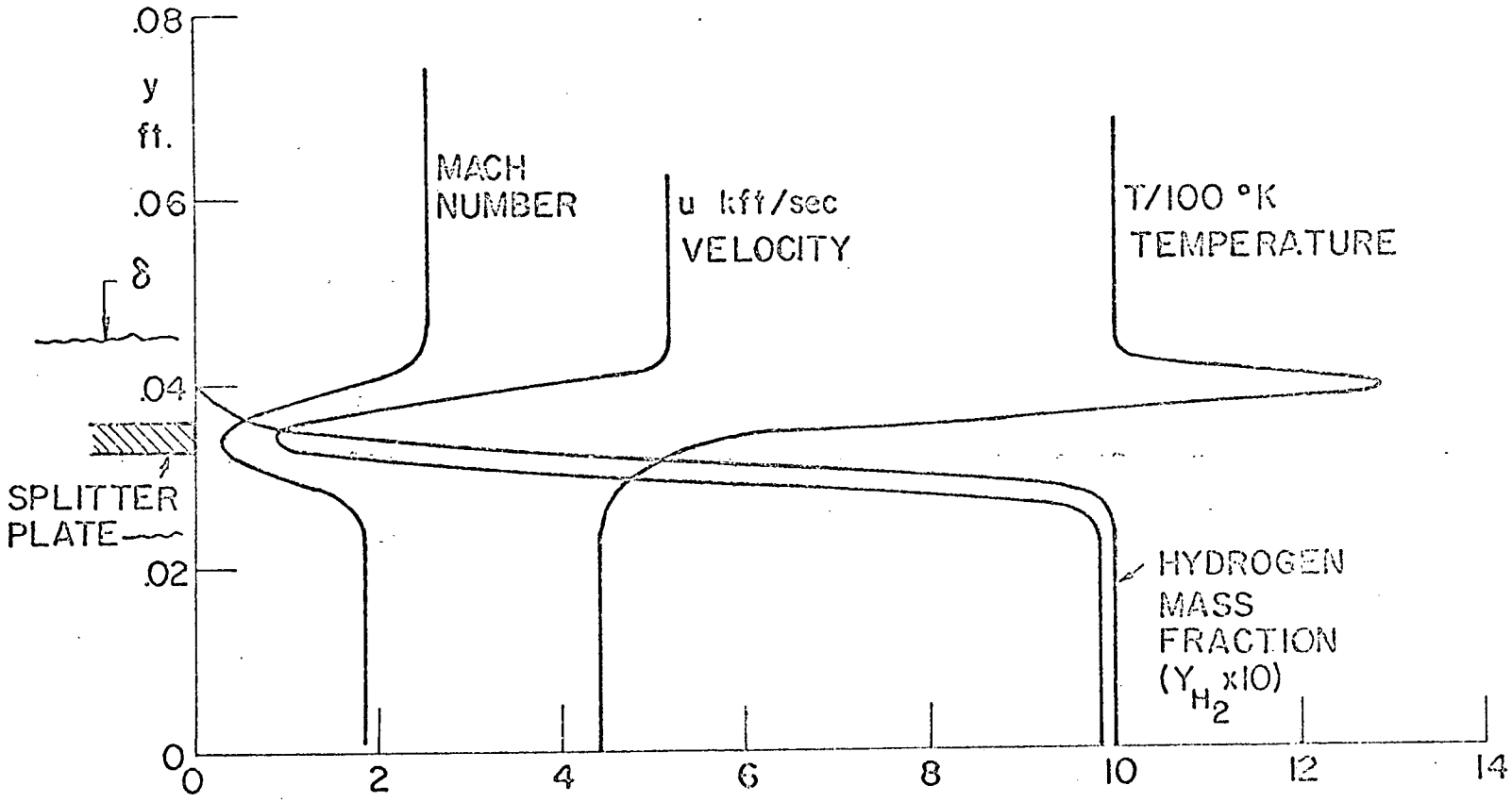

Fig. 8 Initial profiles used in parabolic mixing analysis

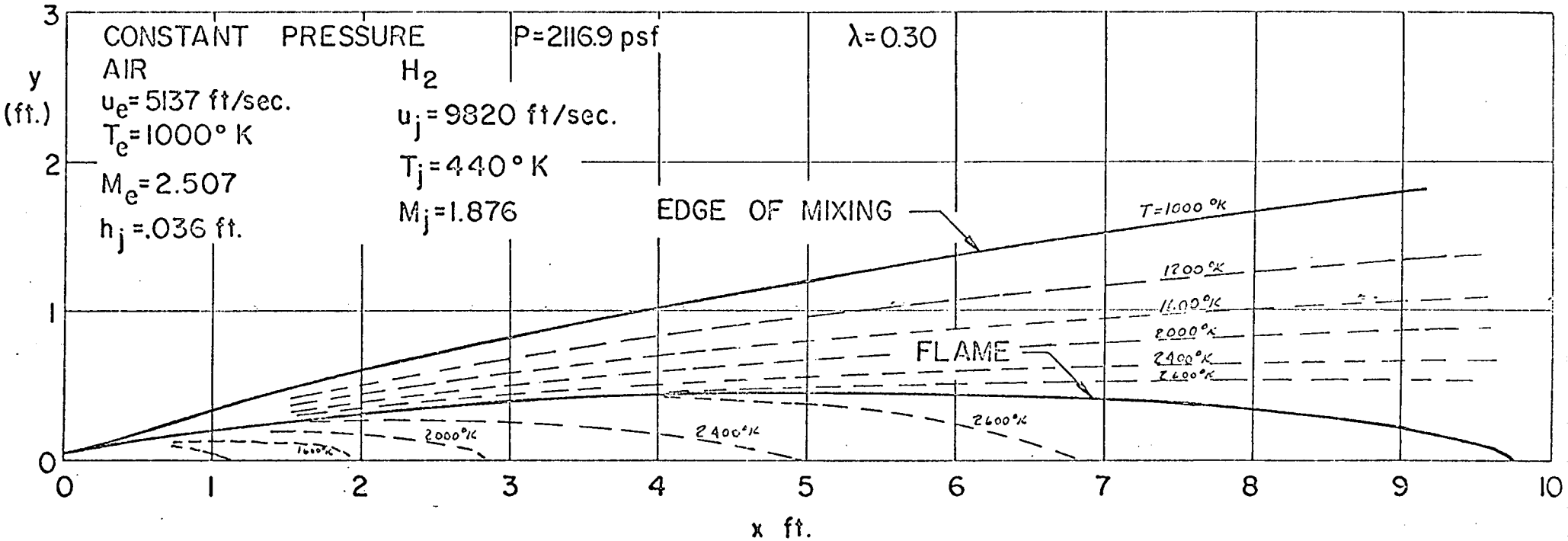

Fig. 9 Flame shape, edge of mixing, and isotherms

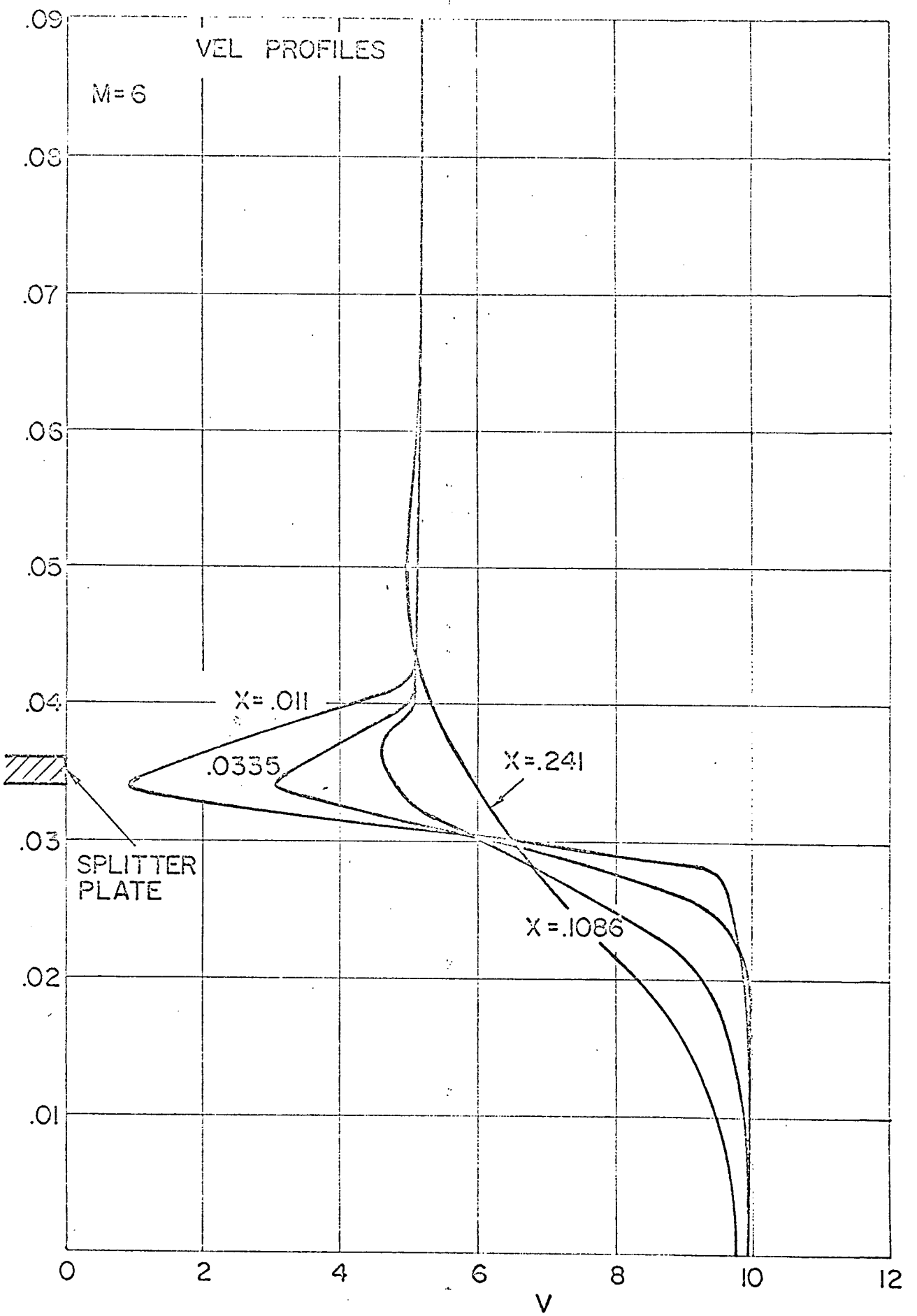

Fig. 10 Velocity profiles at various axial stations

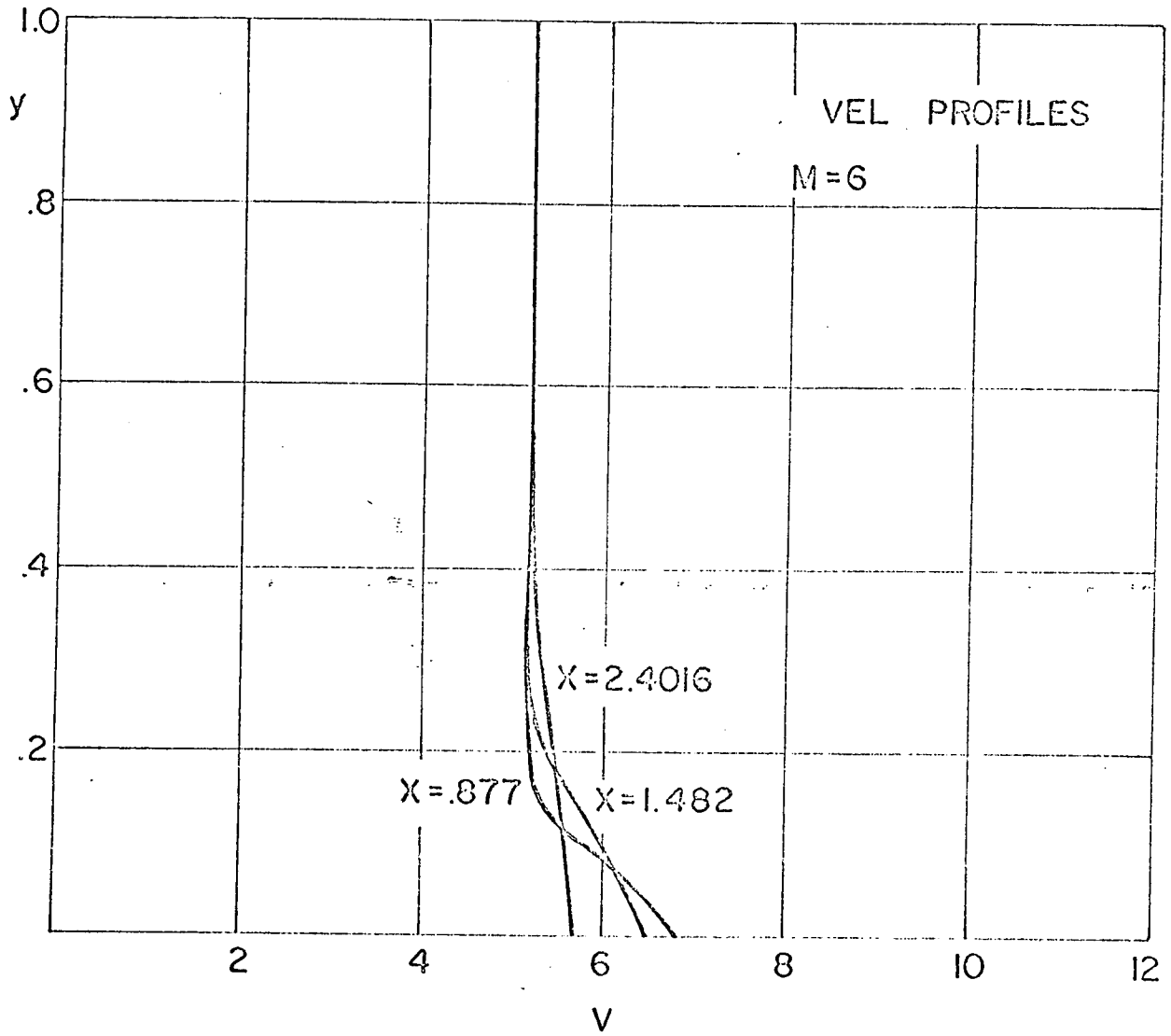

Fig. 10 Cont'd Velocity profiles at various axial stations

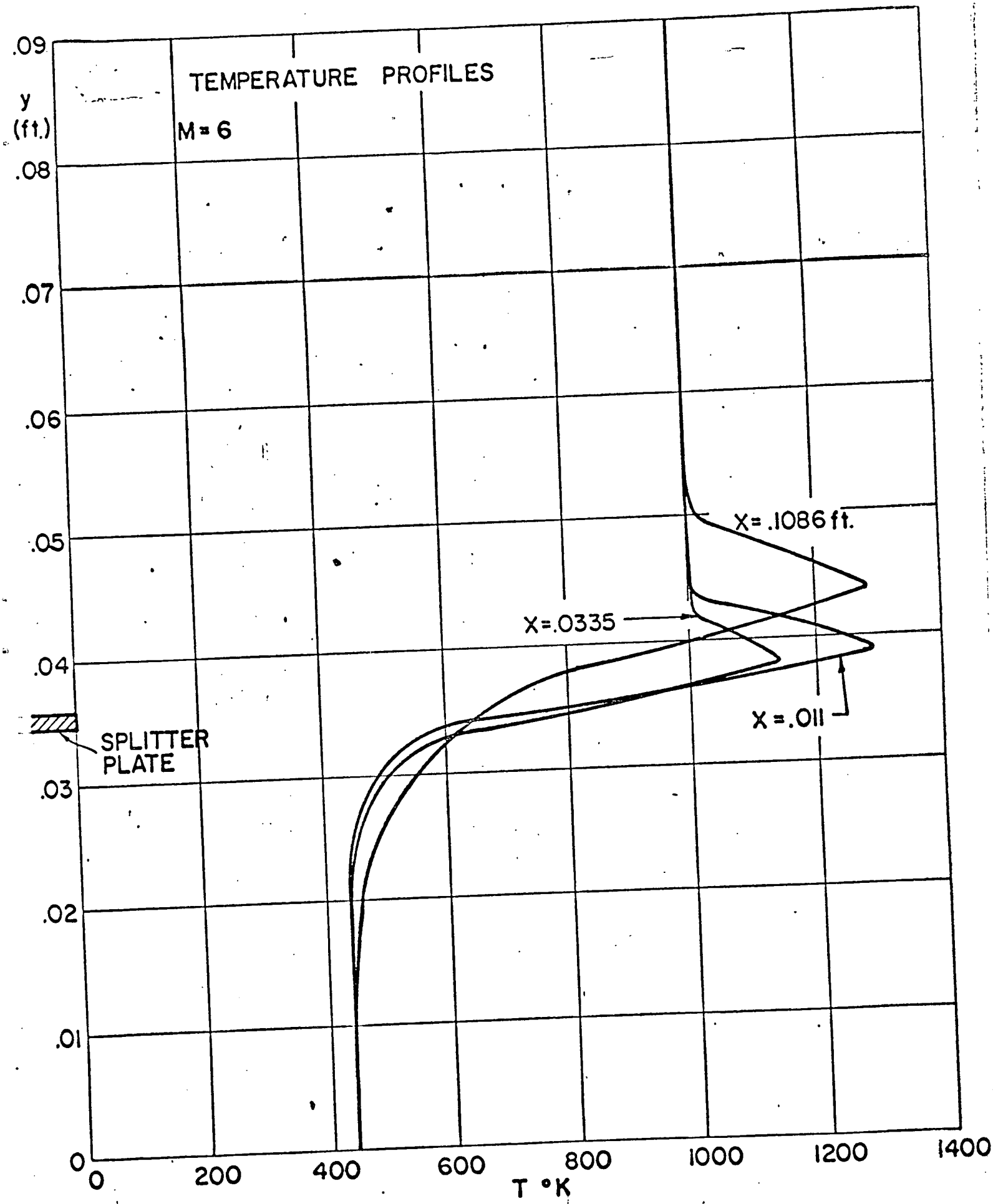

Fig. 10 Temperature profiles at various axial stations

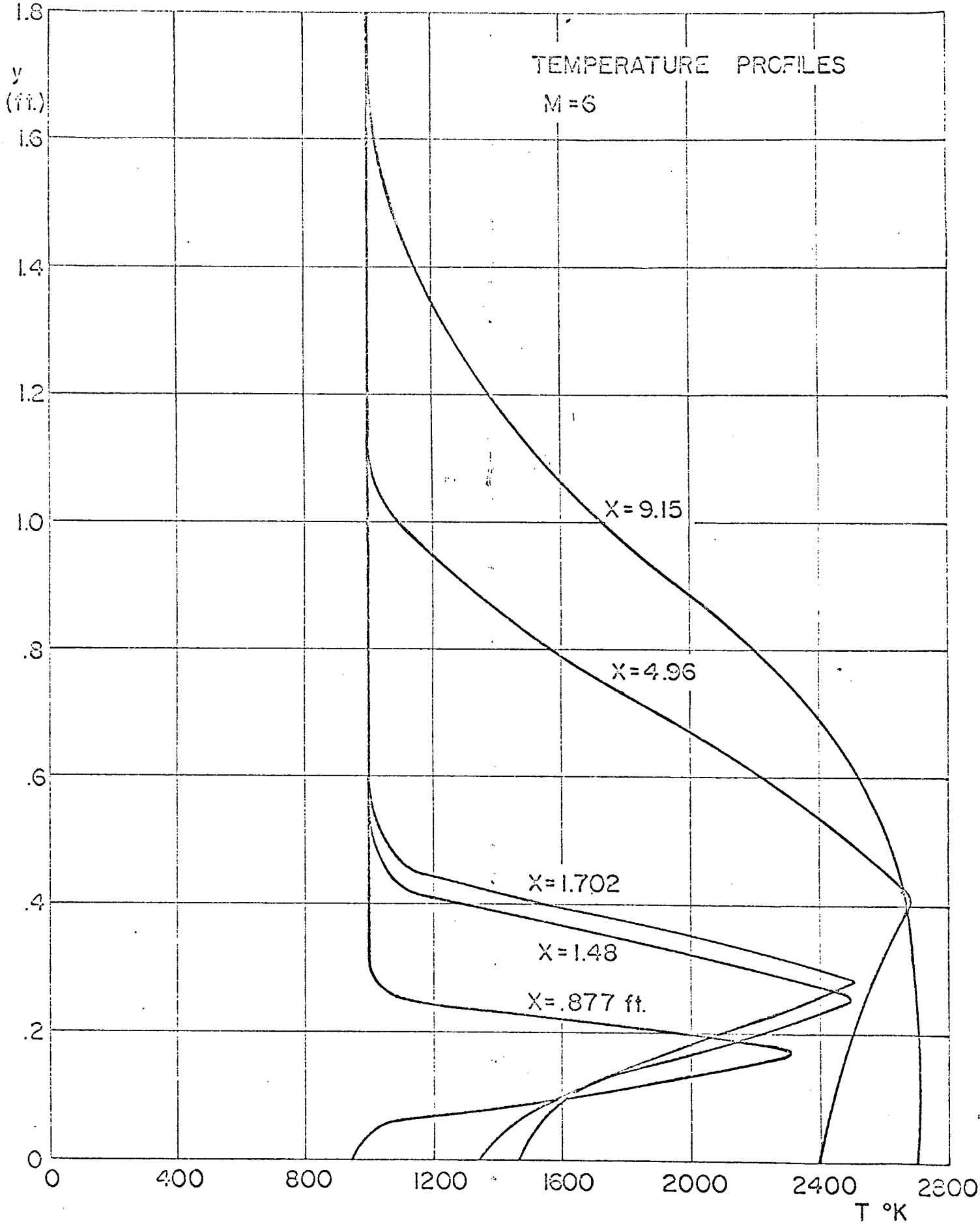

Fig. 10 cont'd Temperature profiles at various axial stations

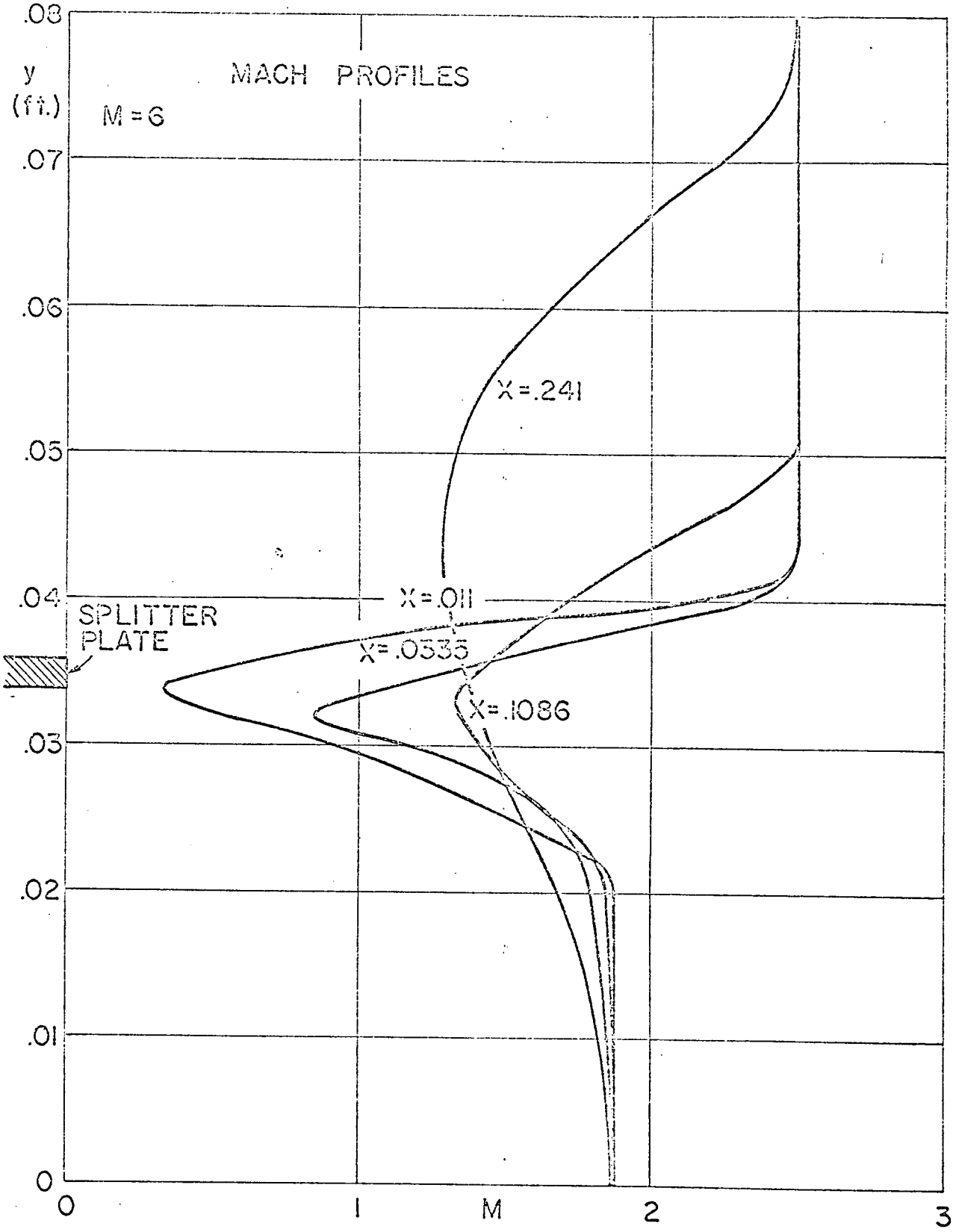

Fig. 10 Mach number profiles at various axial stations

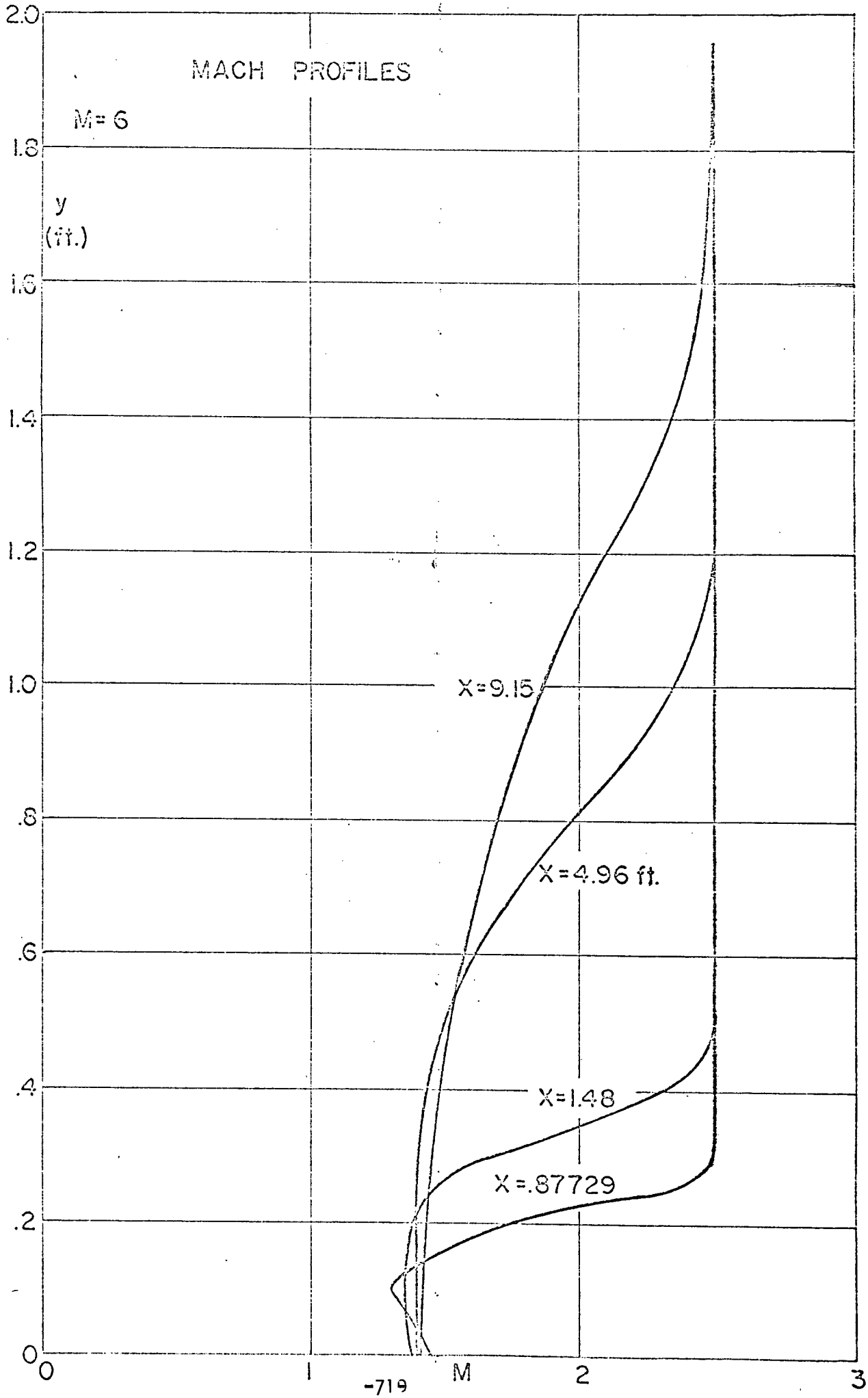
MACH PROFILES
M= 6
y
(ft.)
2.0
1.8
1.6
1.4
1.2
1.0
.8
.6
.4
.2
0
0
1
M
2
3
X=9.15
X=4.96 ft.
X=1.48
X=.87729

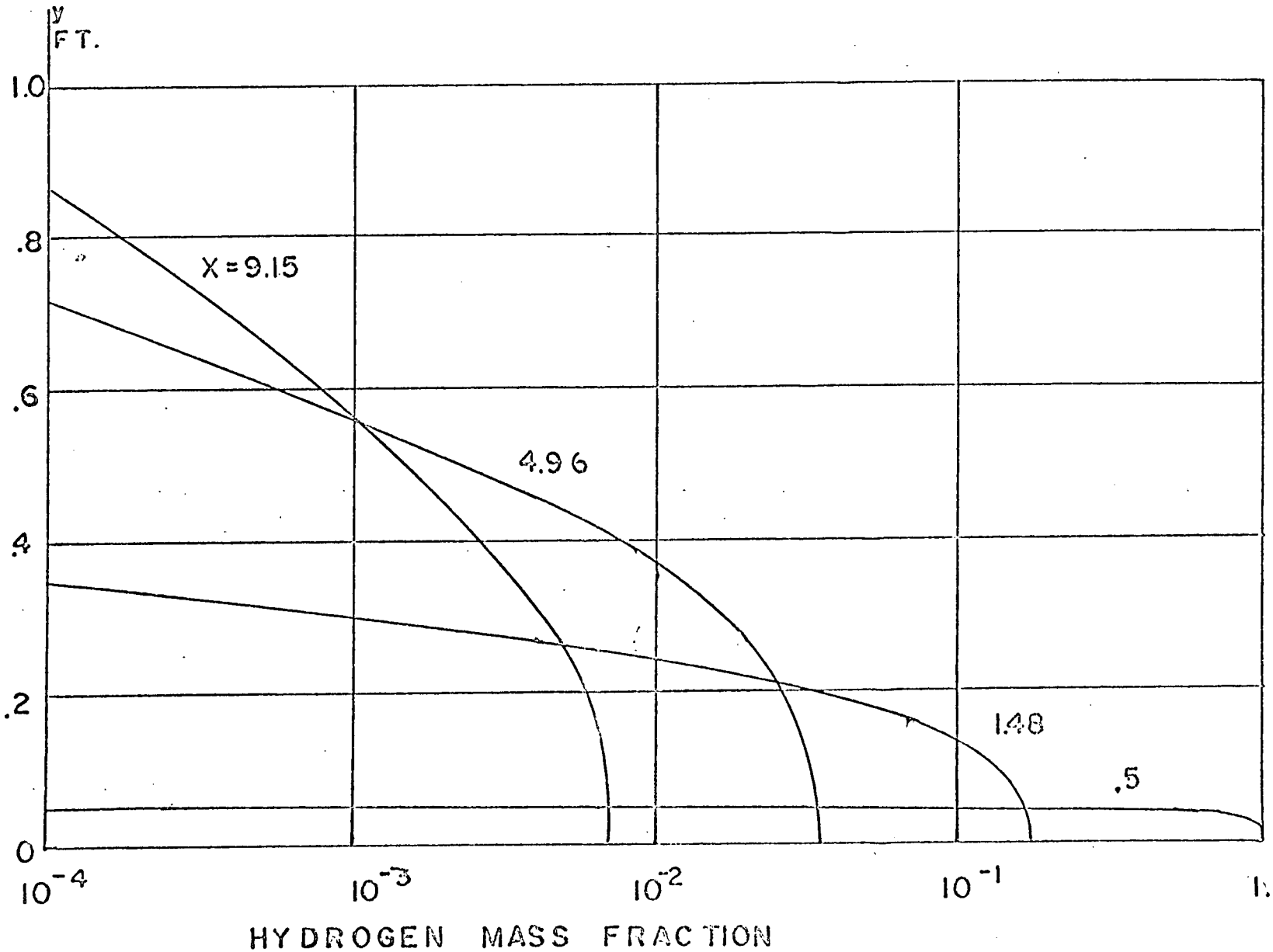

Fig. 10 Cont'd Hydrogen Mass fraction Profiles at various stations

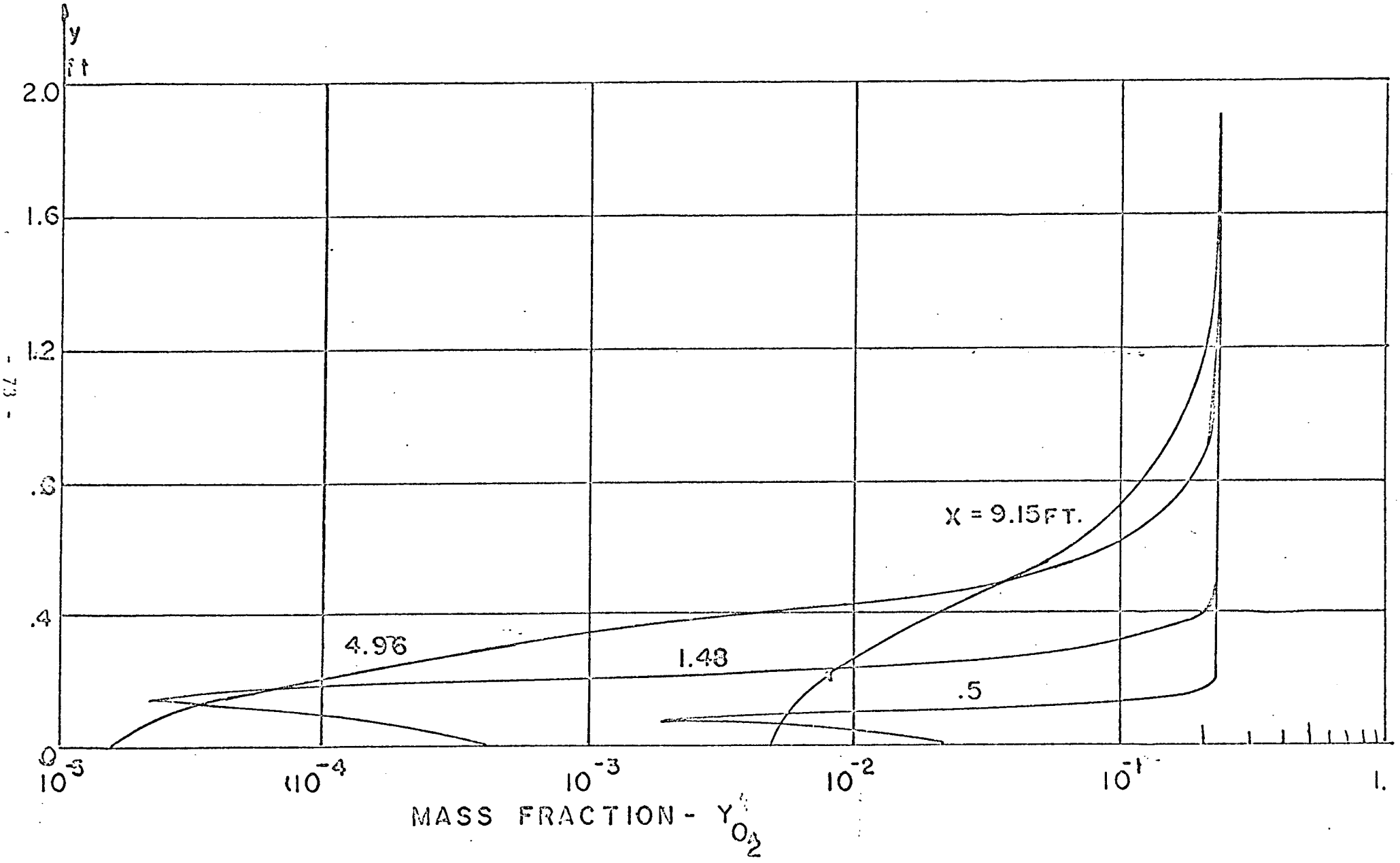

Fig. 10 Cont'd Oxygen mass fraction profiles at various axial stations

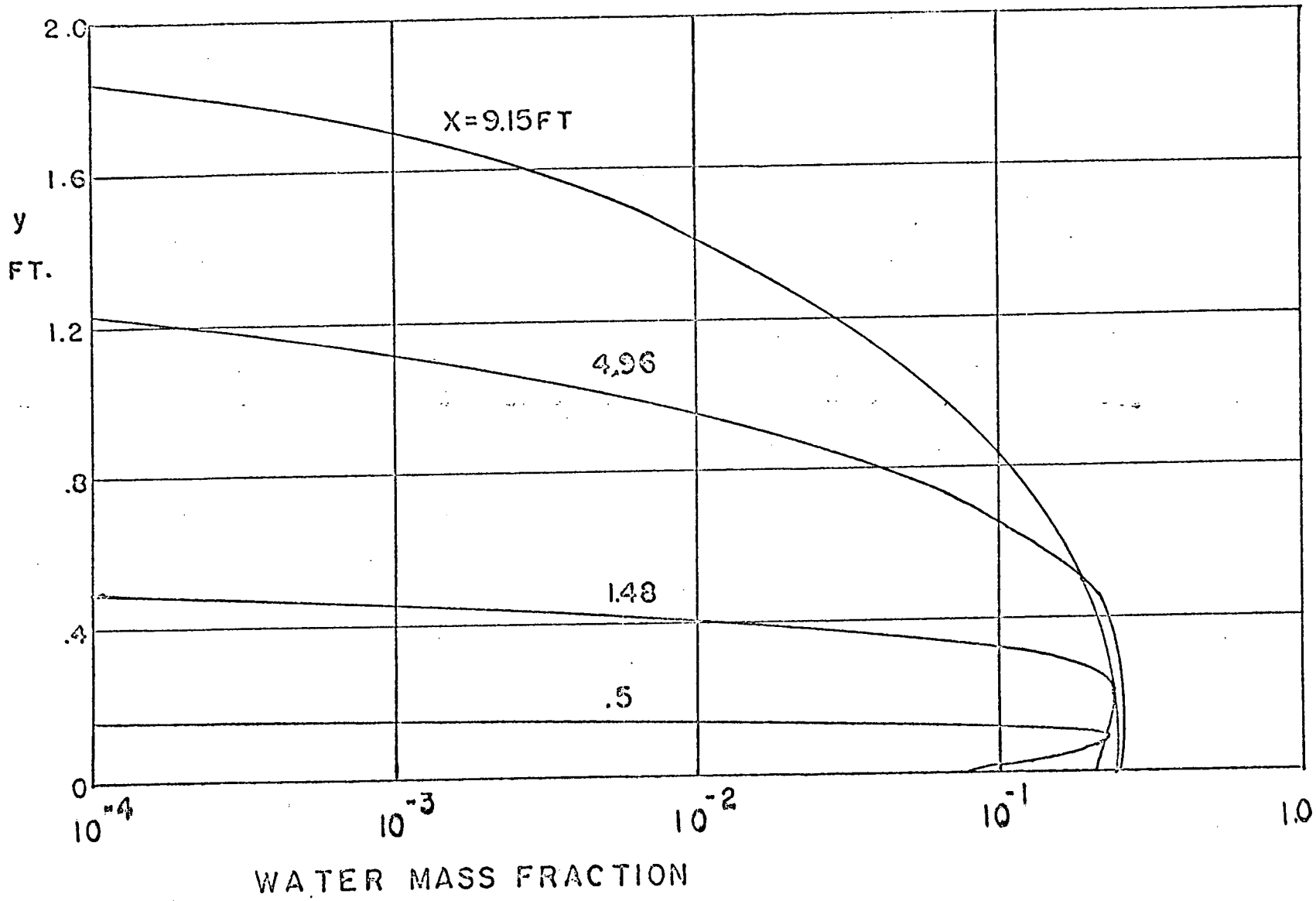

Fig. 10 Cont'd Water mass fraction profiles at various axial stations

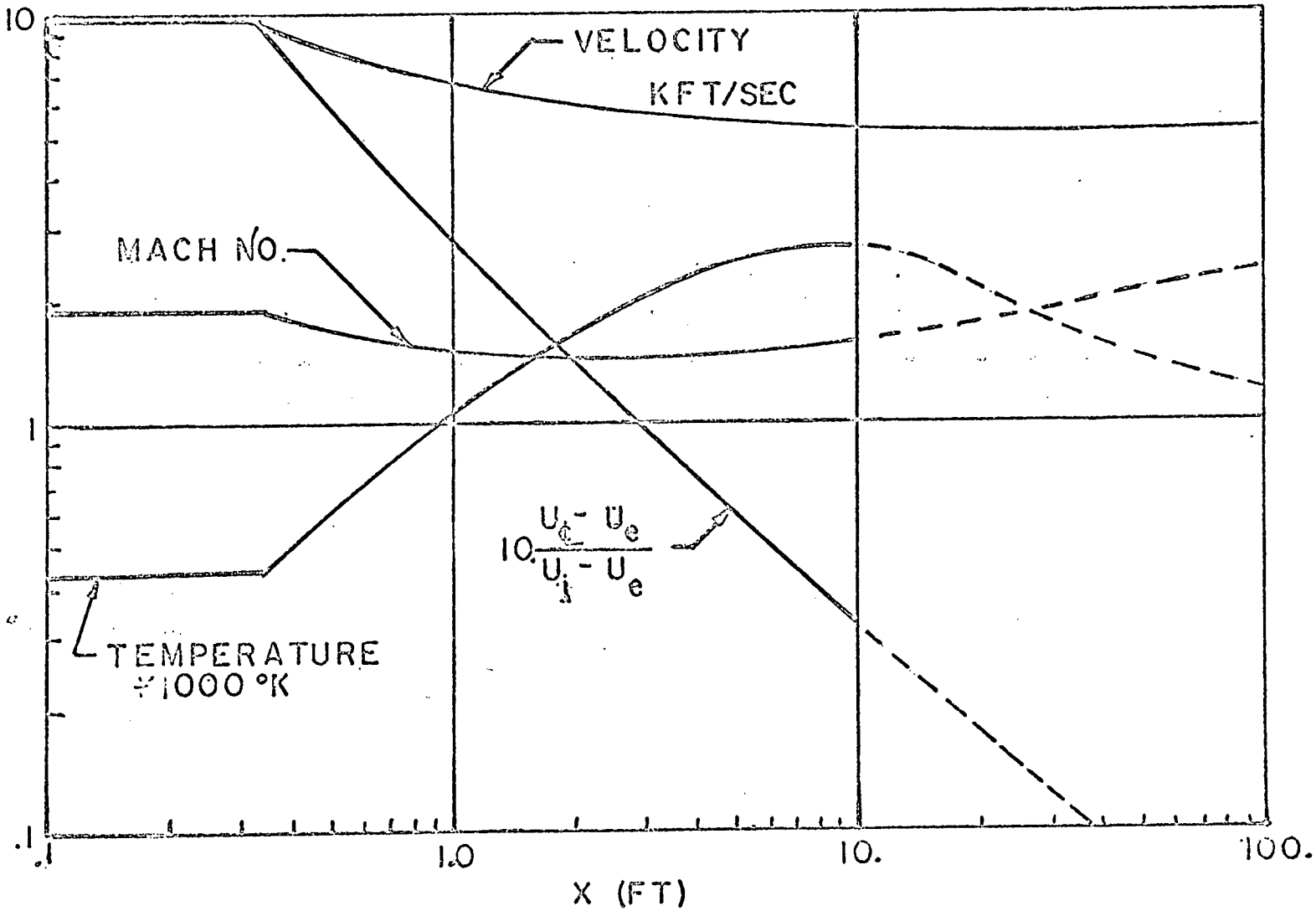

Fig. 11 Centerline properties

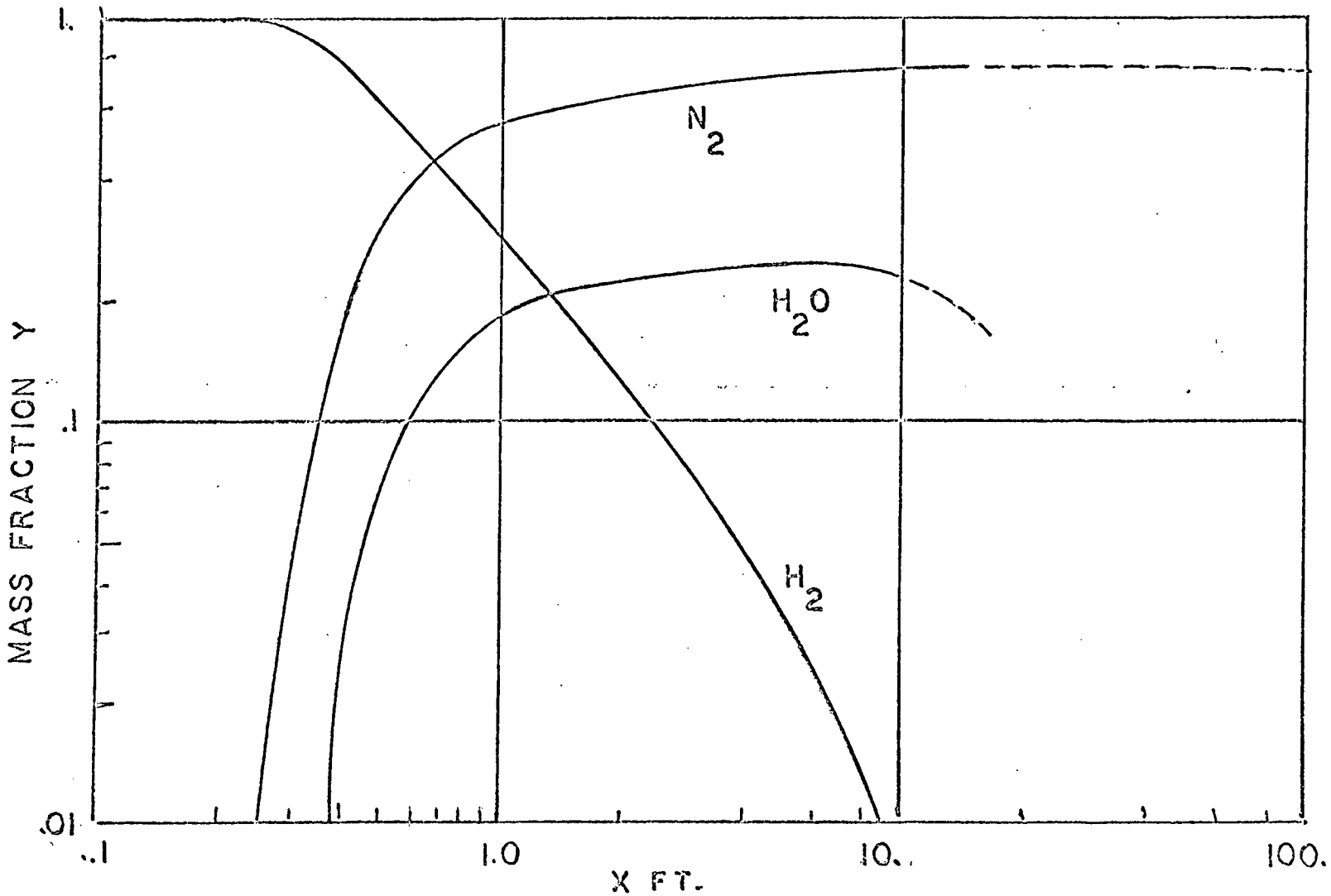

Fig. 11 Cont'd Centerline properties - mass fractions

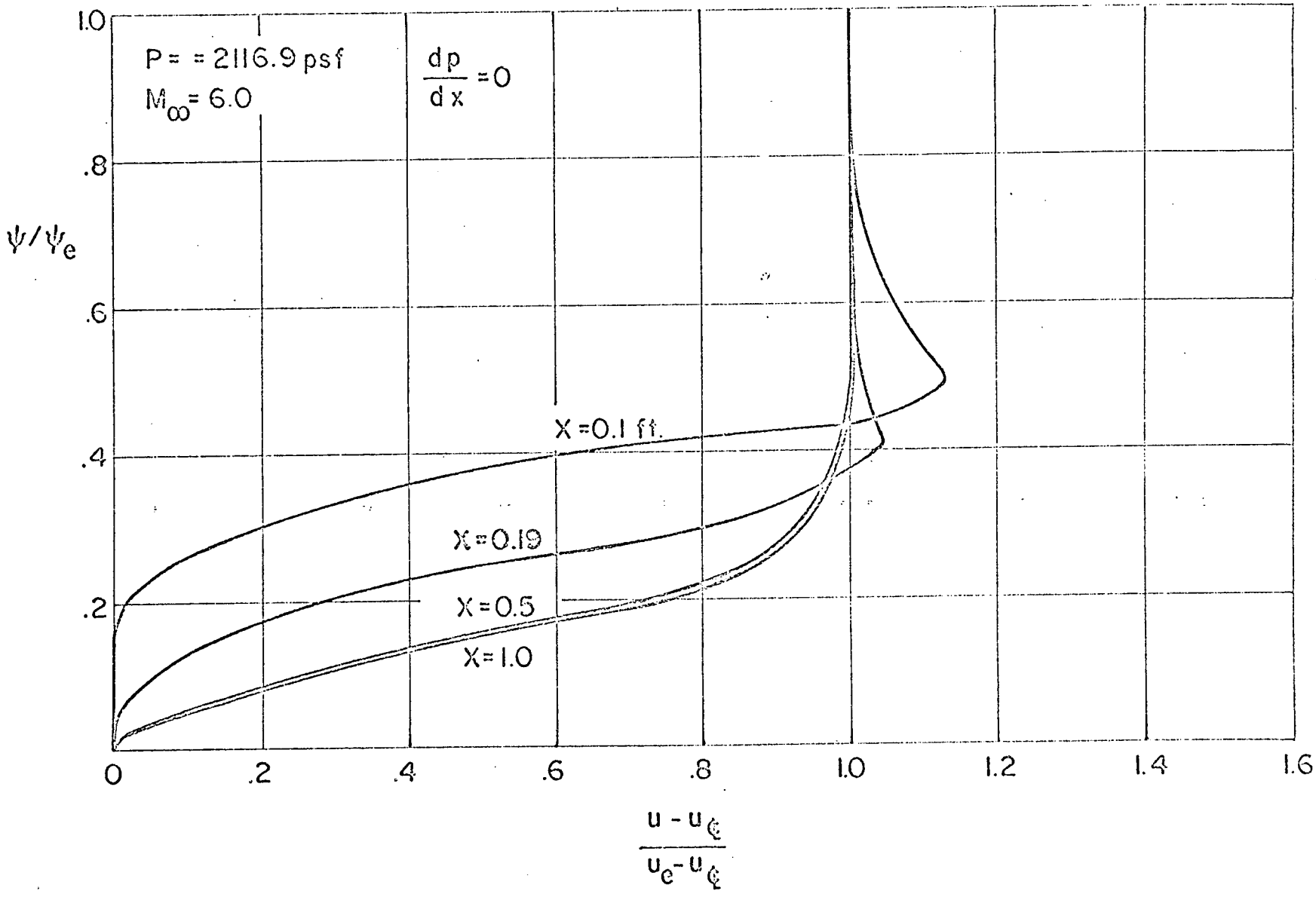

Fig. 12 Development of similar velocity profiles

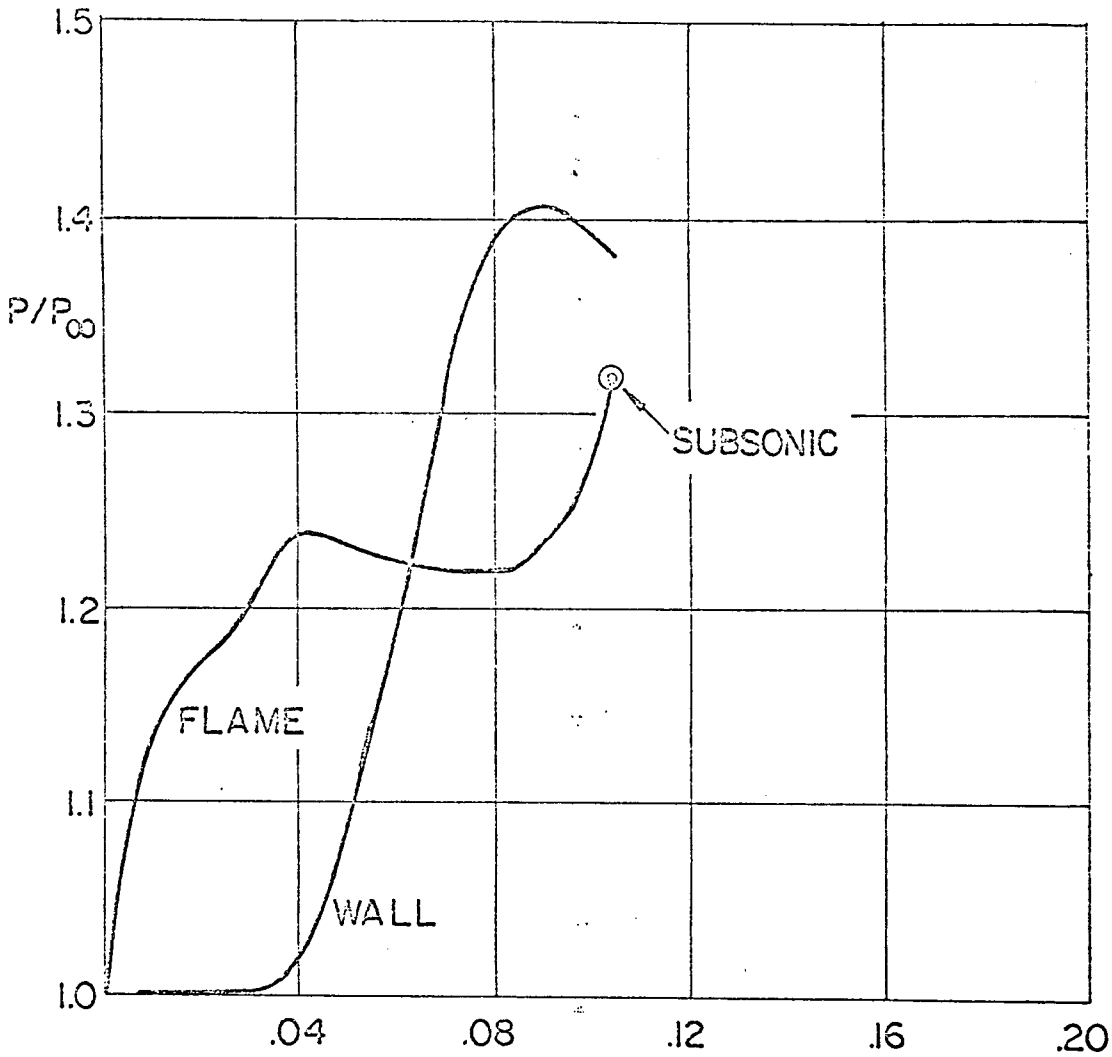

Fig. 13 Static pressure distribution along the flame and wall of a straight wall injector

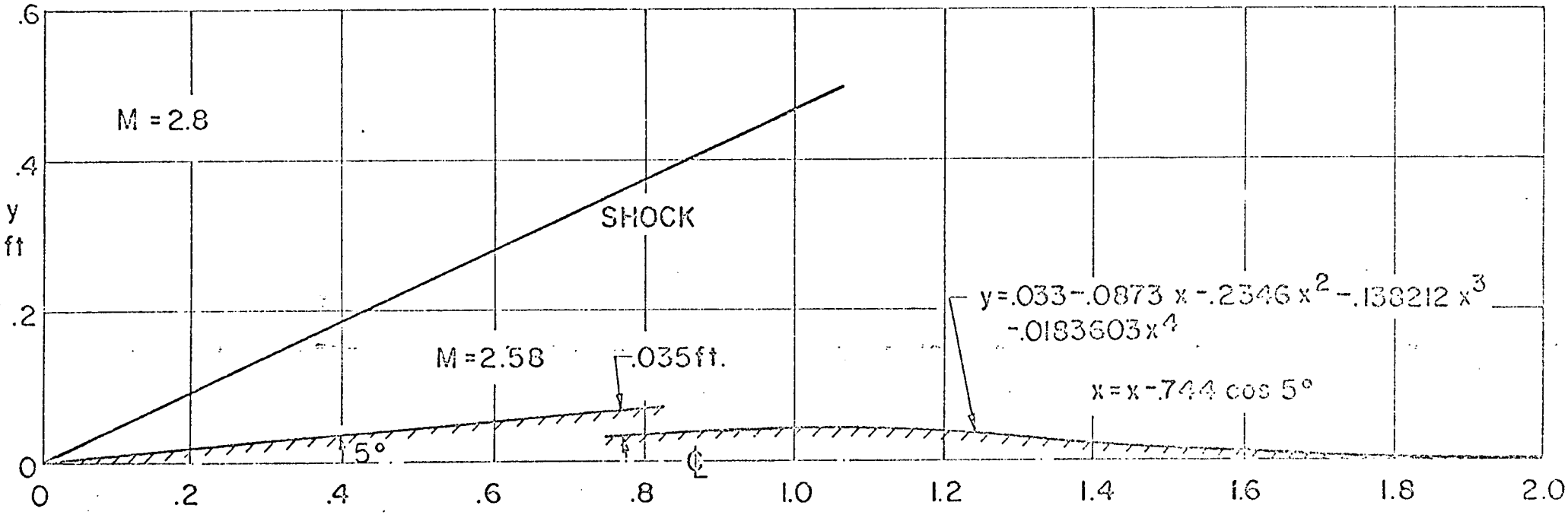

Fig. 14 Geometry of curved wall injector

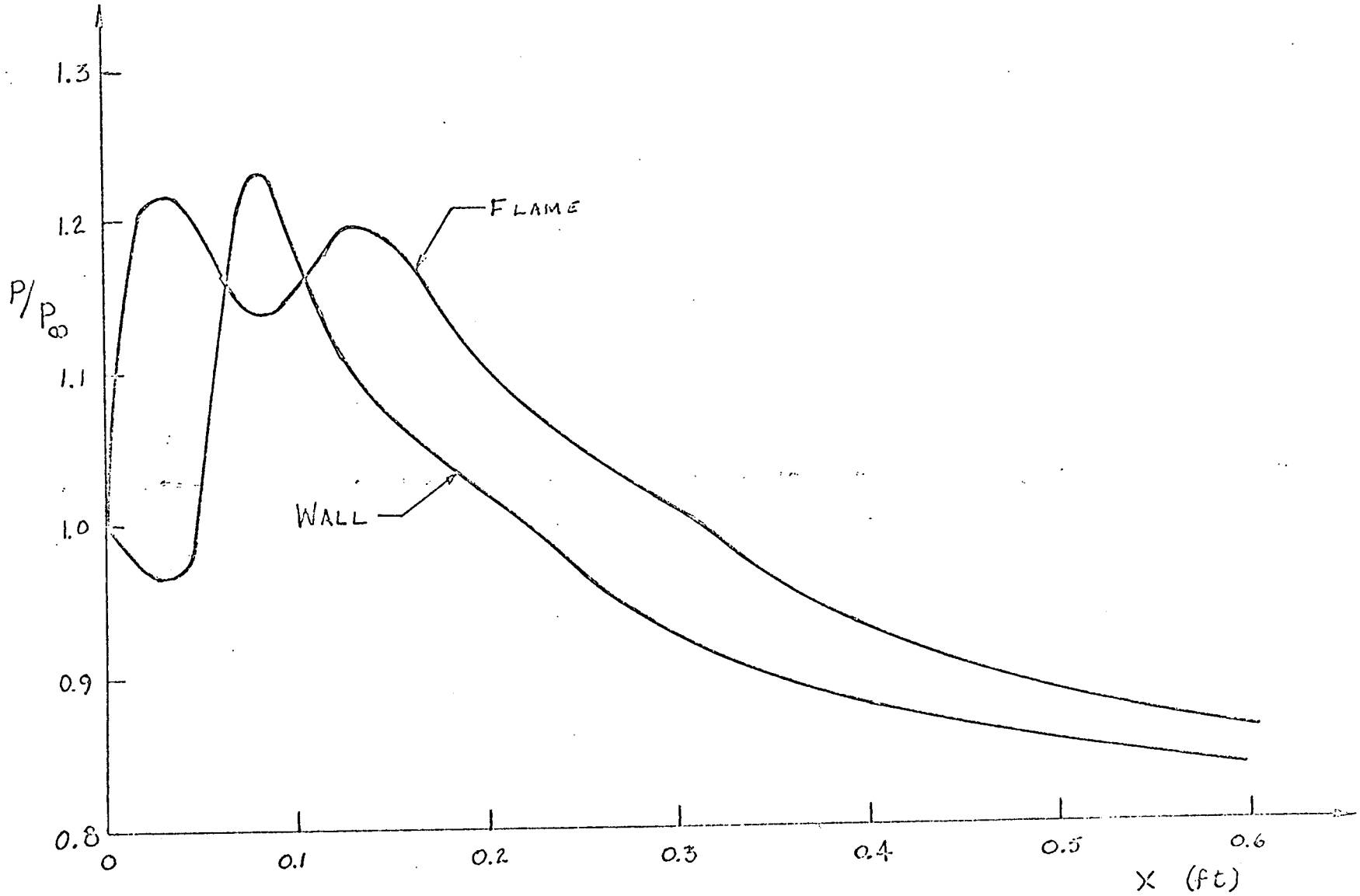

Fig. 15 Pressure distributions for injector of figure 14

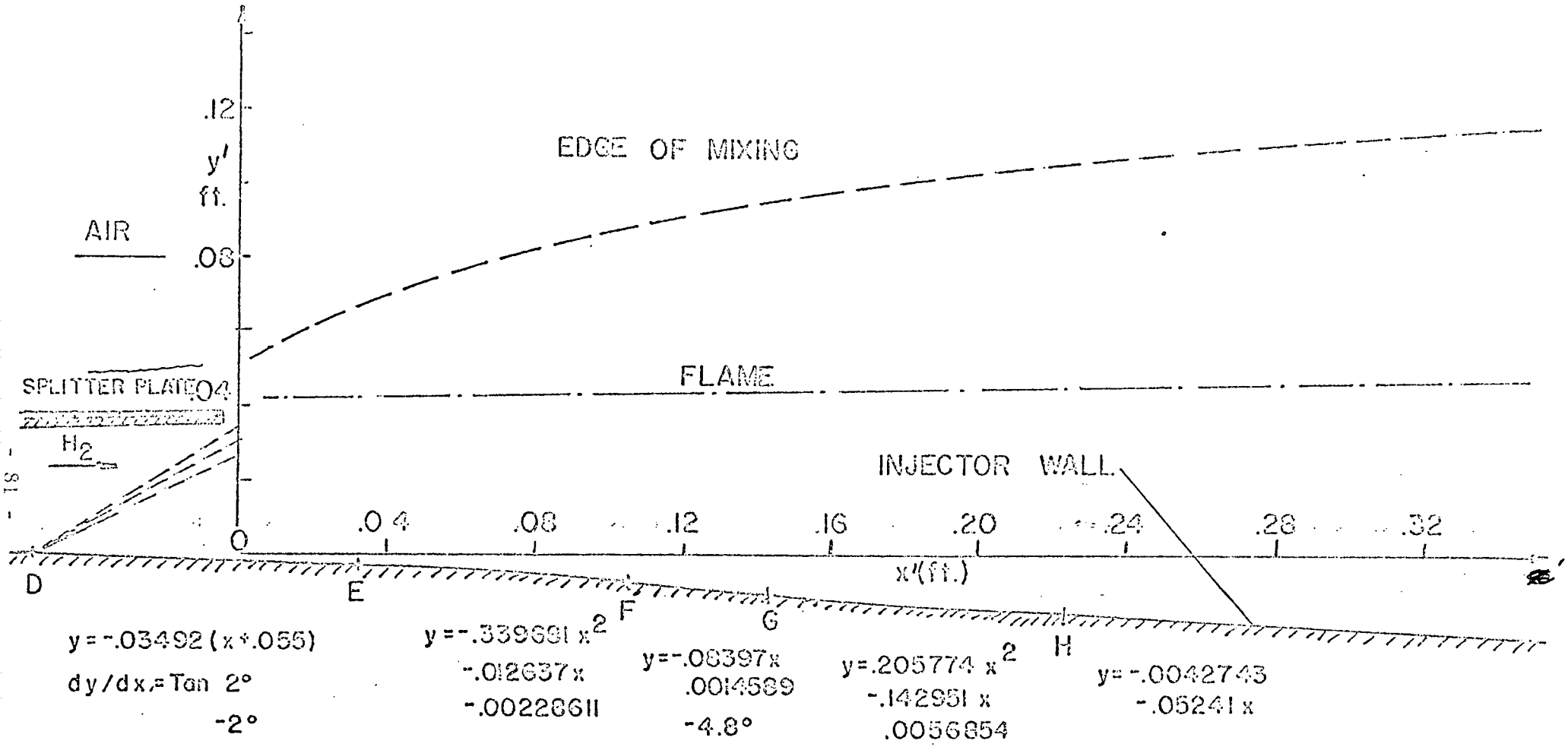

Fig. 16 Injector wall geometry that gives relatively constant pressure at the flame

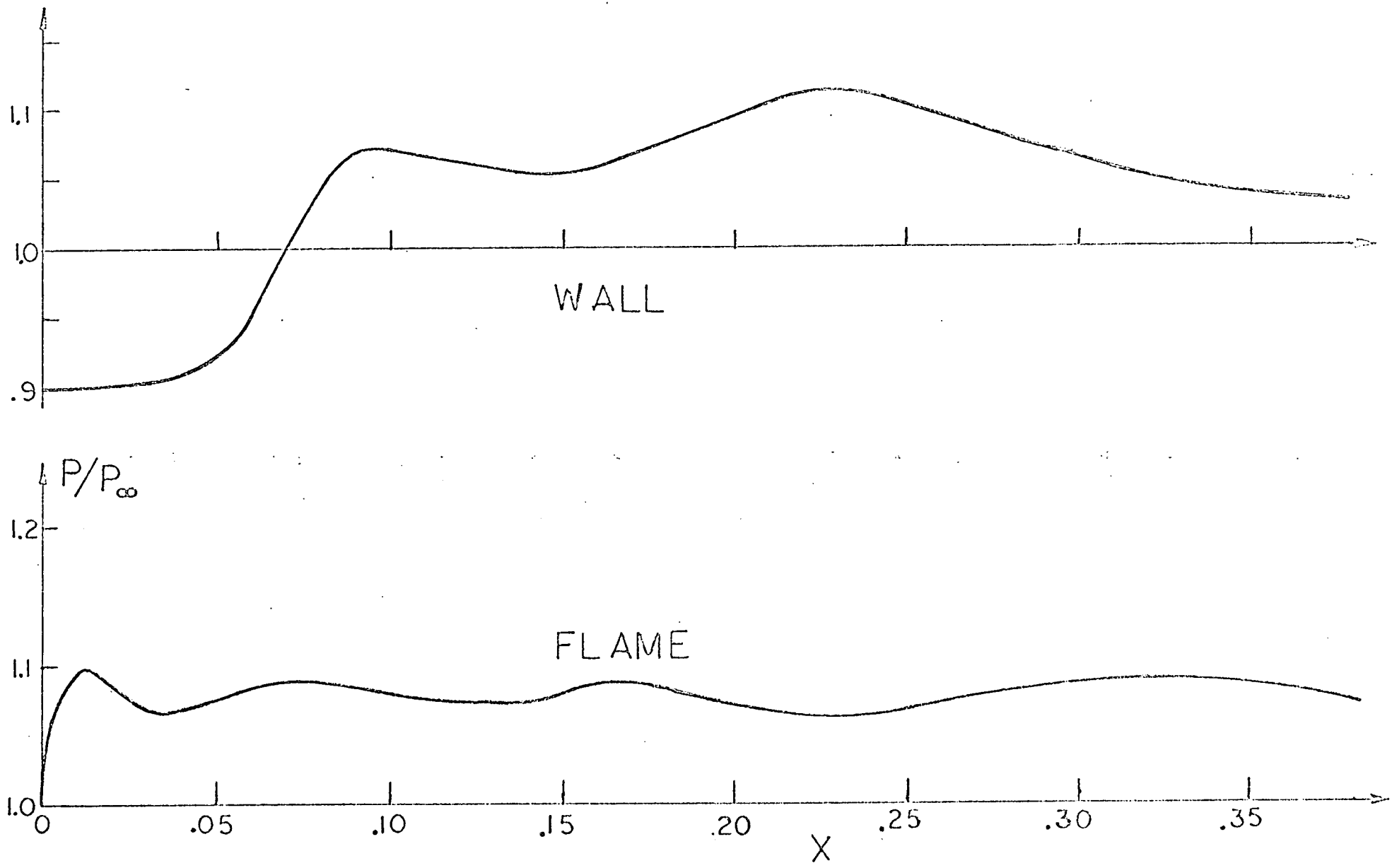

Fig. 17 Pressure distributions for injector shown in figure 16

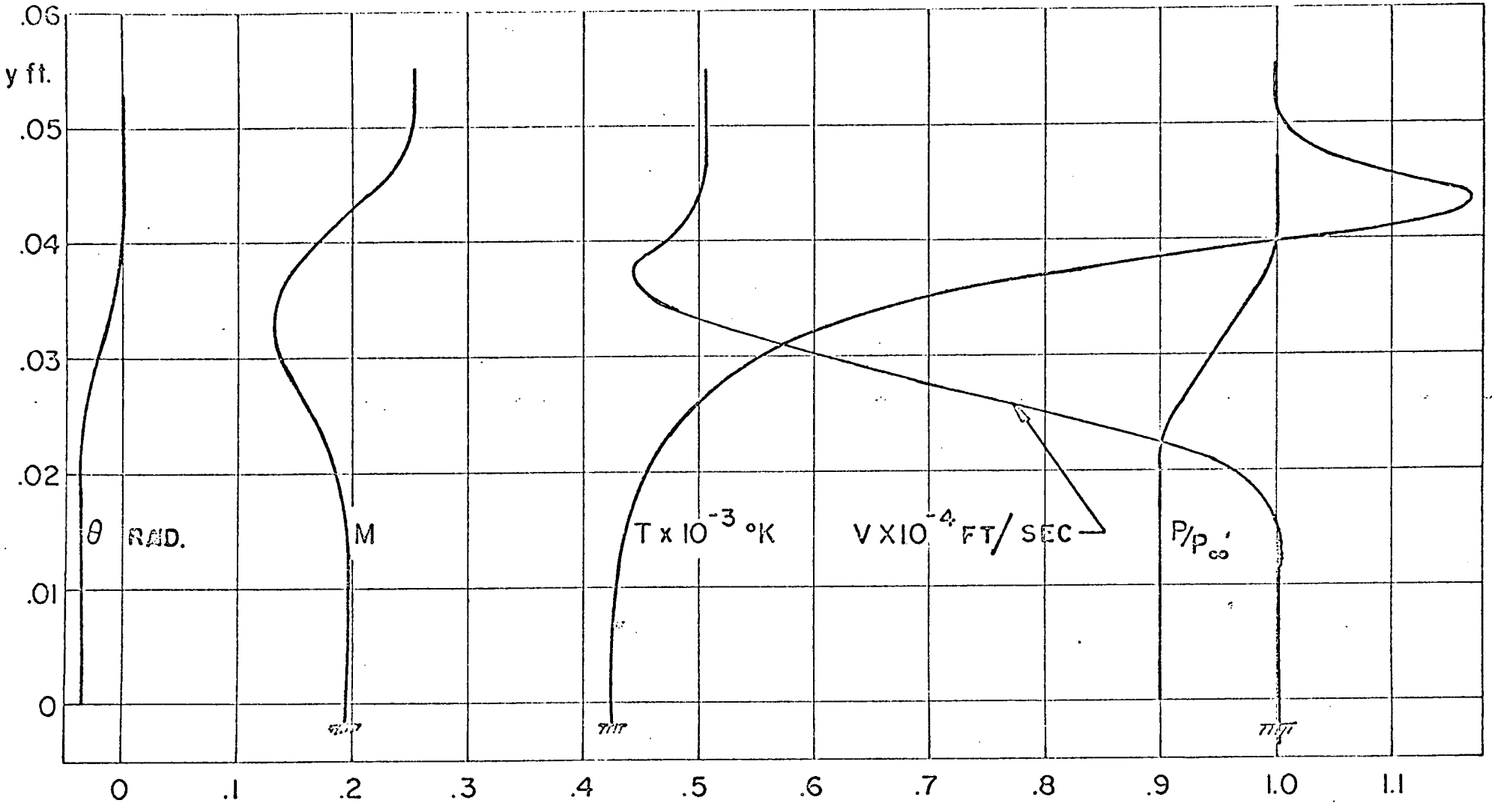

Fig. 18a Initial flow profiles used in the viscous characteristics analysis

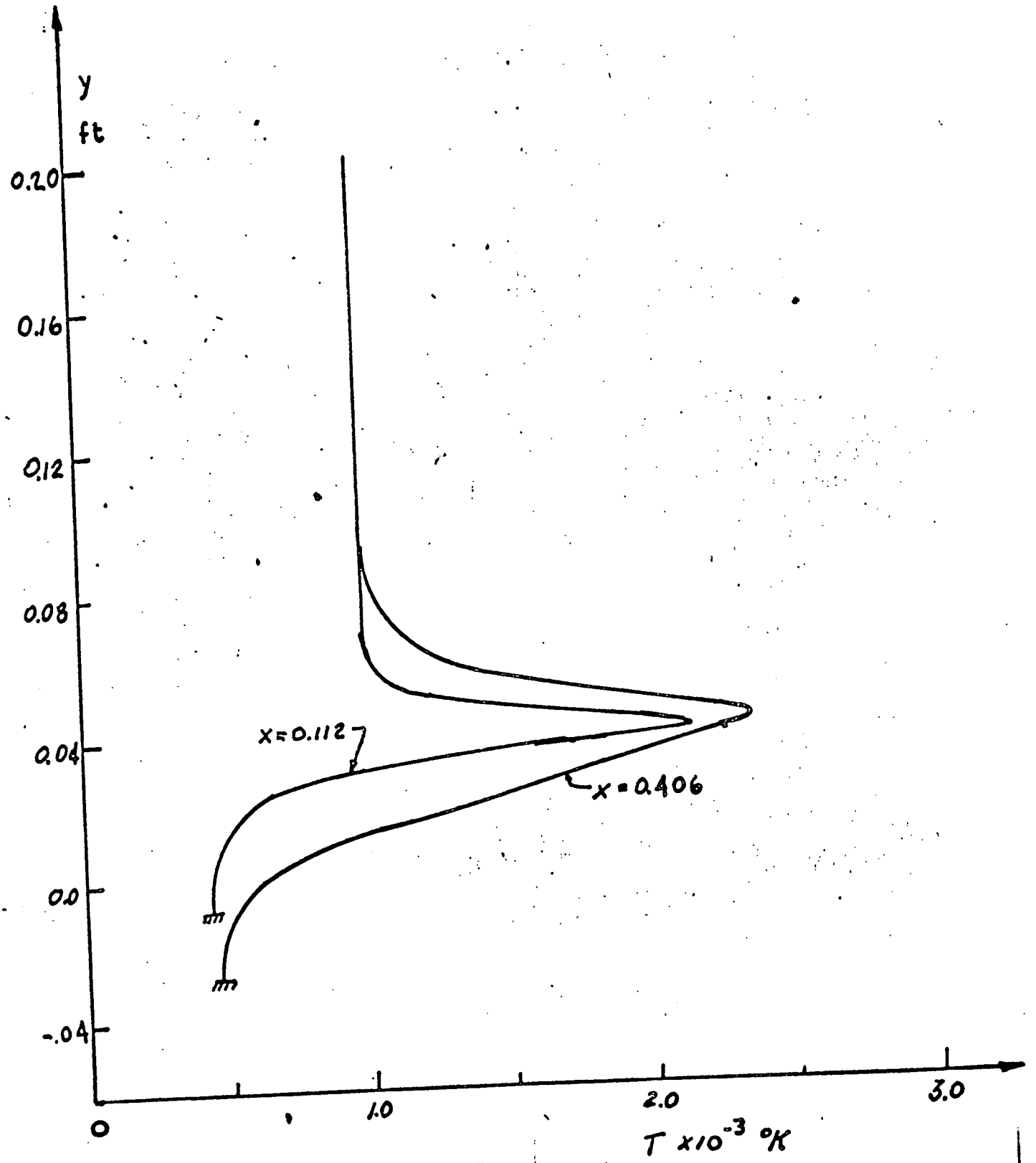

Fig. 18 Flow profiles in the flow field produced by the injector of fig. 16

Temperature profiles

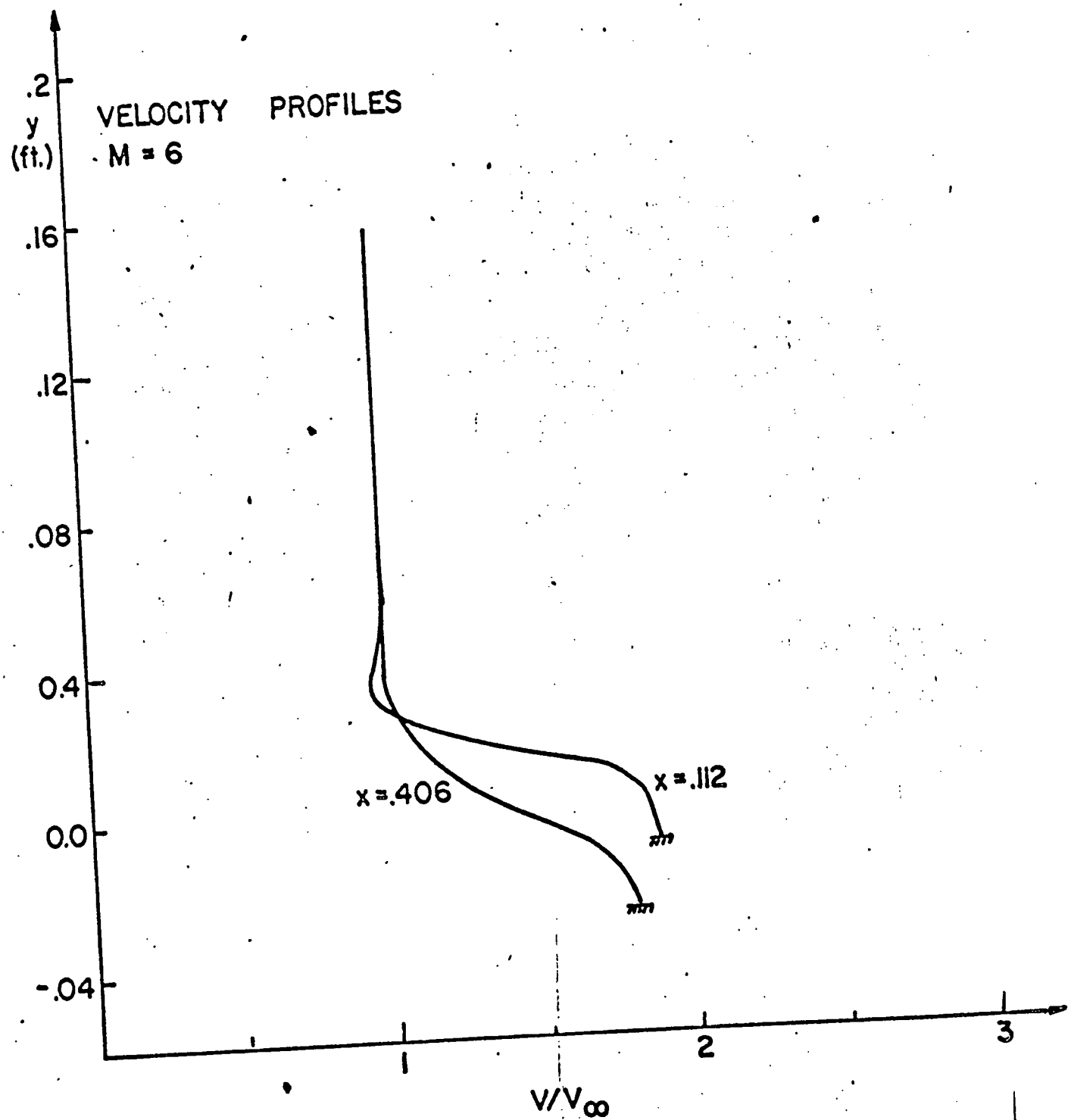

Fig. 18 VCont'd - Velocity profiles

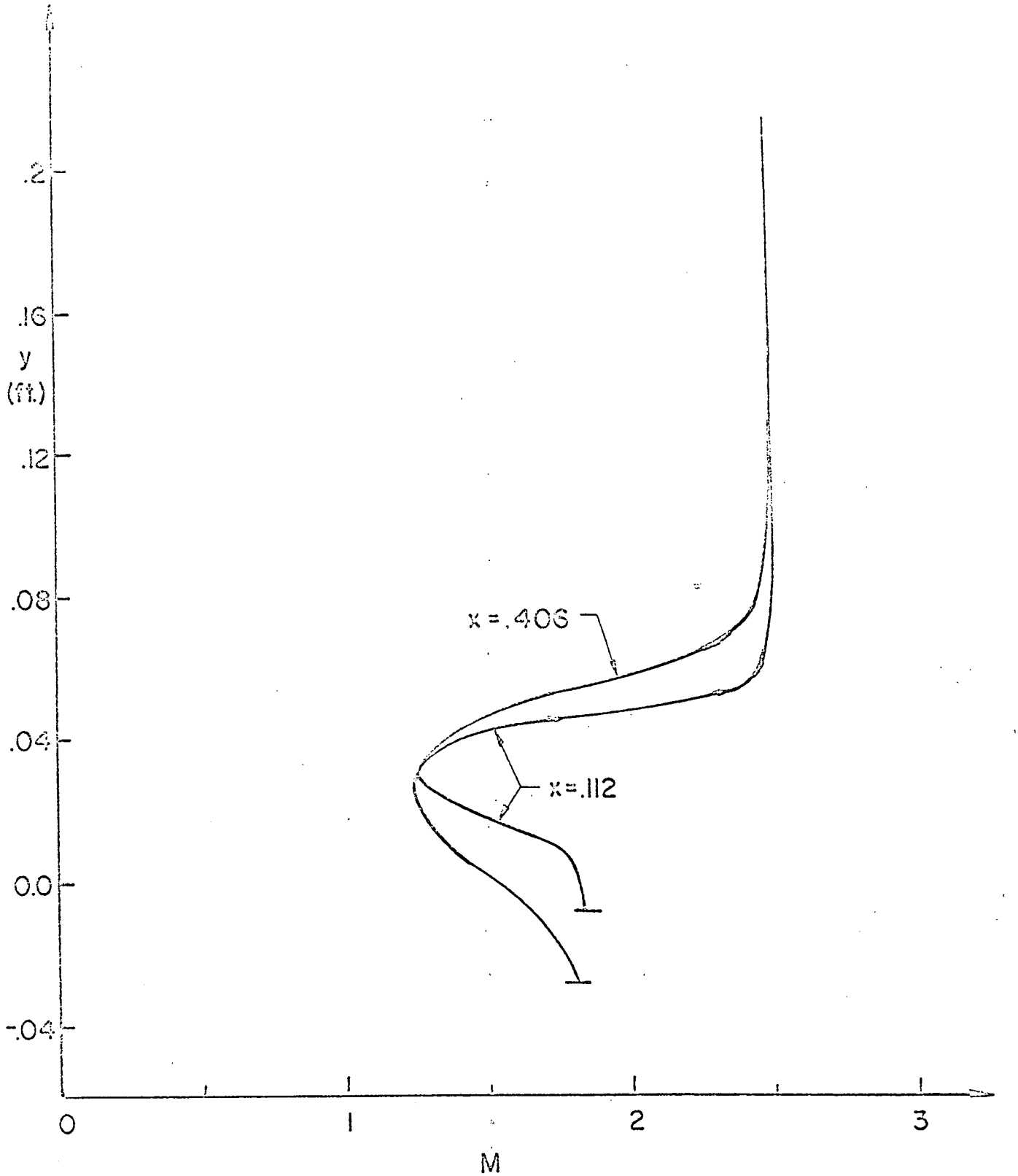

Fig. 18 Cont'd - Mach number profiles

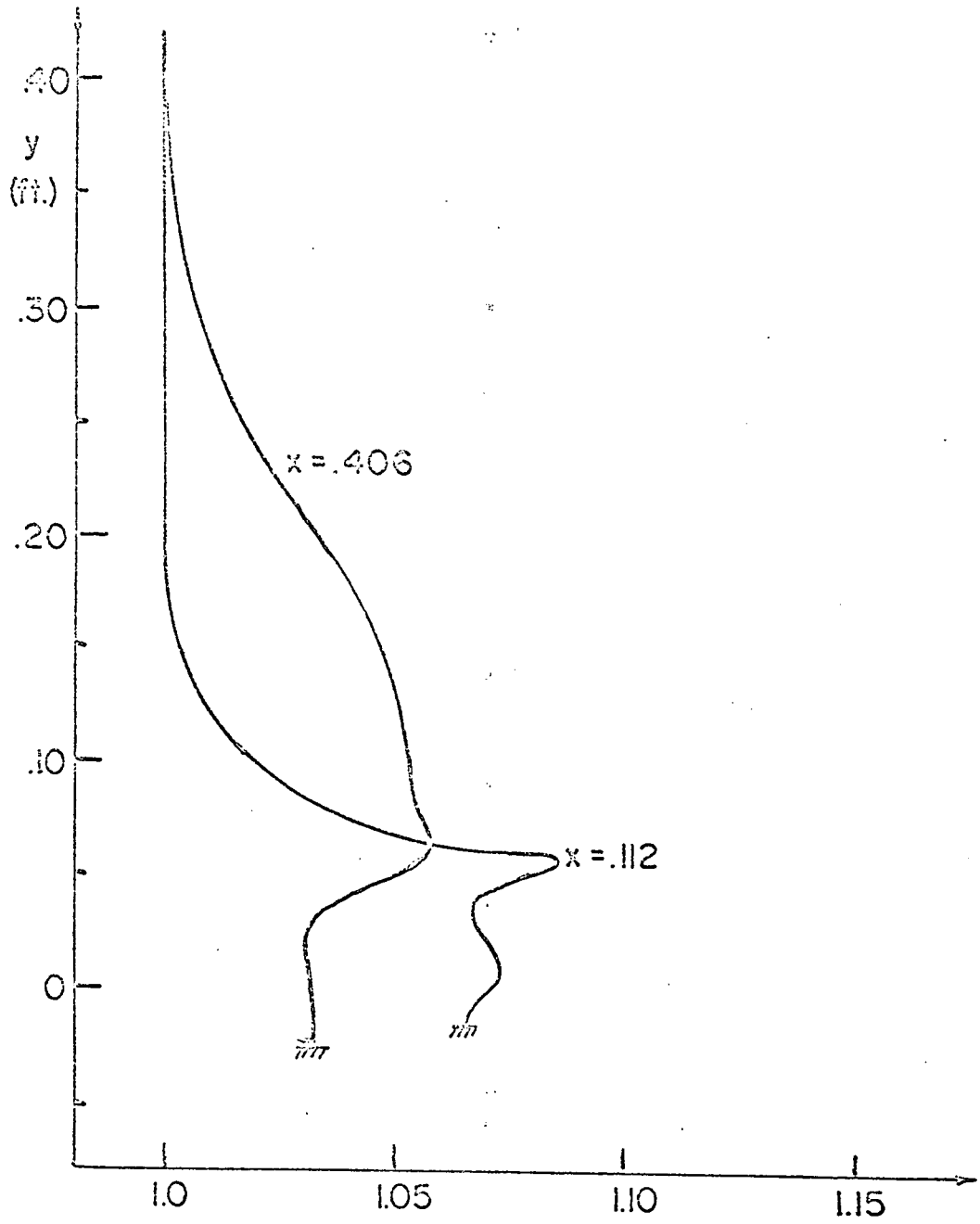

Fig. 18 Cont'd - Static pressure profile

Fig. 18 Cont'd species mass fraction profiles at x=0.0 ft.

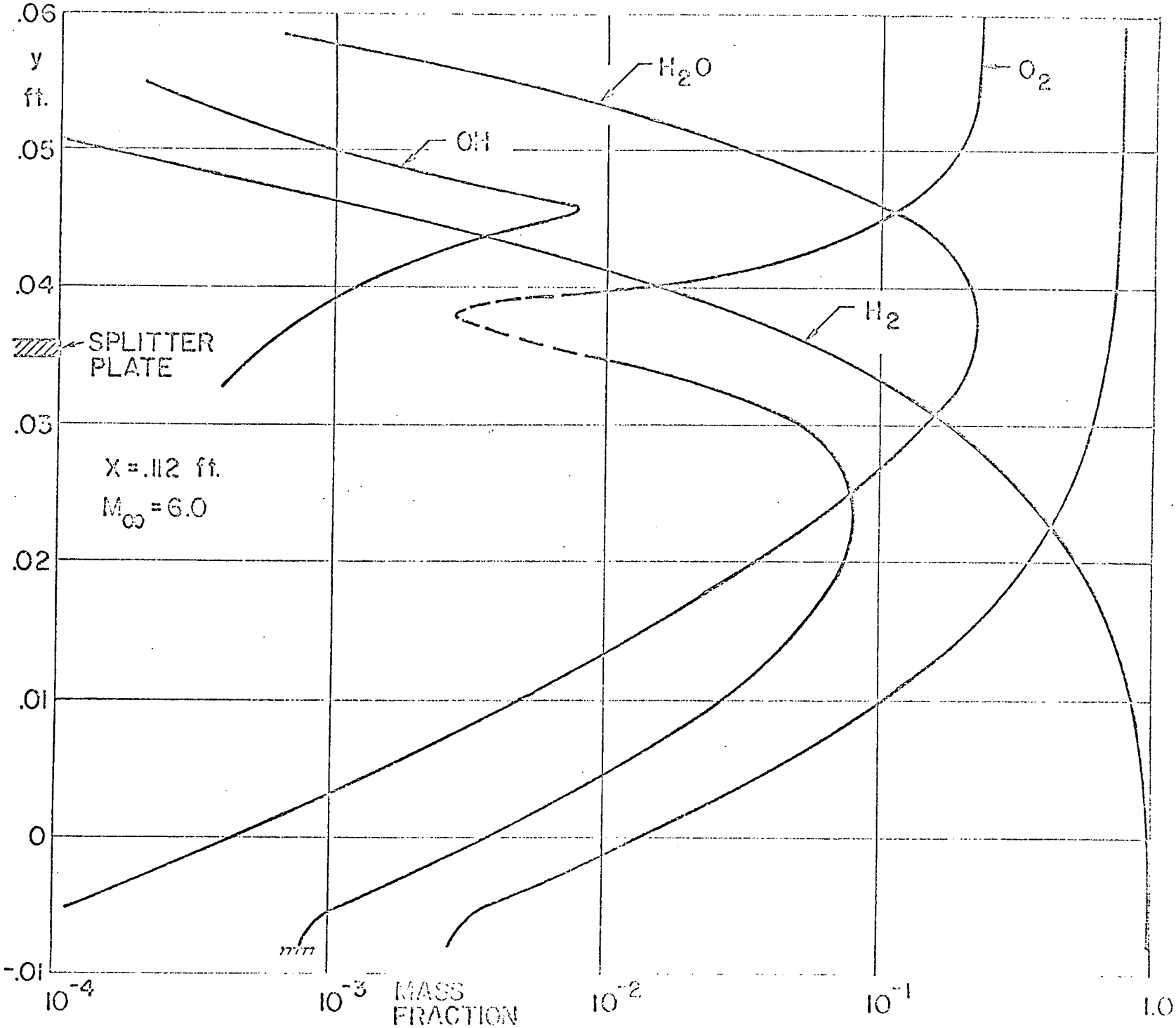

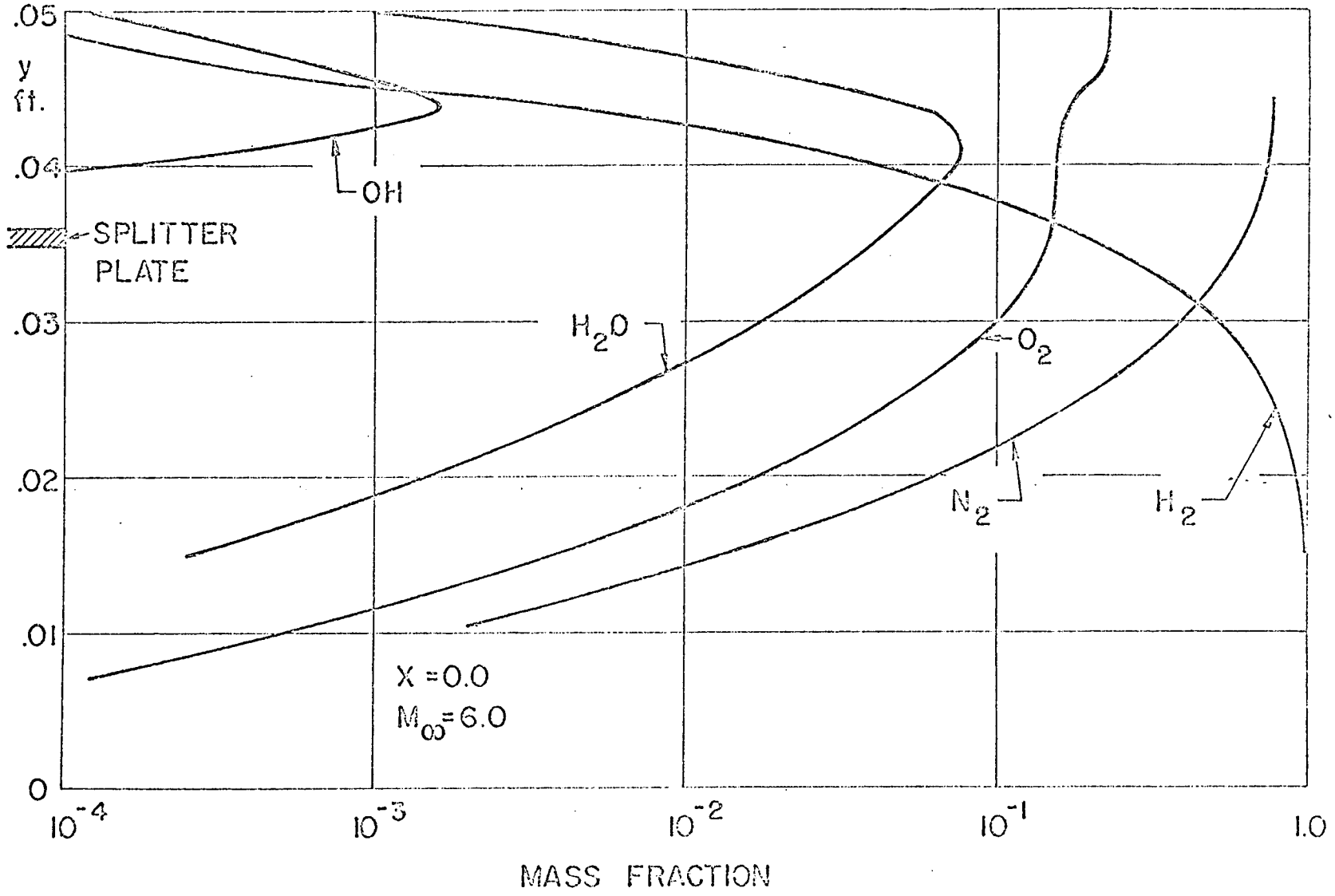

Fig. 18 Cont'd Species mass fraction profiles at x'=0.112 ft.

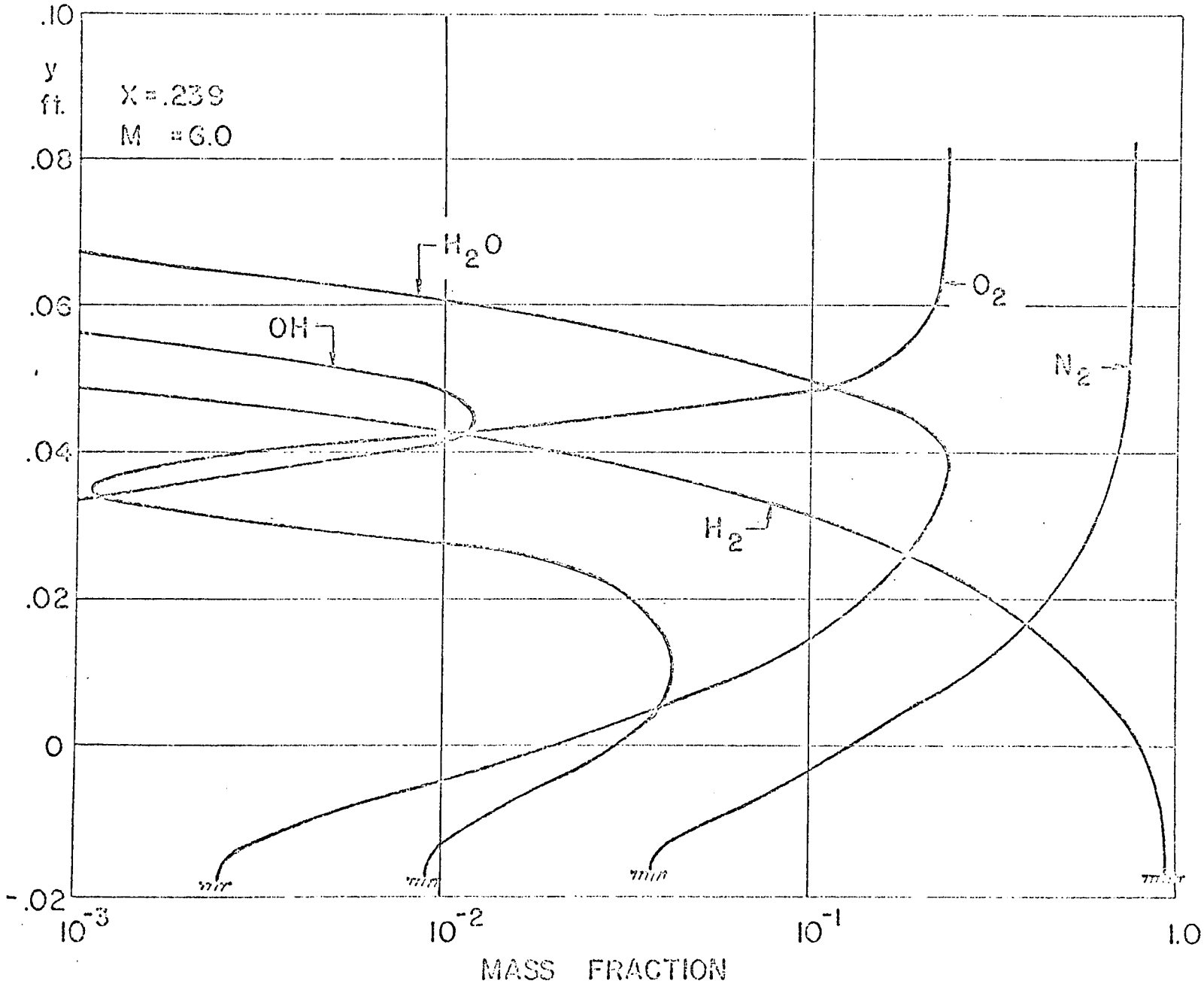

Fig. 18 Cont'd Species mass fraction profiles at x'=0.239 ft

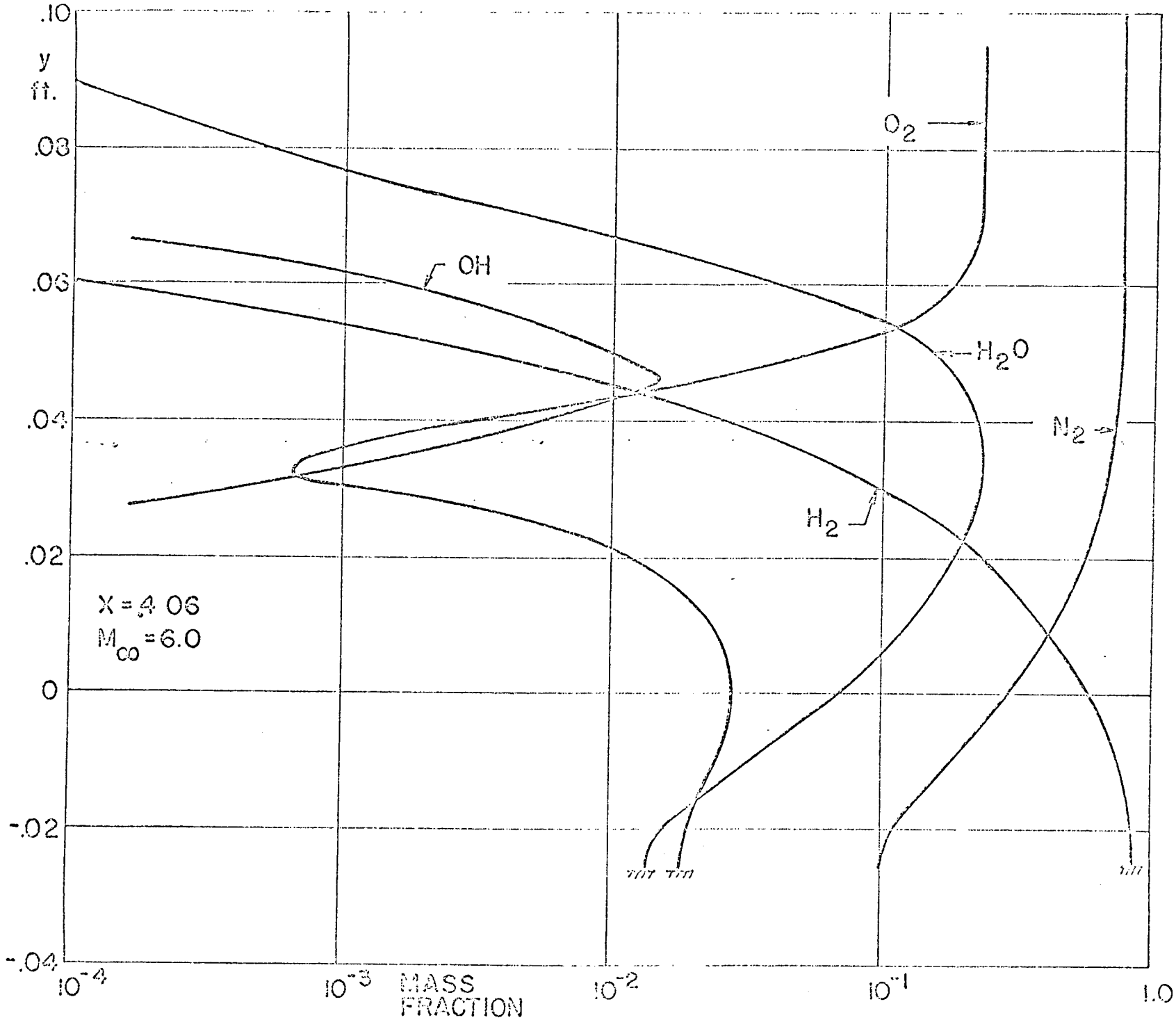

Fig. 18 Cont'd Species mass fraction profiles at t = 0.46 ft.

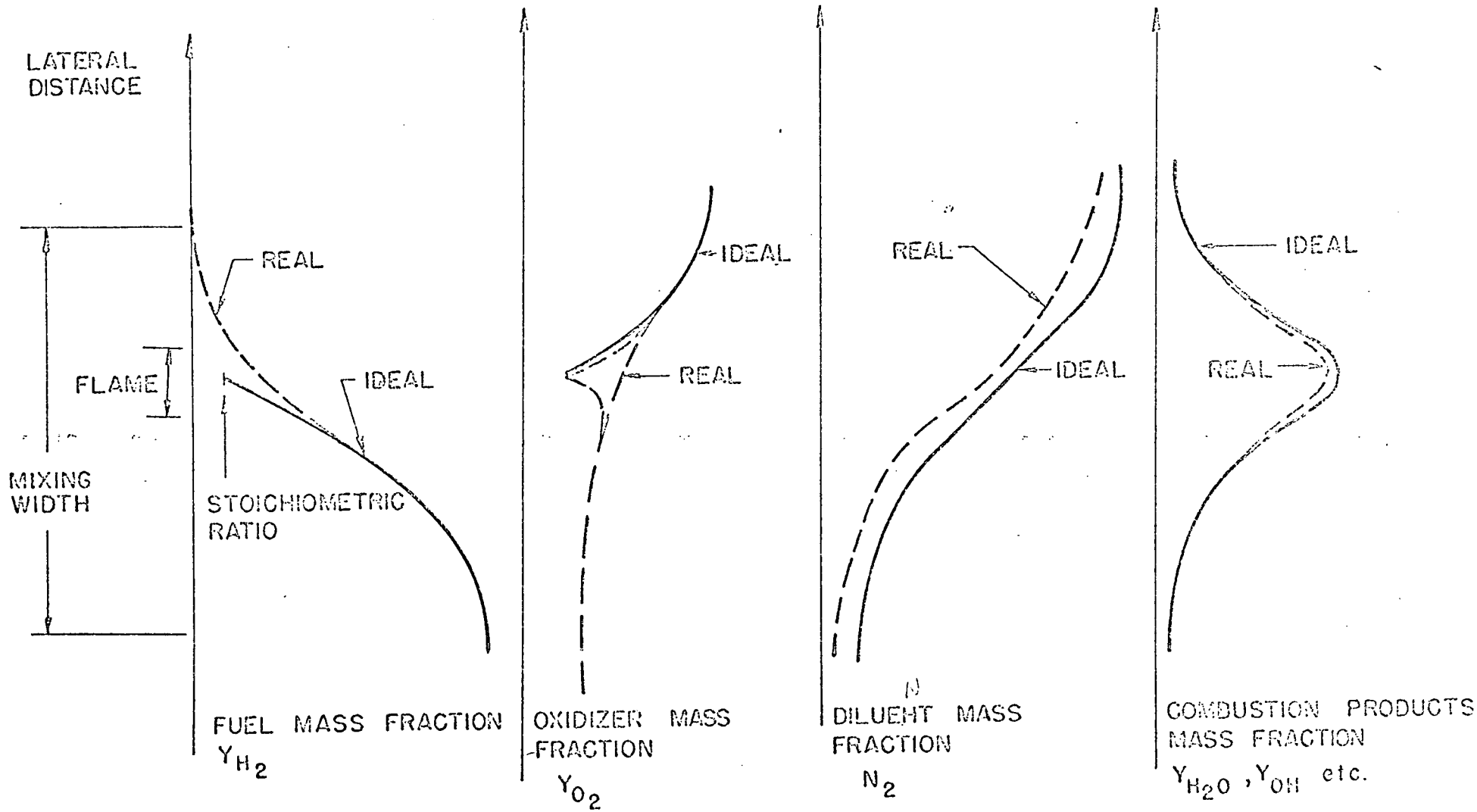

Fig. 19 Flow profiles with ideal and real combustion

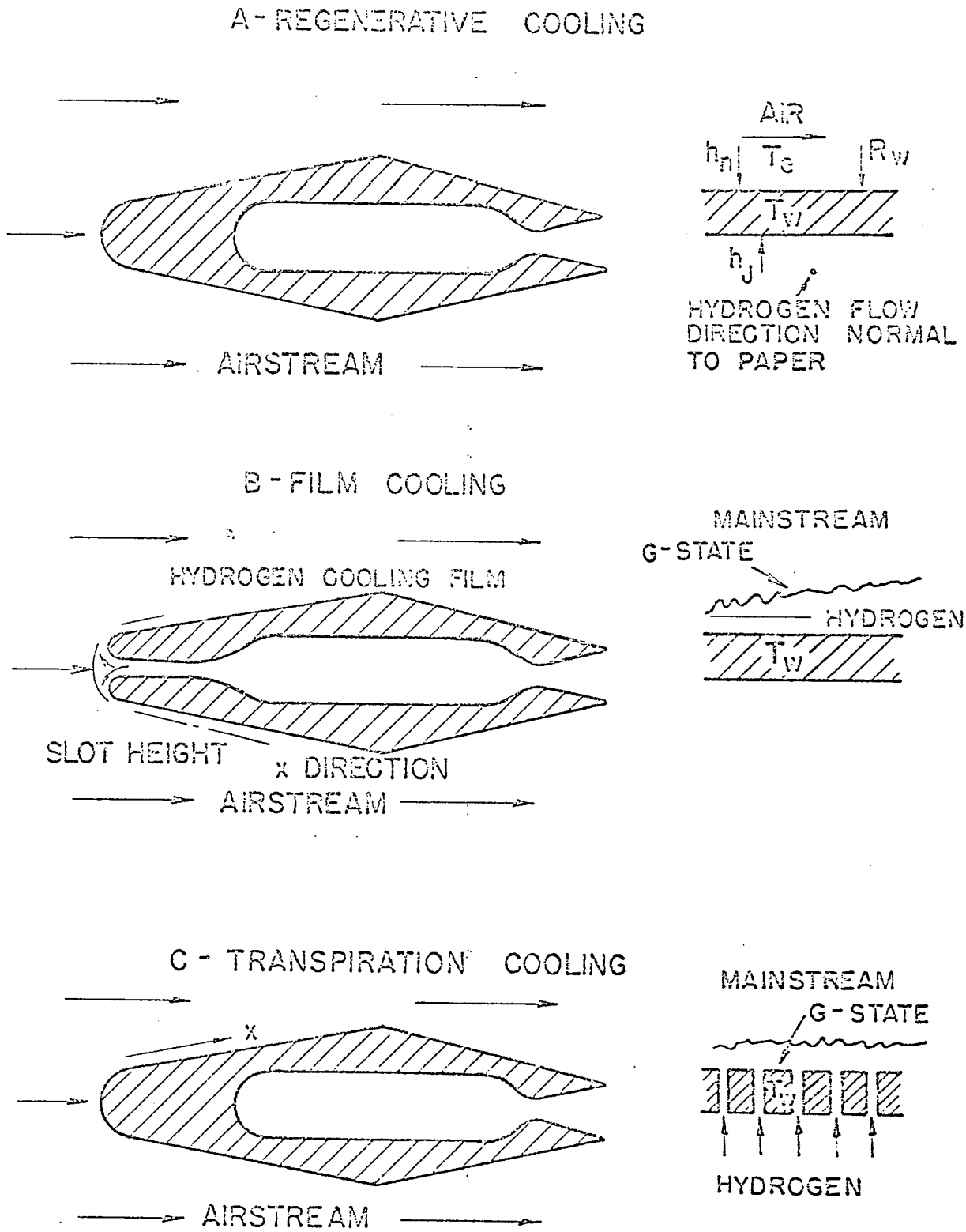

Fig. 20 Standard injectors cooling schemes

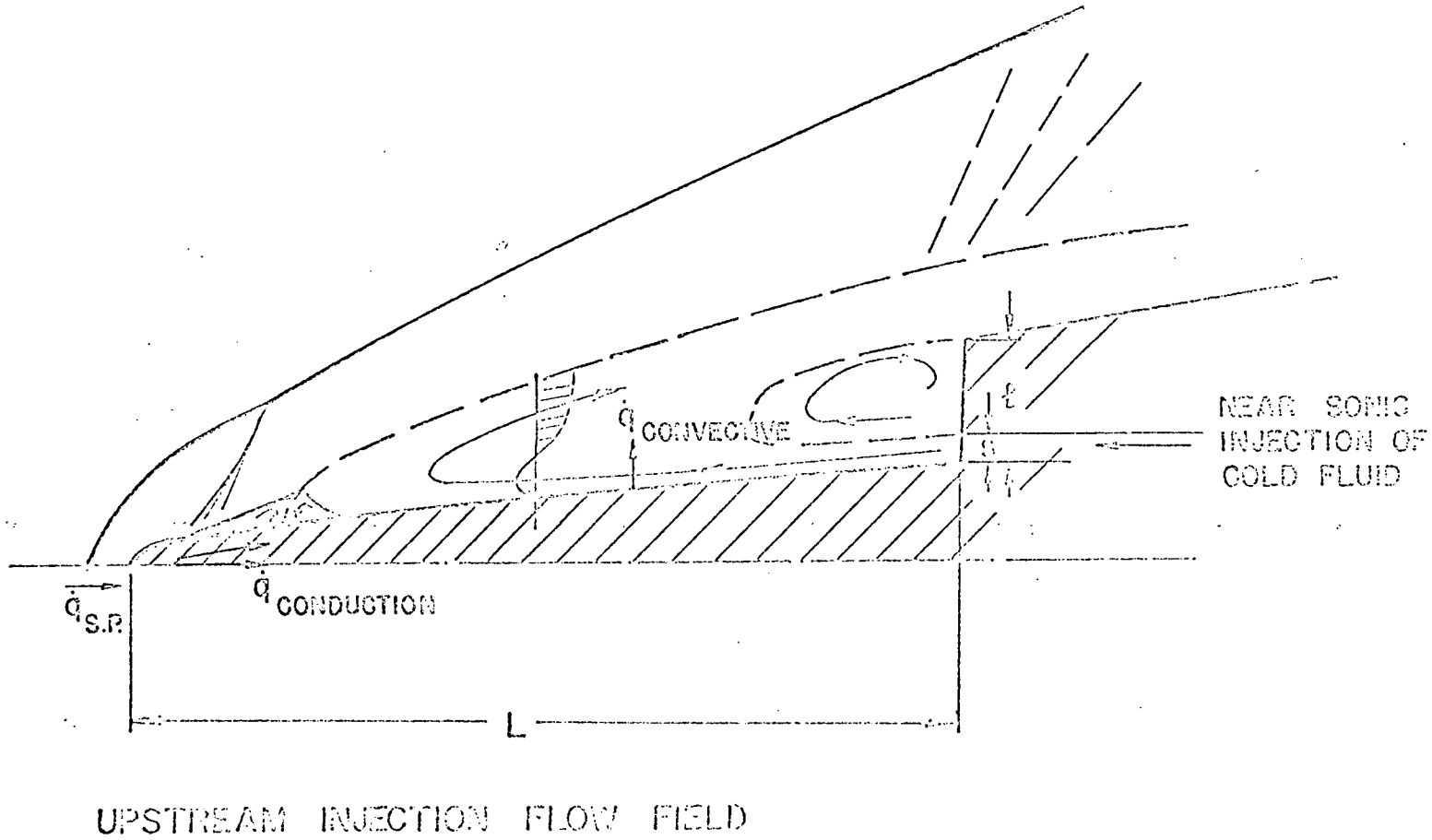

Fig. 21 Leading edge cooling scheme of Ref. 46

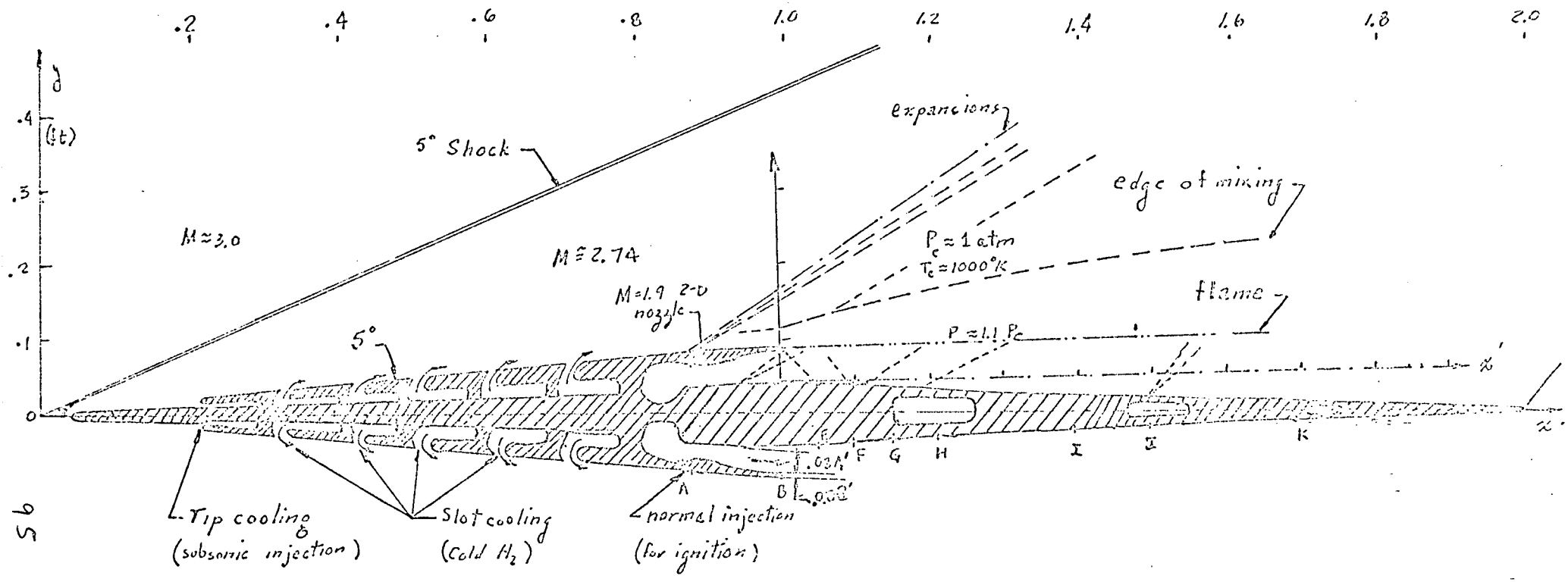

Point	A	B	C	D	E	F	G	H	I	J	K	L
X*	10.200	12.00		11.340	12.384	13.260	13.716	14.640	16.560	18.005	20.40	24.00
Y*	0.8924	0.9552		0.500	0.5002	0.4789	0.4566	0.4058	0.3727	0.2719	0.1257	0.002
slope	+5°	3°		0.0	0.0	-2.8°	-2.8	-1.0°	-4.0°	-4.0°	-2°	—

Fig. 22 Final fuel injector design - flow field and geometry

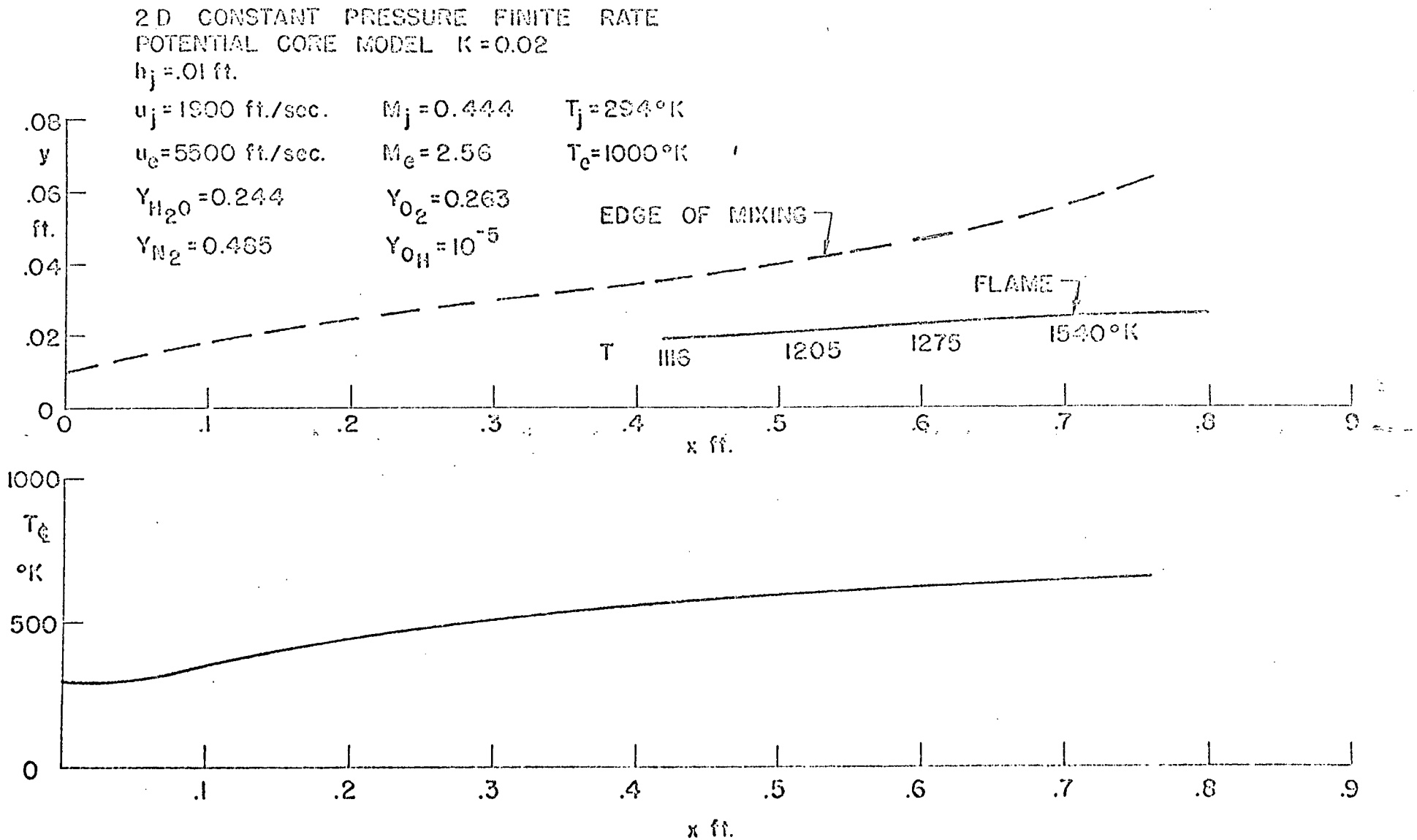

Fig. 23 Injector cooling calculation with a low speed tangential slots of cold hydrogen

Fig. 24 Effect of streamwise pressure gradient on mixing and combustion

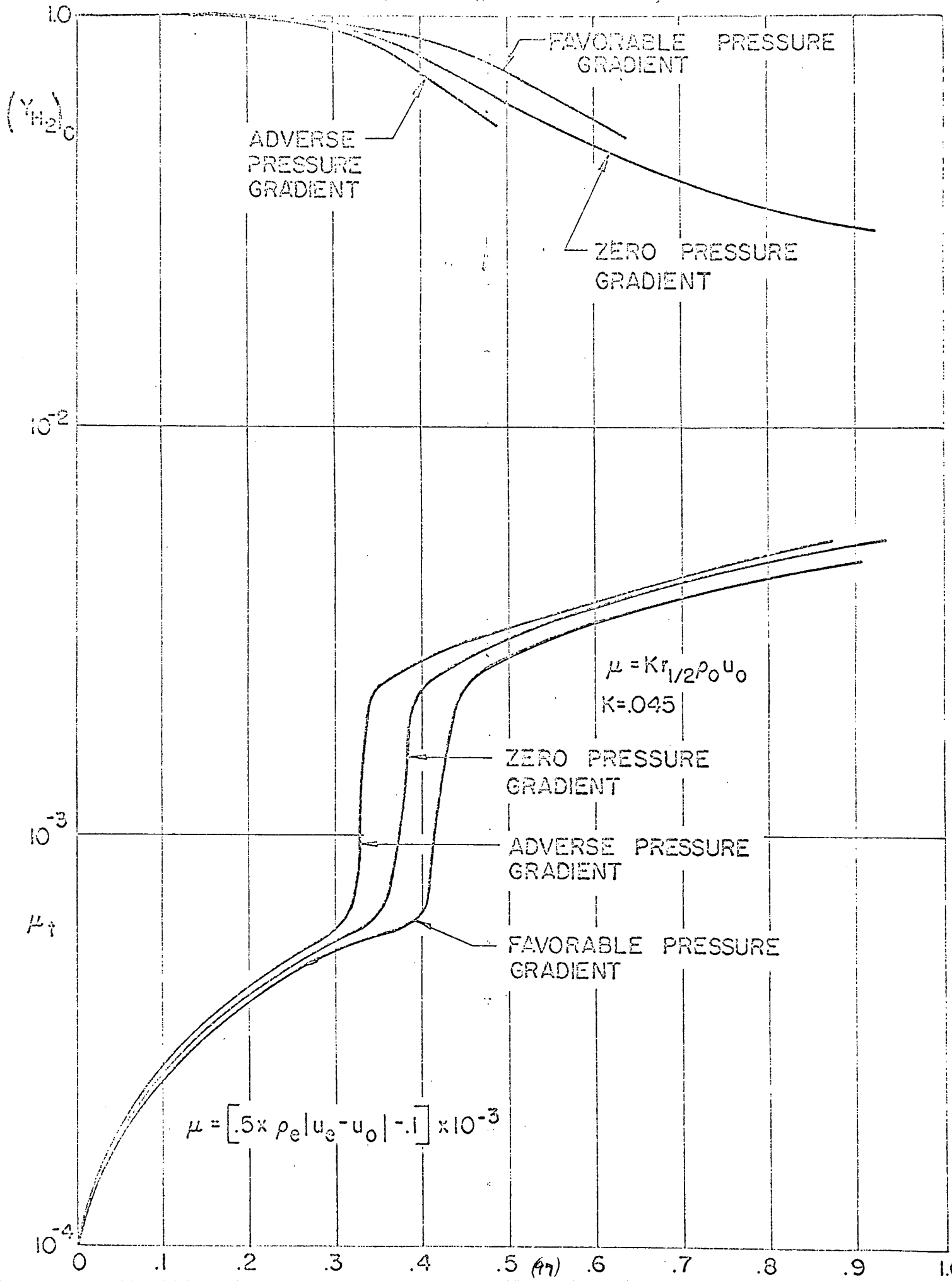

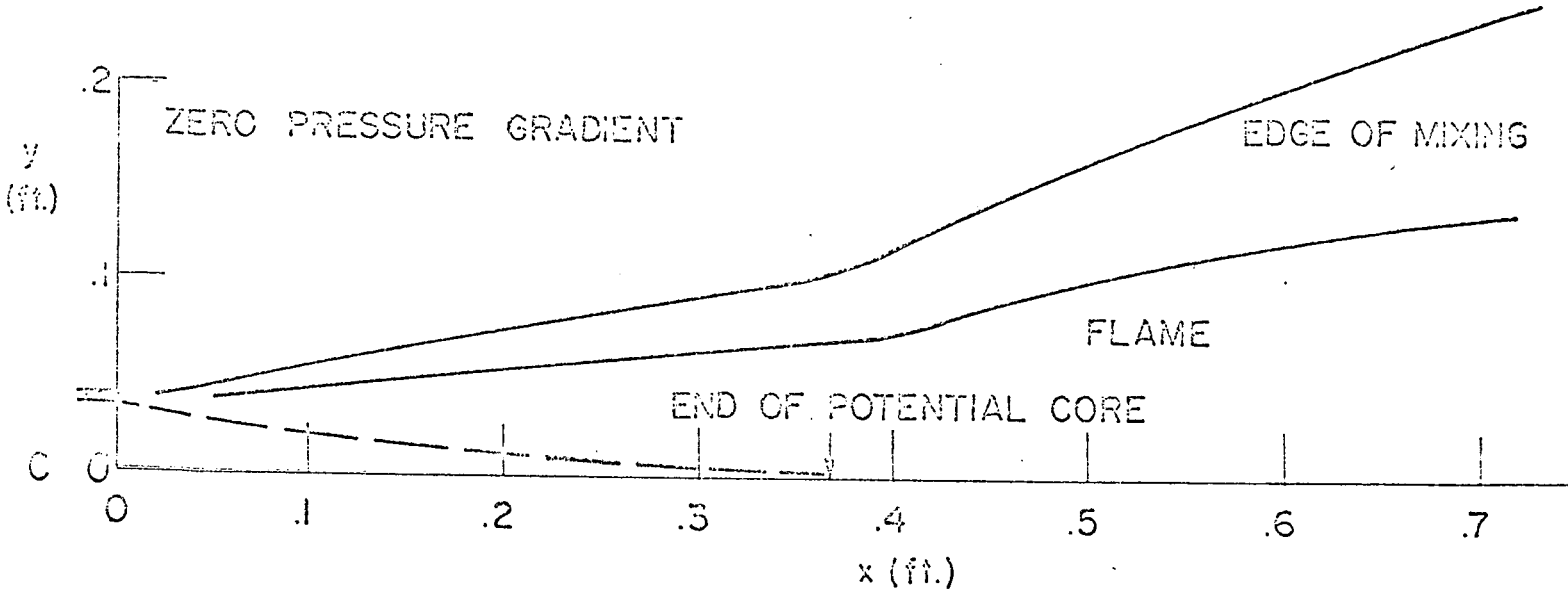

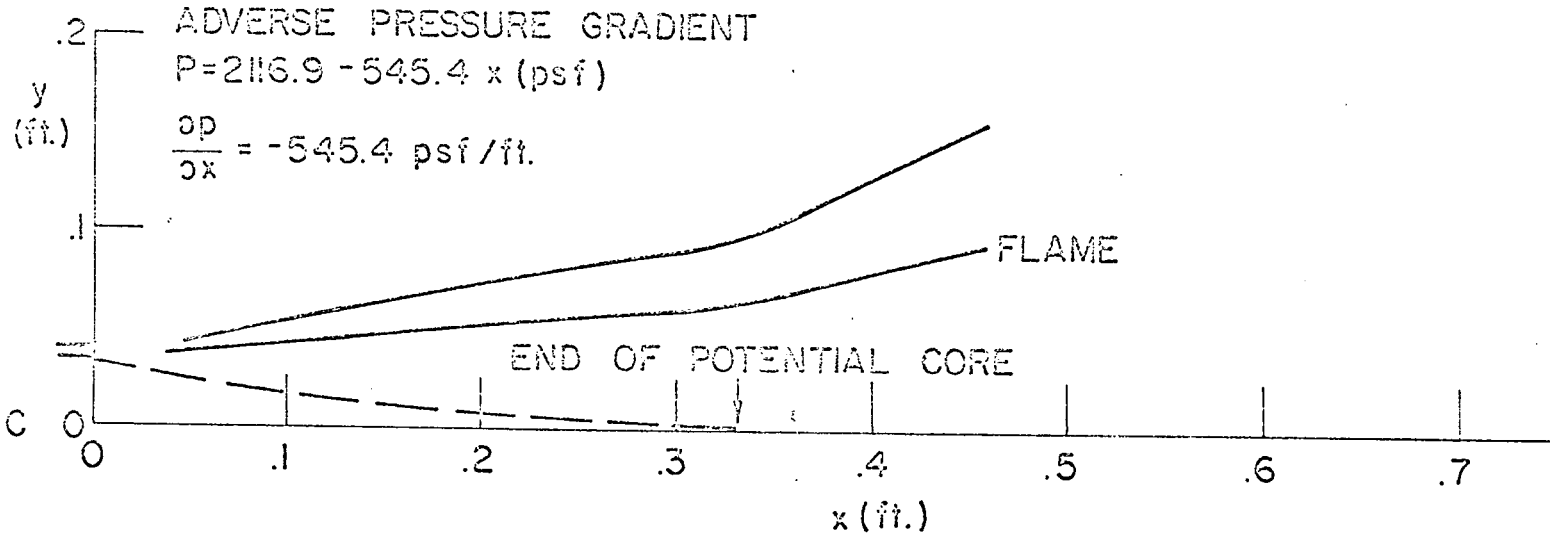

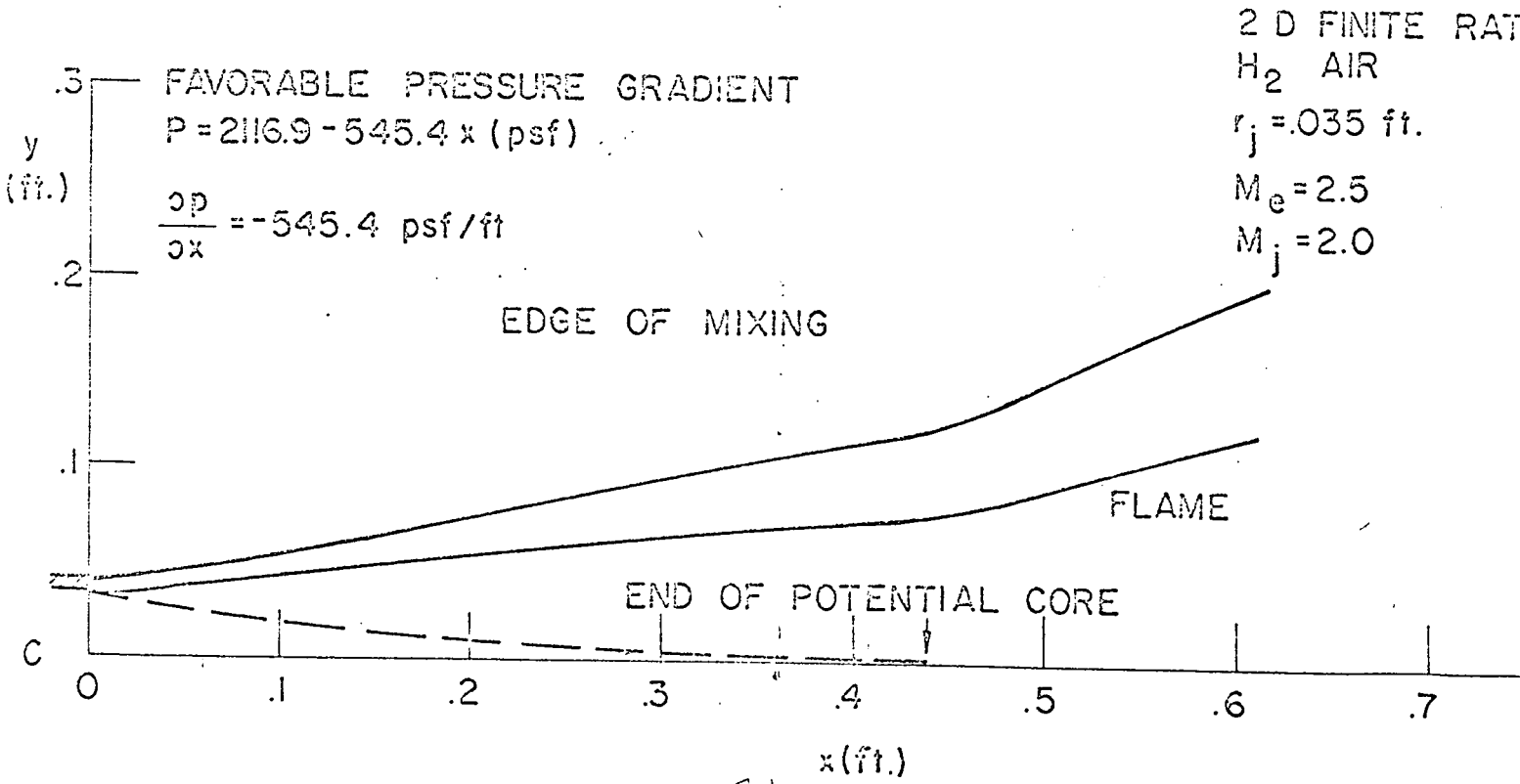

Fig. 24a Effect of Streamwise pressure gradient on mixing and combustion

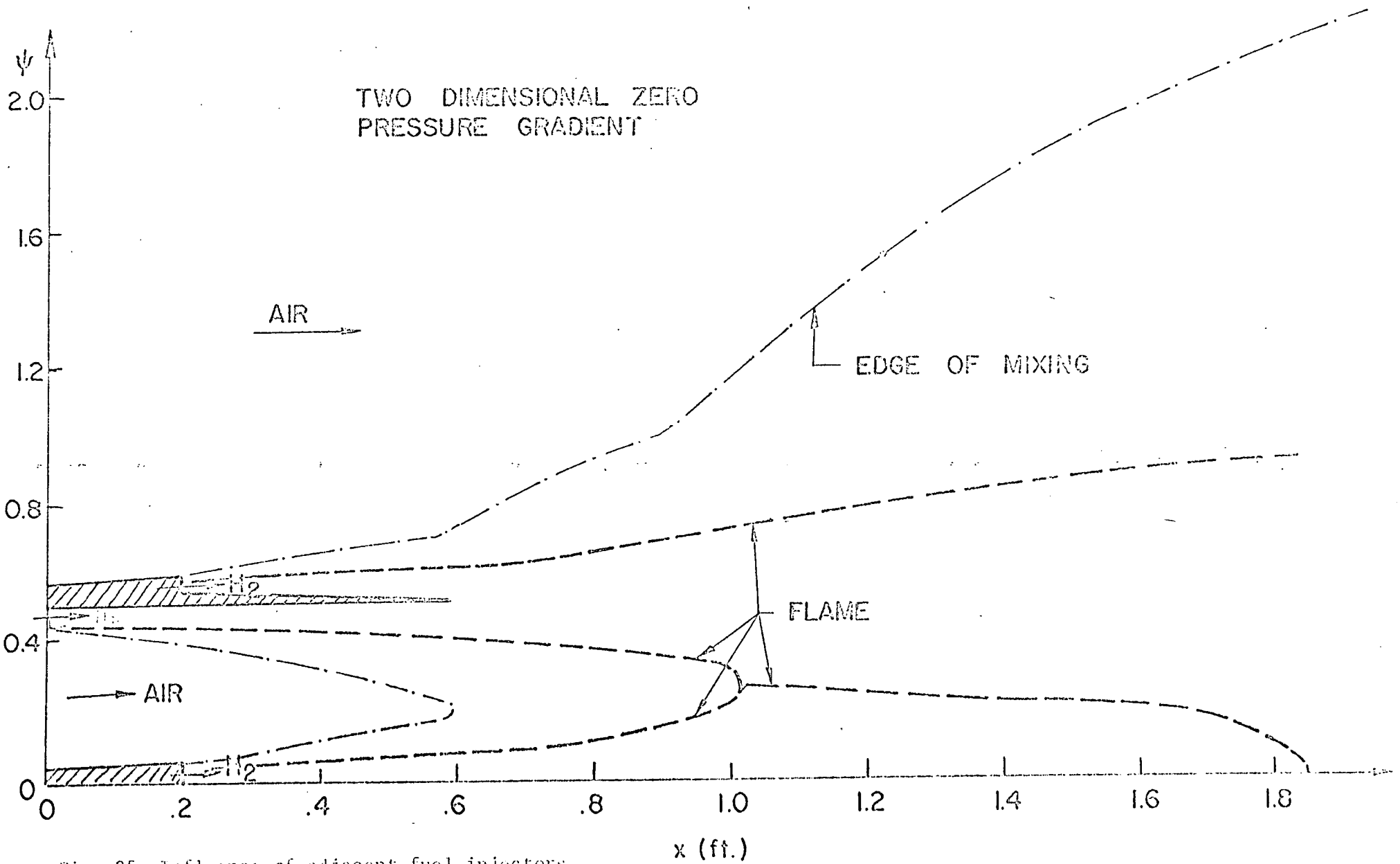

Fig. 25 . Influence of adjacent fuel injectors

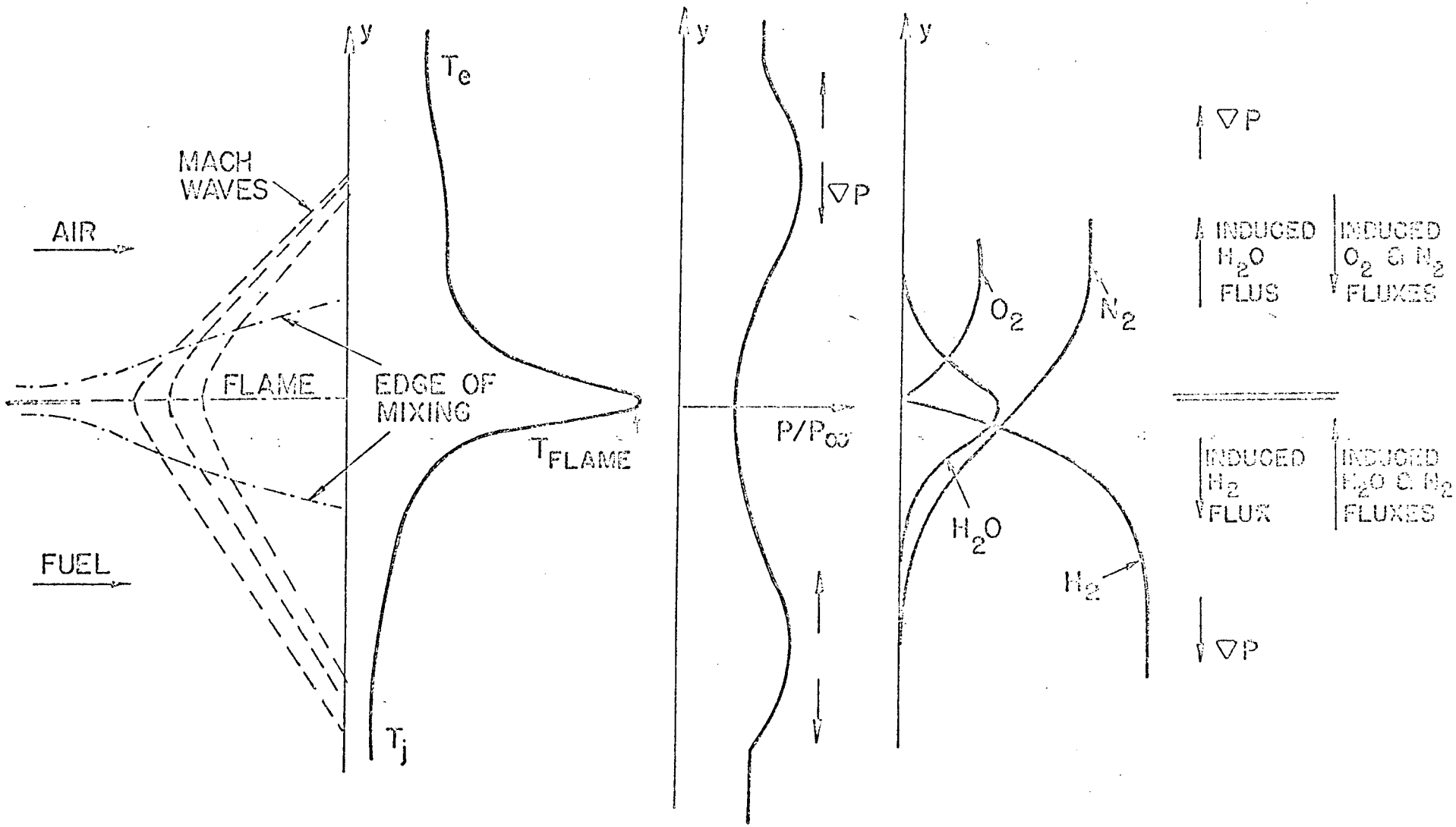

Fig. 26 Qualitative influence of lateral pressure and thermal gradients